Title: SIRT1 and SIRT3 impact host mitochondrial function and host- *Salmonella* pH balance during infection

Dipasree Hajra[1], Vikas Yadav[1], Amit Singh[1], and Dipshikha Chakravortty[1,2]

[1]Department of Microbiology & Cell Biology, Indian Institute of Science

[2]Adjunct Faculty, School of Biology, Indian Institute of Science Education and Research, Thiruvananthapuram

Corresponding author: Prof. Dipshikha Chakravortty

Email: dipa@iisc.ac.in

Tel. No. 0091 80 22932842

ABSTRACT

Mitochondria are an important organelle regulating energy homeostasis. Mitochondrial health and dynamics are crucial determinants of the outcome of several bacterial infections. SIRT3, a major mitochondrial sirtuin, along with SIRT1 regulates key mitochondrial functions. This led to considerable interest in understanding the role of SIRT1 and SIRT3 in governing mitochondrial functions during an intravacuolar pathogen, *Salmonella* infection. Here, we show that loss of SIRT1 and SIRT3 function either by shRNA-mediated knockdown or inhibitor treatment led to increased mitochondrial dysfunction with alteration in mitochondrial bioenergetics alongside increased mitochondrial superoxide generation in the *Salmonella*-infected macrophages. Consistent with dysfunctional mitochondria, mitophagy was induced along with altered mitochondrial fusion-fission dynamics in *S.* Typhimurium-infected macrophages. Additionally, the mitochondrial bioenergetic alteration promotes acidification of the infected macrophage cytosolic pH. This host cytosolic pH imbalance skewed the intra-phagosomal and intra-bacterial pH in the absence of SIRT1 and SIRT3, resulting in decreased SPI-2 gene expression. Our results suggest a novel role of SIRT1 and SIRT3 in maintaining

the intracellular *Salmonella* niche by modulating the mitochondrial bioenergetics and dynamics in the infected macrophages.

KEYWORDS- *Salmonella*, Mitochondrial bioenergetics, mitochondrial ROS, mitophagy, fusion-fission dynamics, macrophage-bacterial pH regulation, SPI-2 secretion

INTRODUCTION

Mitochondria are considered to play a central role in bacterial infections. Numerous microbial pathogens modulate mitochondrial functions and dynamics to evade host immune responses. On the other hand, the host-elicited immune responses are dependent on the overall mitochondrial bioenergetics and their function (Tiku, Tan et al., 2020). Thus, mitochondrial health is a crucial determinant for the outcome of several bacterial infections.

Pathogens like *Listeria monocytogenes* induce mitochondrial fragmentation upon infection via its listeriolysin O protein (Stavru, Bouillaud et al., 2011). Similarly, *Helicobacter pylori* utilize its VacA effector protein to induce mitochondrial network fragmentation(Jain, Luo et al., 2011). DRP-1- (Dynamin-related protein 1) dependent mitochondrial fragmentation is reported in both *Shigella flexneri* (Lum & Morona, 2014) and *Legionella pneumophila* infections(Escoll, Song et al., 2017). On the other hand, *Chlamydia trachomatis* infection promotes mitochondrial elongation in the early phases of infection. Elongated mitochondria contribute to enhanced ATP production, promoting the intracellular proliferation of *C. trachomatis*(Chowdhury, Reimer et al., 2017, Kurihara, Itoh et al., 2019).

Mitochondria, being attributed as the powerhouse of the cell, perform critical functions like governing the regulation of the TCA cycle, oxidative phosphorylation and ATP production. Several bacteria reprogram host metabolism to facilitate their intracellular survival. *Mycobacterium tuberculosis*(Shi, Salamon et al., 2015), *Brucella abortus*(Czyż, Willett et al.,

2017), and *Chlamydia trachomatis*(Siegl, Prusty et al., 2014) infections lead to reduced TCA cycle, increased aerobic glycolysis and augmented lactate production.

Sirtuin 3 (SIRT3) is a mitochondrial NAD+ dependent Class III deacetylase that governs host mitochondrial functions like mitochondrial bioenergetics, metabolism and energy homeostasis(Ahn, Kim et al., 2008, Jing, Emanuelli et al., 2011). It regulates vital enzymatic processes involved in oxidative phosphorylation and fatty acid oxidation in mitochondria(Hallows, Yu et al., 2011, Hirschey, Shimazu et al., 2010). It performs a crucial role in ameliorating oxidative stress by inducing activation of SOD2 (superoxide dismutase 2), and CAT (catalase) that reduces ROS levels(Sundaresan, Gupta et al., 2009). SIRT1, on the other hand, also plays a major role in mitochondrial function in various tissues(Li, Meng et al., 2015, Powell, Swet et al., 2014), and its effect on mitochondrial biogenesis is mediated by PGC1α(Menzies & Hood, 2012). SIRT1 catalyzes the deacetylation of PGC1α, leading to its activation(Nemoto, Fergusson et al., 2005). The activated PGC1α co-ordinates mitochondrial biogenesis by acting as a master regulator. It induces the expression of the nuclear respiratory factors (NRF1 and NRF-2) and transcription factor A of the mitochondria (TFAM) which mediate the transcription of the nuclear and mitochondrial genome respectively(Wu, Puigserver et al., 1999). Recent findings by Kim et al., highlighted the role of SIRT3 in anti-mycobacterial host defences by limiting ROS production and preserving mitochondrial function via autophagy(Kim, Jin et al., 2019). Furthermore, SIRT3 downregulation led to the reprogramming of mitochondrial metabolism and cell-death in *Mycobacterium tuberculosis* infected macrophages(Smulan, Martinez et al., 2021). However, in intravacuolar pathogen like *Salmonella*, the role of SIRT1 or SIRT3 in the modulation of mitochondrial function and establishment of pathogenesis is largely unexplored.

Salmonella enterica is a facultative, anaerobic, flagellated, intracellular pathogen causing food- and water borne enteric typhoid fever and gastroenteritis worldwide. *Salmonella* Typhimurium

causes localized gastroenteritis, however, in certain instances it contributes to systemic invasive infections in immunocompromised individuals(Knodler & Elfenbein, 2019). The emergence of several multi-drug resistant *Salmonella* strains continues to be a major healthcare concern which calls for a comprehensive understanding of the mechanism underlying *Salmonella* pathogenesis and its interaction with its host. The pathogen gain entry into the non-phagocytic intestinal epithelial cells via its *Salmonella* Pathogenicity Island-1 (SPI-1) effectors and with the help of specialized microfold (M) cells breach the intestinal barrier (Haraga, Ohlson et al., 2008). Apart from M cells in Peyer's patches, the dendritic cells can also sample the bacteria from the lumen to the lamina propria. In the lamina propria, it encounters various host immune cells like neutrophils, macrophages, and dendritic cells. Macrophages, dendritic cells and neutrophils are responsible for successful dissemination throughout the body through the reticulo-endothelial system (RES) to the secondary organs such as Mesenteric Lymph Node (MLN), liver and spleen (Haraga et al., 2008). Inside the macrophages, *Salmonella* reside within a modified vacuole, called *Salmonella* -Containing Vacuole (SCV), and utilize various SPI-2 effectors to maintain a replication niche inside their host (Hajra, Nair et al., 2021, Haraga et al., 2008).

In this study, we explored the role of host deacetylases SIRT1 and SIRT3 in modulating mitochondrial bioenergetics and dynamics during *Salmonella* infection. Inhibiting SIRT1 or SIRT3 through shRNA knockdown or specific catalytic inhibitors resulted in increased mitochondrial dysfunction in infected macrophages, leading to elevated mitochondrial superoxide generation and altered mitochondrial dynamics, with increased fission and mitophagy. This was further accompanied by mitochondrial membrane hyperpolarization, increased proton leakage and respiration rate, and reduced ATP production and Electron Transport Chain (ETC) function. Absence of SIRT1 or SIRT3, resulted in increased macrophage cytosol acidification, consequently resulting in reduced intra-phagosomal and

intra-bacterial acidification. This sequalae in the intracytoplasmic pH change in bacteria and the bacterial phagosome led to decreased SPI-2 gene expression. Altogether, our findings indicate the crucial role of SIRT1 and SIRT3 in modulating mitochondrial bioenergetics and pH dynamics during *S*. Typhimurium infection, thereby influencing the bacterial intracellular niche and pathogenesis.

MATERIALS AND METHODS

Bacterial Strains, Cell culture condition and infection

Salmonella enterica serovar Typhimurium (STM) strain ATCC 14028S or ATCC 14028S constitutively expressing green fluorescent protein (GFP) through pFPV25.1 were used. 4% paraformaldehyde fixed STM (PFA) was used as the killed fixed bacteria control. The above-mentioned live bacterial strain was grown overnight at 37 ^{0}C at 160 rpm shaking condition. Macrophages were infected with stationary-phase bacterial culture with MOI of 10. For facilitating the attachment of bacteria to host cells, tissue culture plates were subjected to centrifugation at 600xg for 5 min and plate was incubated at 37 ^{0}C humified incubator with 5% $CO_2$for 25 min. Cells were washed with PBS and were treated with DMEM (Lonza) + 10% FBS (Gibco) containing 100 µg/ml gentamicin for 1 hr. Subsequently, the gentamicin concentration was reduced to 25 µg/ml and maintained until the cells were harvested for further studies.

Cell Culture

RAW 264.7 murine macrophages were cultured in DMEM (Lonza) containing 10% Fetal Bovine Serum (FBS) (Gibco) at 37 ^{0}C in a humified incubator with 5% CO_2. Prior to each experiment, cells were seeded into 24-well or 6-well plates as per requirement at a confluency of 60%.

Peritoneal macrophages were collected in PBS from the peritoneal cavity of C57BL/6 mice aseptically post thioglycolate treatment using 20G needle and 5ml syringe. Following centrifugation, cell pellet was resuspended in RPMI-1640 (Lonza) containing 10% heat-inactivated FBS (Gibco),100 U/ml penicillin and 100 µg/ml streptomycin and seeded into 6 well- plate. 6hr prior to infection, antibiotic containing media was replaced with Penicillin-Streptomycin free RPMI-1640 (Lonza) containing 10% heat-inactivated FBS (Gibco).

Transfection

shRNA mediated knockdown was carried out by PEI mediated transfection protocol. Plasmid harbouring shRNA in pLKO.2 vector backbone specific to SIRT1and SIRT3 were used for transfection. Plasmid harbouring scrambled sequence of shRNA, served as a control, was also used for transfection. Plasmid DNA was used at a concentration of 500ng per well of a 24-well plate. Plasmid and PEI were added in 1:2 ratio in serum free DMEM media and incubated for 20 mins at room temperature. Post incubation, the DNA: PEI cocktail was added to the seeded RAW 264.7 macrophages. After 6-8hrs of incubation, serum-free media was replaced with complete media containing 10% FBS. Post 48hr of transfection, transfected cells were either harvested for knockdown confirmation studies or subjected to infection with STM.

Table 1: List of shRNA used for knockdown

Sirtuins	Construct ID	TRC ID	Sequence (5'---3')

SIRT 1	C4	TRCN000 0218734	GTACCGGCATGAAGTGCCTCAGATATTACTCGAGTA ATATCTGAGGCACTTCATGTTTTTTG
SIRT 1	C12	TRCN000 0018979	CCGGGCAAAGCCTTTCTGAATCTATCTCGAGATAGA TTCAGAAAGGCTTTGCTTTTT
SIRT 3	E8	TRCN000 0038889	CCGGCCCAACGTCACTCACTACTTTCTCGAGAAAGT AGTGAGTGACGTTGGGTTTTTG
SIRT 3	E12	TRCN000 0038893	CCGGCCACCTGCACAGTCTGCCAAACTCGAGTTTGG CAGACTGTGCAGGTGGTTTTTG

Immunofluorescence confocal microscopic studies

At the specified time points post infection with GFP tagged STM, cells were fixed with 3.5% paraformaldehyde for 15 min. Primary antibody staining was performed with specific primary antibody in the presence of a permeabilizing agent, 0.01% saponin (Sigma) dissolved in 2.5% BSA containing PBS at 4°C for overnight or for 6hr at room temperature (RT). Following this, cells were washed with PBS stained with appropriate secondary antibody tagged with fluorochrome for 1 hr at RT. This was followed by DAPI staining and mounting of the coverslip onto a clean glass media. All immunofluorescence images were obtained using Zeiss Multiphoton 880 and were analyzed using ZEN black 2012 software.

For the mitophagy flux determination, we transfected RAW264.7 macrophages with mitoGFP-mCherry traffic light construct which was a generous gift from Prof. Gangi Setty Subba Rao, IISc. Post- 24 hr of transfection, RAW264.7 macrophages were infected with *S*. Typhimurium at an MOI of 10 and were subjected with SIRT1 (EX-527) and SIRT3 (3TYP) treatment at a concentration of 1µM. At the designated time points post-infection, cells were fixed, and intracellular *Salmonella* were stained with rabbit raised anti-*Salmonella* antibody followed by

secondary staining and mounting. Immunofluorescence images were obtained using Zeiss Multiphoton 880 and were analysed using ZEN black 2012 software.

Quantitative Real Time PCR

Total RNA was isolated at specific time points post infection by using TRIzol (Takara) as per manufacturer's protocol. Quantification of RNA was performed in Nano Drop (Thermo-Fischer scientific). Quality of isolated RNA was detected by performing 2% agarose gel electrophoresis. 2 µg of RNA was subjected to DNaseI treatment at 37°C for 1 hr followed by addition of EDTA and heat inactivation at 65°C for 10 mins. The mRNA was reverse transcribed to cDNA using oligo $(dT)_{18}$ primer, buffer, dNTPs and reverse transcriptase (Takara) as per manufacturer's protocol.The expression profile of target gene was evaluated using specific primers by using SYBR green RT-PCR master mix (Takara) in BioRad Real time PCR instrument. βactin was used as an internal control. All the reaction was setup in 384 well plate with two replicates for each sample.

Table 2: List of primers

Primer Name	**Sequence (5'---3')**
SIRT1 FP	ACAAAGTTGACTGTGAAGCTGTAC
SIRT1 RP	GTTCATCAGCTGGGCACCTA
SIRT3 FP	GCTGCTTCTGCGGCTCTATAC
SIRT3 RP	GAAGGACCTTCGACAGACCGT
Ndufa9 FP	GAAGCAGCCGGTGTATGTTG
Ndufa9 RP	ATGCTCCGGGCCTTCTTTTT
Ndufs1 FP	AGCCGGCAGCCATCATGTTA

Ndufs1 RP	AGTTACTTGCTGCTGTGCC
Ndufv1 FP	TTTCTCGGCGGGTTGGTTC
Ndufv1 RP	GGTTGGTAAAGATCCGGTCTTC
Sdhd FP	TGTCACCAAGCCACCACTC
Sdhd RP	CCACAGAGCAGGGATTCAAG
Uqcr FP	TGCCGAGGCCTCAGACACAG
Uqcr RP	TCCAAGGCATAAGAATAAGGTTT
Cox5b FP	CAGAAGGGACTGGACCCATA
Cox5b RP	TTCACAGATGCAGCCCACTA
ATP5B FP	TTTGCTGGTGTTGGTGAGAG
ATP5B RP	GGTGGTTCGTTCATCTGTCC
HO-1 FP	GAACCCAGTCTATGCCCCAC
HO-1 RP	GCGTGCAAGGGATGATTTCC

SOD2 FP	CTGTCCGATGATGTCAGCCA
SOD2 RP	AACCCATTTGCCGCTACTGA
NQO1 FP	TAGCCTGTAGCCAGCCCTAA
NQO1 RP	GCCTCCTTCATGGCGTAGTT
CAT FP	CACTGACGAGATGGCACACT
CAT RP	TGTGGAGAATCGAACGGCAA
Gpx1 FP	AGTCCACCGTGTATGCCTTC
Gpx1 RP	CCTCAGAGAGACGCGACATT
Drp1 FP	GCAACTGGAGAGGAATGCTG
Drp1 RP	CACAATCTCGCTGTTCTCGG
Fis1 FP	AGAGGAACAGCGGGACTATG
Fis1 RP	CCATGCCTACCAGTCCATCT
Mff FP	CACCACCAAATGCTGACCTG

Mff RP	GGTGTTTTCAGTGCCAGAGG
Mid49 FP	TGTCAGCCTCTGTCAACTGG
Mid49 RP	AGTGAACTCCAGGCACTCGT
Mid 51 FP	ATGTACTTGAGTGGCAGCCT
Mid51 RP	TCACGACGAACCAGGAAGAA
Mfn2 FP	GTGGAATACGCCAGTGAGAAGC
Mfn2 RP	CAACTTGCTGGCACAGATGAGC
OPA-1 FP	GAGGCCCTTCTCTTGTTAGGTT
OPA-1 RP	CTTCCGCAGCTCTTTGTTCTC
βactin FP	CAGCAAGCAGGAGTACGATG
βactin RP	GCAGCTCAGTAACAGTCCG
cadA FP	GGCGAAACGGAAGAGGTGTA
cadA RP	CGCACAGCATTTGCAGGAAT
cadB FP	CCGGCACCTTTATCGTCAGT

cadB RP	TCAGCCGTATTGTTGTCGCT
cadC FP	ACGCTGGTGGTGTTTATCGT
cadC RP	GCCGCCTTCAAAACGAACAT
Salmonella 16S rRNA FP	GTGAGGTAACGGCTCACCAA
Salmonella 16S rRNA RP	TAACCGCAACACCTTCCTCC
pipB2 FP	TGGCGCCAATTTACAACACGC
pipB2 RP	CTCGCCTTTCGCAGGTTTGC
steE FP	CCGCAAAAGCCTTAACCACC
steE RP	GTTTTACCGGCACGGCTTTT

Intracellular proliferation or gentamicin protection assay

Following infection of the transfected cells with STM at an MOI of 10, cells were treated with DMEM (Sigma) + 10% FBS (Gibco) containing 100 µg/ml gentamicin for 1 hr. Subsequently, the gentamicin concentration was reduced to 25 µg/ml and maintained until the specified time point. Specific inhibitor treatment was given along with 25 µg/ml gentamicin-containing media at the specified concentration. Post 2hr and 16hr post-infection, cells were lysed in 0.1% triton-X-100. Lysed cells were serially diluted and plated to obtain colony-forming units (CFU). Fold proliferation was calculated as CFU at 16hr divided by CFU at 2hr.

Western Blotting

Post appropriate time points of infection, the cells were harvested in PBS following PBS wash and centrifuged at 1500 rpm for 10 mins at 4°C. Cells were lysed in RIPA buffer containing 10% protease inhibitor cocktail (Roche) for 30 min on ice. Total protein was estimated using Bradford method of protein estimation. Protein samples were subjected to SDS polyacrylamide gel electrophoresis and then were transferred onto 0.45µm PVDF membrane (18V, 2 hrs). The

membrane was blocked using 5% skim milk in TBST for 1hr at RT and subsequently probed with appropriate primary antibody for overnight at 4°C. Following wash in TBST, blot was probed with specific HRP conjugated secondary antibody for 1hr at RT. The membrane was developed using ECL (Biorad) and images were captured using ChemiDoc GE healthcare. All densitometric analysis was performed using ImageJ software.

Table 3: List of Antibodies

Antibody Name	**Catalogue Number**
SIRT1 Polyclonal Antibody	Cat #PA5-85921 (ThermoFisher Scientific)
SIRT3 Polyclonal Antibody	**Cat#** PA5-13222(ThermoFisher Scientific)
OPA1 (D6U6N) Rabbit mAb	Cat #80471 (Cell Signaling Technology)
SOD2 Rabbit pAb	A1340, ABclonal
LC3B Antibody	Sigma
Acetylated-Lysine Antibody	Cat #9441(Cell Signaling Technology)
β actin	A3854 (Sigma)

Immunoprecipitation

For co-immunoprecipitation, cells were washed with PBS and were lysed in native lysis buffer containing 1% Nonidet P-40, 20 mM Tris (pH 8), 2 mM EDTA, 150 mM NaCl and protease

inhibitors mixture (Roche Diagnostics) for 30 min at 4°C. Cell debris was removed by centrifugation at 10,000 rpm for 10 min and the supernatant was treated with the specific capture antibody (SIRT3 or OPA-1). Antibody-lysate complexes were immunoprecipitated using Protein A/G- linked magnetic beads (MagGenome) according to the manufacturer's protocol. Beads were extensively washed with washing buffer and denatured at 95 ^{o}C for 10 min. Denatured precipitates were subjected to SDS-PAGE (12% gel) followed by transfer to 0.45 μ PVDF membrane. The membrane was blocked using 5% skimmed milk in TBST (Tris Buffered Saline containing 0.1% Tween-20) for 1h at room temperature and eventually probed for SIRT3 or Anti-acetylated Lysine (Ac-K) primary antibody overnight at 4°C. The blot was probed with a specific HRP-conjugated secondary antibody for 1hr at RT after rigorous washing in TTBS. ECL (BioRad) was used for detection and images were captured using ChemiDoc GE healthcare.

SOD2 Assay

The cell culture supernatant was harvested at 16h post infection and the assay were performed using Mouse Superoxide dismutase [Mn], mitochondrial ELISA kit (SOD2) (ABclonal, Catalog Number-RK04590) as per the manufacturer's instructions. Briefly, 50µl of standards or the test samples were added to each well. Incubation was carried for 1 h at 37ºC followed by three-time washes with wash buffer. 100µl of the working Streptavidin-HRP solution was added and incubated for 30 minutes at 37ºC. Post-incubation, washing was carried out for a total of five washes. 90µL of TMB substrate solution was added per well and incubated for 15-20 minutes at 37ºC under dark conditions. 50 µL of stop solution was added to each well and the optical density was measured within 5 minutes under 450nm. Correction wavelength was set at 570nm or 630nm. The concentration of the samples were extrapolated from the standard curve.

ATP Estimation Assay

Cells were harvested at the required time points post infection and the ATP content of the sample was estimated using ATP Colorimetric Assay Kit (Sigma, MAK190) according to the manufacturer's protocol. Briefly, 50µL of the samples were added to each of the 96-well plate in duplicates. To each of the 50µL of the master mix containing 44µL of ATP assay buffer, 2µL of ATP probe, 2µL of ATP converter and 2µL of Developer Mix were added. After the addition of the master reaction mix to the sample, they were mixed by horizontal shaker or via pipetting. The plate was incubated for 30 minutes in dark at room temperature. Post incubation, absorbance was measured at 570nm in a microplate reader. The ATP content of the sample was estimated from the ATP standard curve ranging from 0-10 nmole/µl. 10µM oligomycin, an ATP synthase inhibitor, treatment was provided to the cells to serve as a negative control for the assay (Shchepina, Pletjushkina et al., 2002, Zhou & Faraldo-Gómez, 2018).

Seahorse OCR Measurement

Mitochondrial oxidative phosphorylation reaction was assessed by measuring the oxygen consumption rate (OCR) by performing a modified mitostress test(Cumming, Addicott et al., 2018) using a XF Extracellular Flux Analyzer (Agilent Technologies) at 6hr post infection post SIRT3 inhibitor treatment. 8-well XF sensor cartridge containing 200 µl/well of XF calibrate solution was preincubated overnight at 37 °C in a CO2-free incubator. 10-fold concentrated compound of oligomycin (Complex V inhibitor), and a combination of rotenone (Complex I inhibitor) and antimycin A (Complex III inhibitor) were loaded into a sensor cartridge to produce final concentrations of 1.5 µM, and 2 µM, respectively. After a 30-min calibration of the XF sensor with the preincubated sensor cartridge, the cell plate was loaded into the analyzer, and OCR was analyzed under basal conditions. Oxygen use for ATP generation, and net mitochondrial oxygen consumption was analyzed by sequential injection of the complex

inhibitors oligomycin, and the combination of rotenone and antimycin A. Data were analyzed using WAVE software (Agilent Technologies).

Flow Cytometry

At specific time points post infection, the cell growth media was removed, and the cells were washed with 1X PBS and 1X TMRM (Thermoscientific, cat no. T668) staining solution at 100nM concentration were added to the cells. Cells were incubated with the staining solution for 30 mins at 37°C. Cells were washed in 1X PBS and harvested in 1X PBS to analyse the cells via flow cytometry with 488 nm laser for excitation and a 570 ±10 nm emission filter.

Cell growth media was removed at specific time point post infection and stained with 5µM of MitoSox Red (Invitrogen, cat no.M36008) in 1X PBS. Cells treated with 10µM of antimycin served as a positive control for mitochondrial ROS production (Han, Kim et al., 2008, Park, Han et al., 2007). Cells were incubated with the staining solution for 10-30 mins at 37°C, protected from light. Cells were washed thrice with 1X PBS before harvesting the cells in 1X PBS for analysing the cells via flow cytometry.

This similar protocol was followed for BCECF-AM staining wherein after removal of cell growth media at specific time point post infection, the cells were stained with 10µM of BCECF-AM (Invitrogen, cat no.B1150) in 1X PBS. Two hours prior to the specific time points, cells were treated with 50µg/ml of chloroquine in 25µg/ml gentamicin containing DMEM media (Roy Chowdhury, Sah et al., 2022). This chloroquine treated cells served as a control for increased intracellular pH(Di Trani, Savarino et al., 2007). Cells were incubated with the staining solution for 10-30 mins at 37°C, protected from light. Cells were washed thrice with 1X PBS before harvesting the cells in 1X PBS for analysing the cells via flow cytometry (BD FACSVerse) using 405nm and 488nm excitation and 535nm emission channel. The median fluorescence intensity (MFI) of the macrophage population at 488 nm and 405 nm was

estimated using BD FACSuite software. The 488/ 405 ratio was determined to estimate the level of acidification of the bacterial cytosol. A standard curve of known pH versus the ratio metric fluorescence (488nm/405nm) was obtained by exposing the macrophages at different pH buffered solution in presence of 10µM valinomycin and 10µM nigericin. The obtained standard curve was used to interpolate the unknown pH of the test samples.

Intra-phagosomal pH measurement

The *Salmonella*-containing vacuole (SCV) pH of *S*. Typhimurium infected macrophages were measured using a previously reported protocol (Gogoi, Ravikumar et al., 2018). Briefly, overnight grown stationary phase cultures of STM WT was labelled with 20 µM pH rhodo red succinimidyl ester (Molecular Probes, Invitrogen) at 37ºC incubator for 1h. The bacterial cells were washed with 0.1 M sodium bicarbonate buffer (pH= 8.4) both pre- and post- labelling. RAW264.7 cells were infected with these labelled bacteria at MOI 10. 6- and 16 h post-infection, the macrophages were washed with PBS and were resuspended in PBS for flow cytometric analysis (CytoFLEX by Beckman Coulter Life Sciences) using 560 nm excitation and 585 nm emission filter. To generate a standard curve of known pH, the macrophages were infected with pH rhodo red labelled bacteria as described. The macrophages were subjected to different pH- buffered solution ranging from pH 5.0 to 8.0 in presence of valinomycin (10µM) and nigericin (10µM) for equilibration. Post, equilibration for 1h, the macrophages were harvested in PBS and subjected to flow cytometric analysis. The percentage pH rhodo-red positive population was plotted as a function of pH to obtain a standard curve. The resulting standard curve was used to obtain the SCV pH of the infected macrophages.

Intracellular bacterial pH Measurement

S. Typhimurium wildtype (STM WT) and STM Δ*ompR* strains were transformed with a pH sensitive fluorescent plasmid pBAD-pHUji (Plasmid#61555)(Shen, Rosendale et al., 2014).

Both the overnight grown bacterial strains were subjected to pH range of 5.0 to 9.0 in buffered solution in presence of 40µM of sodium benzoate to ensure equilibration to the desired pH. The resulting fluorescence intensity ratio as obtained from flow cytometric analysis was plotted as a function of pH and fitted to obtain a standard curve. The standard curve was used to interpolate ratios measured within the intracellular bacteria in infected macrophages.

S. Typhimurium wildtype (STM WT) and STM Δ*ompR* expressing pBAD-pHUji was used to infect the murine macrophages (knockdown macrophages or inhibitor treated). 16hr post infection, the cells were harvested for flow cytometric analysis to obtain fluorescence ratios. The standard curve was used to interpolate ratios measured to obtain intracellular bacterial pH within infected macrophages.

Statistical analysis

Data were analysed and graphed using the GraphPad Prism 5 software (San Diego, CA). Statistical significance was determined by Student's t-test or Two-way ANOVA and Bonferroni post-t-test to obtain p values. Adjusted p-values below 0.05 are considered statistically significant. The results are expressed as mean ± SEM.

RESULTS

SIRT3 inhibition only led to enhanced mitochondrial superoxide generation in the infected macrophages

Salmonella Typhimurium strain 14028S infection triggered an increase in mitochondrial superoxide generation in RAW264.7 murine macrophages in comparison to the uninfected control in flow cytometric studies. This increment in mitochondrial superoxide was further aggravated (around 2-fold) in knockdown condition of SIRT3 in infected RAW264.7 macrophages. However, the mitochondrial ROS production within SIRT1 knocked down macrophages remained comparable to scrambled control under infection scenario

(Supplementary Fig. S1, Fig. 1 A). This result was further corroborated by the findings in the *Salmonella* infected primary peritoneal macrophages (PMs) treated with SIRT1 or SIRT3 inhibitors EX-527 (Morató, Astori et al., 2022), and 3TYP (Hu, Wang et al., 2022), respectively. Treatment with only SIRT3 inhibitor resulted in heightened production of mitochondrial ROS (mtROS) in the infected PMs in comparison to the untreated control (Fig. 1B). Immunofluorescence data further showed increased mitoSOX Mean Fluorescence Intensity (MFI) and elevated coefficient of colocalization of mitoSOX with mitochondria in SIRT3 knockdown RAW264.7 macrophages when compared to the scrambled control (Fig. 1C-D). Together, these results implicate the role of SIRT3 in mitigating mitochondrial ROS generation in the *Salmonella* infected murine macrophages.

Heightened mitochondrial ROS (mtROS) production restricted the intracellular proliferation of *Salmonella* within SIRT3 knockdown macrophages

As depicted earlier, SIRT3 knockdown triggered increased mitochondrial oxidative stress in infected RAW264.7 macrophages. Therefore, we hypothesized that the elevated mtROS leads to attenuated intracellular replication of bacteria in the SIRT3 knockdown RAW264.7 macrophages. To investigate this hypothesis, we performed the intracellular bacterial proliferation assay in the or absence of mitochondrial superoxide scavenger, mitoTEMPO (Supplementary Fig. S2) in SIRT3 knockdown macrophages. In the untreated data set, the SIRT3 knockdown macrophages depicted attenuated intracellular proliferation of *S.* Typhimurium in comparison to the scrambled control. However, upon alleviation of the mtROS by mitoTEMPO treatment, there was a restoration in intracellular proliferation of *Salmonella* in the SIRT3 knockdown macrophages (Fig.2). Therefore, the increased mitochondrial oxidative burst within the SIRT3 knockdown limited the intracellular proliferation of *Salmonella* which got reversed upon alleviation of the mtROS production by mitoTEMPO.

SIRT1 and SIRT3 inhibition compromised the mitochondrial antioxidant defence in the *S.* Typhimurium infected macrophages

Our previous data suggested increased mitochondrial ROS-mediated mitochondrial oxidative stress in SIRT3 knockdown RAW264.7 macrophages in *S.* Typhimurium infected macrophages. The host mitochondrial antioxidant machinery tends to combat the oxidative stress caused by diverse insults (Chen, Zhou et al., 2018, Forman & Zhang, 2021). To evaluate the mitochondrial antioxidant arsenals in the infected macrophages, we carried out RT-qPCR mediated gene expression studies of several mitochondrial antioxidant genes such as *Gpx*, *Ho-1*, *Cat*, and *Sod2* upon knockdown of SIRT1 and SIRT3 in RAW264.7 macrophages and in peritoneal macrophages upon SIRT1 (EX-527) or SIRT3 (3TYP) inhibitor treatment. Both SIRT1 or SIRT3 knockdown and SIRT1 or SIRT3 inhibition treatments led to decreased transcript level expression of the mitochondrial antioxidant genes in the infected RAW264.7 and peritoneal macrophages (Fig. 3A-B). Subsequently, we evaluated the bacterial antioxidant gene expression status within the SIRT1 or SIRT3 knockdown macrophages. Our results depict decreased bacterial antioxidant gene expression (*sodA*, *sodB*, *katE*, *katG*) in shSIRT3 infected macrophages in comparison to the scrambled infected control. However, within shSIRT1 infected macrophages, the bacterial antioxidant gene expression showed heightened expression profiles when compared to the scrambled control. (Supplementary Fig. S3). In literature, SIRT3 has been reported to deacetylate SOD2 at two critical lysine residues K53 and K89 and promote its antioxidant activity(Qiu, Brown et al., 2010). Therefore, we checked the interaction of SOD2 with SIRT3 upon *S.* Typhimurium infection condition. Immunoprecipitation studies revealed interaction of SOD2 with SIRT3 upon infection. However, this interaction got dampened in SIRT3 knockdown, and SIRT3 inhibitor-treated infected RAW264.7 macrophages alongside SOD2 hyperacetylation (Fig. 3C-D). Further, we performed the SOD2 activity assay to evaluate the active SOD2 in infected RAW264.7 macrophages upon SIRT3

knockdown or inhibitor treated condition. The assay revealed reduced active SOD2 or MnSOD2 concentration in the *S*. Typhimurium infected RAW264.7 macrophages in both SIRT3 knockdown or inhibited condition (Fig. 3E-F). Together, our results highlight the role of SIRT1 and more predominantly SIRT3 in rendering protection against mitochondrial oxidative stress upon *Salmonella* infection by deacetylating SOD2 and thereby promoting its antioxidant properties.

SIRT1 or SIRT3 inhibition resulted in compromised ETC function and lowered ATP generation in the infected macrophages

SIRT3 has been shown to possess association with subunit of ATP synthase which is fundamental for the maintenance of healthy mitochondrial homeostasis(Yang, Nagasawa et al., 2016). Additionally, SIRT3 also regulates basal ATP levels in vivo (Ahn et al., 2008). Therefore, we asked whether inhibition or downregulation of SIRT3 in the macrophages leads to alteration in ATP production in the *Salmonella* infection scenario. *Salmonella* infected SIRT1 or SIRT3 knockdown murine RAW264.7 macrophages exhibited decreased ATP production in the later phases of infection at 16hr p.i. compared to the infected scrambled or un-transfected control (Fig. 4A). Moreover, previous data showed exacerbated production of mitochondrial ROS (mtROS) upon knockdown or inhibition of SIRT3 in *Salmonella* infected murine macrophages. Since both mtROS production and ATP synthesis are governed by mitochondrial ETC, we speculated whether SIRT1 and SIRT3 inhibition or knockdown leads to dysregulation of ETC function in the *Salmonella* infection scenario. We investigated the ETC function of the *S*. Typhimurium infected macrophages via qPCR mediated ETC Complex gene profiling under SIRT1 or SIRT3 knockdown condition. Knockdown of either SIRT1 or SIRT3 resulted in decreased expression of Complex I subunit genes (*NDUFV1*, *NDUFS1*, *NDUFA9*), Complex II (*SDHD)*, Complex III (*UQCR*), Complex IV (*COX5B*) and Complex V genes (*ATP5B*) in infected RAW 264.7 at 16hr p.i (Fig. 4B). Similar findings were obtained

from infected peritoneal macrophages upon SIRT1 or SIRT3 catalytic inhibitor treatment (Fig. 4C). Therefore, SIRT1 or SIRT3 knockdown as well as inhibition triggers mitochondrial ETC dysfunction in the infected macrophages which could result in enhanced mitochondrial ROS generation and reduced ATP production.

SIRT3 modulated the mitochondrial membrane potential of the infected macrophages

Mitochondrial function, ATP production and mtROS generation are also dependent on mitochondrial membrane potential. To investigate alteration in the mitochondrial membrane potential of the macrophages upon *S.* Typhimurium infection, we undertook Mito Tracker Red CMXRos staining and TMRM staining of the infected macrophages in SIRT1 or SIRT3 knockdown condition through flow cytometry. Mitotacker Red CMXRos stains the live mitochondria and their accumulation in the cell is dependent upon membrane potential (Totzke, Essmann et al., 2006). Tetramethylrhodamine Methyl Ester, Perchlorate (TMRM) is a cell-permeant fluorescent dye that assesses mitochondrial membrane potential (Chen, Cai et al., 2002). Upon SIRT3 knockdown of the infected macrophages, there is an increased staining of the mitochondria by Mito tracker Red CMXRos with respect to the scrambled control at 16hr p.i., which is suggestive of mitochondrial hyperpolarization (Fig. 5A). Further, TMRM staining of the infected RAW 264.7 macrophages revealed enhanced membrane potential under the knockdown condition of SIRT3 only at 16hr post-infection in comparison to the scrambled control (Fig. 5B). SIRT1 knockdown alone did not exert any significant alteration in the mitochondrial membrane potential within the infected macrophages (Fig. 5A-B). Mitochondrial hyperpolarization has been shown to be caused by Complex I inhibition which subsequently triggers reduced activity of Complex II, III, and IV and reduced forward action of Complex V(Forkink, Manjeri et al., 2014). Our data of mitochondrial hyperpolarization in *Salmonella* infected RAW264.7 macrophages also coincides with decreased expression of Complex I, II, III, IV and V (as shown earlier).

SIRT1 and SIRT3 inhibition led to altered mitochondrial respiration in *S.* Typhimurium infected macrophages

Since we had observed a reduction in ATP production upon inhibition of SIRT1 or SIRT3, we sought to determine mitochondrial bioenergetics under SIRT1 and SIRT3 inhibitor treatment in the infected peritoneal macrophages. Multiple parameters related to mitochondrial respiration were assessed through a stepwise introduction of pharmaceutical compounds into infected peritoneal macrophages treated with SIRT1 or SIRT3 inhibitor. In order to evaluate these parameters, we performed a modified Seahorse Mito stress test (Cumming et al., 2018) to assess the mitochondrial measurements of oxygen consumption rates (OCR) post 6hr of infection and inhibitor treatment in peritoneal macrophages over a 60 min interval (Fig. 6A). Initially, the baseline OCR of the cellular system was gauged, from which the basal respiration was determined by eliminating the non-mitochondrial respiration. Subsequently, the addition of an inhibitor targeting complex V (oligomycin) allowed for the computation of both ATP-linked OCR (by subtracting the post-oligomycin OCR from the baseline OCR) and the rate of proton leakage (OCR after oligomycin addition minus the nonmitochondrial respiration). Finally, the introduction of antimycin A, a complex III inhibitor, and rotenone, a complex I inhibitor, simultaneously hindered the function of ETC, thereby uncovering the rate of nonmitochondrial respiration. Simultaneously, the extracellular acidification rate (ECAR), which is proportional to the lactate efflux, was also measured and interpreted as an indicator of glycolytic flux in the macrophages. The results revealed an increase in basal respiration (Fig. 6B) , non-mitochondrial respiration (Fig.6C), proton leakage (Fig. 6D) and mitochondrial ATP-linked respiration (Fig. 6E) and an increase in ECAR in the infected peritoneal macrophages upon both SIRT1 (EX-527) and SIRT3 (3TYP) catalytic inhibitor treatment in comparison to the infected untreated control (Fig. 6F), thereby highlighting the function of SIRT1 and SIRT3 in the regulation of mitochondrial bioenergetics upon *Salmonella* infection

(Fig. 6A-F). The overall increase in mitochondrial respiratory flux and proton leakage could be a major cause of augmented mitochondrial ROS production and mitochondrial hyperpolarization (Amorim, Coppotelli et al., 2022) (as depicted earlier). Previous reports have indicated the incidence of enhanced respiration alongside decreased ATP production could be due to compensation by increased glycolysis (Hajra, Rajmani et al., 2022) or non-mitochondrial respiration (Yang, Darwish et al., 2021). Additionally, the enhanced respiration lead to increased superoxide generation, resulting in proton leakage across the inner mitochondrial membrane and decreased ATP synthesis (Amorim et al., 2022, BUTLER, JANSON et al., 2003).

pH homoeostasis within *S.* Typhimurium infected macrophages is mediated by SIRT3

Our earlier data showed mitochondrial bioenergetics defect with loss in ETC function along with increased mtROS generation, mitochondrial membrane hyperpolarization and lowered ATP production in STM infected macrophages upon SIRT3 or SIRT1 inhibition. Mitochondrial membrane potential alteration has the potential to influence cytosolic pH(Bonora, Giorgi et al., 2022, Poburko, Santo-Domingo et al., 2011) and therefore we examined the cytosolic pH of the infected RAW264.7 macrophages under the knockdown condition of SIRT1 and SIRT3 by BCECF-AM staining. The host cytosolic pH sensing is an important determinant of *Salmonella* intravacuolar life as it governs effector translocation (Yu, McGourty et al., 2010). BCECF-AM is a cell-permeant dye that is ideal for monitoring intracellular cytosolic pH alterations. It acts as a dual-excitation ratio metric pH indicator by measuring the pH-dependent ratio of emission intensity at 535nm when the dye is excited at 488nm versus the emission intensity upon excitation at 405nm. Knockdown of SIRT3 and not SIRT1 within *S.* Typhimurium infected RAW264.7 macrophages intensified the cytosolic acidity of the macrophages (pH~4.8) as indicated by the decreased fluorescence ratio of BCECF-AM (Fig.7A-B). Similar observations were obtained from the peritoneal macrophages

wherein SIRT3 enzymatic inhibitor treatment resulted in decreased fluorometric ratio of BCECF-AM, indicative of lowered intracellular pH (pH~4.43) (Fig.7B-C). Altogether, our findings suggest the role of SIRT3 in the maintenance of cytosolic pH by maintaining the mitochondrial membrane potential and bioenergetics.

SIRT3 triggered host cytosolic pH alterations influenced both intra-phagosomal and intra-*Salmonella* pH and its T3SS mediated virulence protein secretion

Previous reports suggested the prerequisite for host cytosol sensing by *Salmonella* to facilitate *Salmonella* Pathogenicity Island 2 (SPI-2) (Chakravortty, Rohde et al., 2005) encoded complex dissociation, degradation, and effector secretion(Yu et al., 2010). Therefore, we hypothesized whether the host cytosolic pH alteration by SIRT1 or SIRT3 knockdown or inhibition could impact the intra-phagosomal and intra-bacterial pH and in turn, SPI-2 effector secretion. Upon investigating the SCV pH within the pH rhodo labelled STM infected SIRT1 or SIRT3 RAW264.7 macrophages, we observed an increase in intra-vacuolar pH (pH~7.0) when compared to the scrambled control (pH~5.7 to 6.0) (Fig. 8A-C, Supplementary Fig. S4 A-C). Similarly, in SIRT1 or SIRT3 inhibitors treated RAW264.7 macrophages; a loss in intra-vacuolar or intra-phagosomal acidification (pH~7.0) was observed relative to the untreated control (pH~4.5 to 5.8) (Fig. 8D-F, Supplementary Fig. S4 D-F). Subsequently, we evaluated the intra-bacterial pH within the SIRT1 and SIRT3 knockdown macrophages by infecting the RAW264.7 macrophages with *S.* Typhimurium 14028S expressing pBAD-pHuji (Shen et al., 2014) (a plasmid encoding pH sensitive red fluorescent protein). The intra-*Salmonella* pH in the SIRT1 or SIRT3 knockdown macrophages exhibited loss in acidic pH with pH closer to neutrality (pH~7.2 to 7.6) in comparison to the scrambled control (pH~5.4) (Fig.8G). Similar results were obtained in inhibitor treated peritoneal macrophages wherein both SIRT1 and SIRT3 inhibitor treatment resulted in loss of acidification in the intra-bacterial pH (Fig.8H). Along with the host cytosolic pH, a major factor triggering the SPI-2 effector secretion is the

acidic pH of the bacterial cytosol which consequently causes OmpR activation, a known regulator of SPI-2(Chakraborty, Mizusaki et al., 2015). Inside the macrophages, the cadaverine operon *cadC/B* was repressed by OmpR and the *Salmonella* cytoplasm remained acidified. In *ompR* deficient *Salmonella*, the intracellular pH is returned to a near neutral in a CadC/BA-dependent manner. This activation of EnvZ/OmpR by acid stress stimulates the production of the SsrA/B, another two-component system, and subsequently, expression of SPI-2-secreted effectors(Chakraborty et al., 2015, Garmendia, Beuzón et al., 2003, Wang, Morgan et al., 2012). This phenomenon holds true in bacteria residing inside the SIRT1 and SIRT3 knockdown macrophages wherein the *S.* Typhimurium within the knockdown or inhibitor treated macrophages exhibit increased pH similar to that of *ompR* deficient *S.* Typhimurium strain and consequently exhibit increased expression of *cadA*, *cadB* and *cadC* together amounting to decreased SPI-2 gene expression such as *pipB2*, and *steE* (Fig.8I-M).

Inhibition of SIRT3 triggered mitophagy in the S. Typhimurium-infected macrophages by altering mitochondrial fusion-fission dynamics

Since our previous data suggested disruption of mitochondrial bioenergetics in the murine macrophages along the course *S.* Typhimurium infection in SIRT1 and SIRT3 knockdown condition, we sought to examine whether SIRT1 or SIRT3 knockdown also results in alteration in mitochondrial dynamics upon *S.* Typhimurium infection. We determined the occurrence of mitophagy in the infected macrophages in the knockdown condition of SIRT1 and SIRT3 via both immunoblotting and immunofluorescence studies. SIRT3 knockdown RAW 264.7 macrophages exhibited increased co-localization of mitochondria stained with Mito Tracker Red with LC3B upon *S.* Typhimurium infection at 6hr and 16 hr p.i. whereas SIRT1 knockdown resulted in heightened LC3B co-localization with Mitotracker Red at 6hr p.i. in immunofluorescence studies (Supplementary Fig. S5). We validated this result by assessing the mitophagic flux within the infected macrophages by using mito-eGFP-mCherry traffic light

construct. Upon induction of mitophagy, the lysosomal acidic pH results in degradation of eGFP triggering loss of eGFP fluorescence. We observed increased mitophagy induction in the SIRT1 and SIRT3 inhibitor treated infected RAW264.7 macrophages with loss of eGFP expression in comparison to the untreated control at 16hr post infection (Fig.9A-B). Immunoblotting studies revealed increased mitophagic initiation in the SIRT3 knockdown infected RAW264.7 macrophages as early as 2hr post infection in comparison to the scrambled control. In comparison to the scrambled control, the SIRT3 knockdown infected macrophages showed reduced levels of mitochondrial outer membrane protein TOM20 and displayed elevated LC3B II protein levels (Fig. 9C-D). Similarly, SIRT3 knockdown RAW 264.7 macrophages exhibited increased co-localization of mitochondria stained with Mito Tracker Red with LC3B upon *S.* Typhimurium infection at 2hr p.i. in immunofluorescence studies (Supplementary Fig. S6). Altogether, our data depicts increased mitophagy influx upon knockdown of SIRT3 in the *Salmonella* infected murine macrophages.

Since we observed an increased mitophagy induction upon SIRT3 knockdown condition in infected murine macrophages, we hypothesized whether increased mitophagy coincides with increased incidences of mitochondrial fission. Therefore, we assessed the mitochondrial fission and fusion genes via qPCR in the infected SIRT1 or SIRT3 knockdown RAW264.7 macrophages or infected peritoneal macrophages under the chemical inhibitor treatment of either SIRT1 (EX-527) or SIRT3 (3TYP). We observed an increased transcript level expression of several mitochondrial fission genes such as *Drp1*, *Fis1*, *Mid49* and *Mid51* with concomitant decline in mitochondrial fusion genes such as *Mff*, *Mfn2*, and *Opa1* in the infected murine macrophages and in the infected SIRT1 or SIRT3 knockdown (Fig. 9 E-F) or inhibitor treated macrophages (Supplementary Fig.S7) with SIRT3 inhibitor treatment rendering more prominent effect. Previous studies have shown the role of SIRT3 in deacetylating OPA-1 and thereby causing activation of OPA-1 in cardiac tissues (Samant, Zhang et al., 2014). In line

with this observation, we have evaluated the interaction of SIRT3 with OPA-1 in infected RAW 264.7 macrophages and have observed an enhanced interaction of OPA-1 with SIRT3 in the infected macrophages in comparison to the uninfected control (Fig. 9 G) .However upon knockdown of SIRT3 or with catalytic inhibitor treatment of SIRT3, 3TYP, we observed a similar decline in OPA-1 protein interaction with SIRT3 upon pulldown of OPA-1 with corresponding increase in the acetylation of OPA-1at 16hr p.i. in the infected RAW264.7 macrophages thereby suggesting the role of SIRT3 in the activation of OPA-1 (Fig.9 H-J). Therefore, our study reveals the role of SIRT3 in controlling the mitochondrial fusion dynamics in *Salmonella* infected macrophages.

DISCUSSION

Mitochondrial health is one of the vital determinant in governing the outcome of infection (Ramond, Jamet et al., 2019). For instance, the Gram-positive *L. monocytogenes*, induces transient mitochondrial fragmentation by utilizing its secreted effector protein listeriolysin O, LLO to gain a survival advantage(Stavru et al., 2011). *Shigella flexneri* also adopt a similar mechanism wherein it induces mitochondrial fission at 3.5h post infection (Lum & Morona, 2014). It also depletes the cellular ATP pool by causing dissipation of the mitochondrial membrane potential(Carneiro, Travassos et al., 2009, Koterski, Nahvi et al., 2005). Similarly, the intracellular pathogen *Legionella pneumophila* triggers mitochondrial fragmentation via its type IV secretion system effector MitF which coincides with increased cellular glycolysis and reduced mitochondrial respiration leading to decreased ATP production(Escoll et al., 2017). On the other hand, *Chlamydia trachomatis* preserves the mitochondrial framework to maintain the mitochondrial ATP production capacity by preventing Drp-1 mediated mitochondrial fission(Chowdhury et al., 2017). On the contrary, *C. pneumoniae* causes mitochondrial dysfunction by inducing mitochondrial hyperpolarization, increased ROS production and induction of host metabolic shift to glycolysis(Käding, Kaufhold et al., 2017).

In our study, we observed how *S.* Typhimurium infection in murine macrophages governed the alteration in mitochondrial fusion-fission dynamics and bioenergetics by modulation of SIRT1 and SIRT3 and how it eventually impacts the progression of infection and its intravacuolar niche. We have shown that inhibition of SIRT3 function leads to increased production of mitochondrial superoxide generation and decline in mitochondrial antioxidant SOD2 activity in the infected macrophages. The increased mitochondrial ROS generation in the infected macrophages coincides with mitochondrial membrane hyperpolarization, increased proton leak and respiration rate and decline in ATP production and ETC function. However, mitochondrial ROS production and membrane hyperpolarization remained unperturbed by inhibition of SIRT1, implicating the predominant role of the mitochondrial Sirtuin, SIRT3 in the regulation of mitochondrial energy homeostasis and oxidative stress (Ahn et al., 2008, Jing et al., 2011). This data is in agreement with the recent publication on *Mycobacterium tuberculosis* infection wherein SIRT3 deficiency led to increased accumulation of dysfunctional mitochondria with heightened oxidative stress (Kim et al., 2019). Nevertheless, both SIRT1 and SIRT3 deficiency led to decrease in antioxidant host gene transcript expression. This could be owing to the role of overlapping role of both SIRT1 and SIRT3 in activation of the antioxidant defense via the Nrf2 pathway (Kim, Koo et al., 2022, Yang, Song et al., 2020, Yao, Chen et al., 2023). The mitostress profile suggested overall increase in respiration parameters such as basal respiration, non-mitochondrial respiration, proton leakage and ATP-linked respiration along with increase in Extracellular Acidification Rate (ECAR) upon both SIRT1 and SIRT3 inhibitor treatment. The increased respiratory flux and proton leak gets dissipated in the production of mitochondrial ROS generation leading to decreased ATP content and increased ECAR upon SIRT1 and SIRT3 inhibitor treatment in *S.* Typhimurium infected macrophages. Proton leak and electron slip are the two critical mechanisms contributing to incomplete coupling of ATP generation and substrate oxygen resulting in disproportionate increase in oxygen consumption

rate at high protonmotive force and mitochondrial membrane potential with lower ATP yield (Cheng, Nanayakkara et al., 2017, Kadenbach, 2003, Murphy, 1989).

An important underlying question is how these alterations in the mitochondrial energetics impact the intracellular life of the *Salmonella* within the infected macrophages. Our data indicates that the mitochondrial bioenergetic alteration triggers increased acidification of the macrophage cytosolic pH. This alteration in turn skewed the intra-phagosomal and intra-bacterial pH of the intracellular bacteria within the SIRT1 and SIRT3 knockdown and inhibitor treated macrophages. The host cytosolic pH sensing (Yu et al., 2010) and the intra-bacterial pH (Chakraborty et al., 2015) regulate the T3SS machinery and its secretion. Here, we show that loss or inhibition of SIRT1 or SIRT3 trigger increased acidification of the macrophage cytosol which consequently lead to loss in intra-bacterial acidification together resulting in decreased SPI-2 gene expression and attenuated intracellular bacterial proliferation.

Numerous evidences suggest how different pathogen assaults lead to remodeling of the mitochondria that eventually dictates the fate of the war between the host and the pathogen (Carvalho, Spier et al., 2020, Cervantes-Silva, Cox et al., 2021, Chen, Lin et al., 2021, Shi, Jiang et al., 2019, Suzuki, Danilchanka et al., 2014). Our work highlights the increased occurrence of mitochondrial fusion dynamics upon *S.* Typhimurium infection via SIRT3 mediated deacetylation of OPA-1. This observation is in similar line with *Chlamydia trachomatis* infection studies wherein the infection induces mitochondrial elongation at the early stages and the abrogation of the fusion dynamics led to attenuated chlamydial proliferation(Kurihara et al., 2019). In our study, the *S.* Typhimurium infected macrophages depicted alteration in mitochondrial dynamics with increased mitophagy and decreased mitochondrial fusion dynamics under SIRT3 silenced or inhibited condition. The induction of mitophagy during infection holds a controversial status regarding the outcome of infection battle. In certain instances, like in the case of *Pseudomonas aeruginosa* (Kirienko, Ausubel et

al., 2015), *Vibrio splendidus* (Sun, Shao et al., 2022) or *Mycobacterium tuberculosis* (Lee, Kang et al., 2020) infection, the host promote mitophagic induction to initiate pathogen clearance. Contrastingly, pathogens like *Listeria monocytogenes* (Zhang, Yao et al., 2019), *Yersinia pestis* (Jiao, Cao et al., 2022), *Brucella abortus* (Verbeke, Fayt et al., 2023) and *Helicobacter pylori* (Jain et al., 2011) (Verbeke, De Bolle et al., 2023) induce mitophagy within their infected host to promote survival, persistence, or dissemination.

In summary, our results suggest the role of SIRT1 and predominantly, SIRT3 in governing the intracellular niche of *Salmonella* by the regulation of the mitochondrial energetics, mitochondrial fusion-fission remodeling and host-bacterial intracellular pH balance during *S.* Typhimurium infection. In addition, our work adds to the existing knowledge of host-pathogen crosstalk in the regulation of infection progression and opens up future avenues for *Salmonella* infection control.

AUTHOR CONTRIBUTION

DH and DC have conceptualized the study. DH has contributed to the experiment designing, visualization, methodology, investigation, formal analysis, literature survey, validation, writing (original draft), reviewing and editing of the manuscript. VY has performed the Seahorse mitostress test. AS supervised and provided valuable inputs for the mitochondrial stress test experiments. DC has contributed to the funding acquisition, project administration, and overall supervision of the work. All authors approved the final version of the manuscript.

DECLARATION OF INTEREST

The authors are unaware of any conflicting interests and thereby declare no conflict of interest.

ACKNOWLEDGEMENT

This work was supported by the DAE SRC fellowship (DAE00195) and DBT-IISc partnership umbrella program for advanced research in biological sciences and Bioengineering to DC. Infrastructure support from ICMR (Centre for Advanced Study in Molecular Medicine), DST (FIST), and UGC (special assistance) is highly acknowledged. AS acknowledges funding from India Alliance grant IIA/S/16/2/502700), DBT grants (BT/PR13522/COE/34/27/2015, BT/PR29098/Med/29/1324/2018), DST-SERB grant (SPR/2021/000175), Crypto Relief grant (ODAA/INT/20-21), and the Revati and Satya Nadham Atturi Chair Professorship. DH sincerely acknowledges the CSIR- SPM fellowship for her financial support. The funders had no role in study design, data collection and analysis, decision to publish, or preparation of the manuscript.

REFERENCES

Ahn BH, Kim HS, Song S, Lee IH, Liu J, Vassilopoulos A, Deng CX, Finkel T (2008) A role for the mitochondrial deacetylase Sirt3 in regulating energy homeostasis. Proceedings of the National Academy of Sciences of the United States of America 105: 14447-52

Amorim JA, Coppotelli G, Rolo AP, Palmeira CM, Ross JM, Sinclair DA (2022) Mitochondrial and metabolic dysfunction in ageing and age-related diseases. Nature Reviews Endocrinology 18: 243-258

Bonora M, Giorgi C, Pinton P (2022) Molecular mechanisms and consequences of mitochondrial permeability transition. Nature reviews Molecular cell biology 23: 266-285

BUTLER A, JANSON J, BONNER-WEIR S, RITZEL R, RIZZA R, BUTLER P (2003) β-Cell deficit and increased β-cell apoptosis in humans with type 2 diabetes.(ON LINE) Diabetes 52: 102-110. In

Carneiro LAM, Travassos LH, Soares F, Tattoli I, Magalhaes JG, Bozza MT, Plotkowski MC, Sansonetti PJ, Molkentin JD, Philpott DJ, Girardin SE (2009) Shigella Induces Mitochondrial Dysfunction and Cell Death in Nonmyleoid Cells. Cell host & microbe 5: 123-136

Carvalho F, Spier A, Chaze T, Matondo M, Cossart P, Stavru F (2020) Listeria monocytogenes Exploits Mitochondrial Contact Site and Cristae Organizing System Complex Subunit Mic10 To Promote Mitochondrial Fragmentation and Cellular Infection. mBio 11

Cervantes-Silva MP, Cox SL, Curtis AM (2021) Alterations in mitochondrial morphology as a key driver of immunity and host defence. EMBO reports 22: e53086

Chakraborty S, Mizusaki H, Kenney LJ (2015) A FRET-based DNA biosensor tracks OmpR-dependent acidification of Salmonella during macrophage infection. PLoS biology 13: e1002116

Chakravortty D, Rohde M, Jäger L, Deiwick J, Hensel M (2005) Formation of a novel surface structure encoded by Salmonella Pathogenicity Island 2. The EMBO journal 24: 2043-52

Chen LT, Lin CT, Lin LY, Hsu JM, Wu YC, Pan CL (2021) Neuronal mitochondrial dynamics coordinate systemic mitochondrial morphology and stress response to confer pathogen resistance in C. elegans. Developmental cell 56: 1770-1785.e12

Chen Y, Cai J, Murphy TJ, Jones DP (2002) Overexpressed human mitochondrial thioredoxin confers resistance to oxidant-induced apoptosis in human osteosarcoma cells. The Journal of biological chemistry 277: 33242-8

Chen Y, Zhou Z, Min W (2018) Mitochondria, Oxidative Stress and Innate Immunity. Frontiers in physiology 9: 1487

Cheng J, Nanayakkara G, Shao Y, Cueto R, Wang L, Yang WY, Tian Y, Wang H, Yang X (2017) Mitochondrial Proton Leak Plays a Critical Role in Pathogenesis of Cardiovascular Diseases. Advances in experimental medicine and biology 982: 359-370

Chowdhury SR, Reimer A, Sharan M, Kozjak-Pavlovic V, Eulalio A, Prusty BK, Fraunholz M, Karunakaran K, Rudel T (2017) Chlamydia preserves the mitochondrial network necessary for replication via microRNA-dependent inhibition of fission. J Cell Biol 216: 1071-1089

Cumming BM, Addicott KW, Adamson JH, Steyn AJC (2018) Mycobacterium tuberculosis induces decelerated bioenergetic metabolism in human macrophages. eLife 7: e39169

Czyż DM, Willett JW, Crosson S (2017) Brucella abortus Induces a Warburg Shift in Host Metabolism That Is Linked to Enhanced Intracellular Survival of the Pathogen. J Bacteriol 199

Di Trani L, Savarino A, Campitelli L, Norelli S, Puzelli S, D'Ostilio D, Vignolo E, Donatelli I, Cassone A (2007) Different pH requirements are associated with divergent inhibitory effects of chloroquine on human and avian influenza A viruses. Virology journal 4: 39

Escoll P, Song OR, Viana F, Steiner B, Lagache T, Olivo-Marin JC, Impens F, Brodin P, Hilbi H, Buchrieser C (2017) Legionella pneumophila Modulates Mitochondrial Dynamics to Trigger Metabolic Repurposing of Infected Macrophages. Cell host & microbe 22: 302-316.e7

Forkink M, Manjeri GR, Liemburg-Apers DC, Nibbeling E, Blanchard M, Wojtala A, Smeitink JAM, Wieckowski MR, Willems PHGM, Koopman WJH (2014) Mitochondrial hyperpolarization during chronic complex I inhibition is sustained by low activity of complex II, III, IV and V. Biochimica et Biophysica Acta (BBA) - Bioenergetics 1837: 1247-1256

Forman HJ, Zhang H (2021) Targeting oxidative stress in disease: promise and limitations of antioxidant therapy. Nature Reviews Drug Discovery 20: 689-709

Garmendia J, Beuzón CR, Ruiz-Albert J, Holden DW (2003) The roles of SsrA-SsrB and OmpR-EnvZ in the regulation of genes encoding the Salmonella typhimurium SPI-2 type III secretion system. Microbiology (Reading, England) 149: 2385-2396

Gogoi M, Ravikumar V, Dixit NM, Chakravortty D (2018) Salmonella escapes antigen presentation through K63 ubiquitination mediated endosomal proteolysis of MHC II via modulation of endosomal acidification in dendritic cells. Pathogens and disease 76

Hajra D, Nair AV, Chakravortty D (2021) An elegant nano-injection machinery for sabotaging the host: Role of Type III secretion system in virulence of different human and animal pathogenic bacteria. Physics of life reviews 38: 25-54

Hajra D, Rajmani RS, Chakravortty D (2022) SIRT1 and SIRT3 mediated immuno-metabolic switch govern Salmonella survival within infected macrophages both in vitro and <em>in vivo</em&gt. bioRxiv: 2022.11.21.517246

Hallows WC, Yu W, Smith BC, Devries MK, Ellinger JJ, Someya S, Shortreed MR, Prolla T, Markley JL, Smith LM, Zhao S, Guan KL, Denu JM (2011) Sirt3 promotes the urea cycle and fatty acid oxidation during dietary restriction. Molecular cell 41: 139-49

Han YH, Kim SH, Kim SZ, Park WH (2008) Antimycin A as a mitochondrial electron transport inhibitor prevents the growth of human lung cancer A549 cells. Oncology reports 20: 689-93

Haraga A, Ohlson MB, Miller SI (2008) Salmonellae interplay with host cells. Nat Rev Microbiol 6: 53-66

Hirschey MD, Shimazu T, Goetzman E, Jing E, Schwer B, Lombard DB, Grueter CA, Harris C, Biddinger S, Ilkayeva OR, Stevens RD, Li Y, Saha AK, Ruderman NB, Bain JR, Newgard CB, Farese RV, Jr., Alt FW, Kahn CR, Verdin E (2010) SIRT3 regulates mitochondrial fatty-acid oxidation by reversible enzyme deacetylation. Nature 464: 121-5

Hu B, Wang P, Zhang S, Liu W, Lv X, Shi D, Zhao L, Liu H, Wang B, Chen S, Shao Z (2022) HSP70 attenuates compression-induced apoptosis of nucleus pulposus cells by suppressing mitochondrial fission via upregulating the expression of SIRT3. Experimental & molecular medicine 54: 309-323

728 Jain P, Luo ZQ, Blanke SR (2011) Helicobacter pylori vacuolating cytotoxin A (VacA) engages the
729 mitochondrial fission machinery to induce host cell death. Proceedings of the National Academy of
730 Sciences of the United States of America 108: 16032-7
731 Jiao Y, Cao S, Zhang Y, Tan Y, Zhou Y, Wang T, You Y, Chen H, Ren Y, Yang R, Du Z (2022) Yersinia
732 pestis-Induced Mitophagy That Balances Mitochondrial Homeostasis and mROS-Mediated
733 Bactericidal Activity. Microbiology spectrum 10: e0071822
734 Jing E, Emanuelli B, Hirschey MD, Boucher J, Lee KY, Lombard D, Verdin EM, Kahn CR (2011) Sirtuin-3
735 (Sirt3) regulates skeletal muscle metabolism and insulin signaling via altered mitochondrial oxidation
736 and reactive oxygen species production. Proceedings of the National Academy of Sciences of the
737 United States of America 108: 14608-13
738 Kadenbach B (2003) Intrinsic and extrinsic uncoupling of oxidative phosphorylation. Biochimica et
739 biophysica acta 1604: 77-94
740 Käding N, Kaufhold I, Müller C, Szaszák M, Shima K, Weinmaier T, Lomas R, Conesa A, Schmitt-
741 Kopplin P, Rattei T, Rupp J (2017) Growth of Chlamydia pneumoniae Is Enhanced in Cells with
742 Impaired Mitochondrial Function. Front Cell Infect Microbiol 7: 499
743 Kim A, Koo JH, Lee JM, Joo MS, Kim TH, Kim H, Jun DW, Kim SG (2022) NRF2-mediated SIRT3
744 induction protects hepatocytes from ER stress-induced liver injury. FASEB journal : official
745 publication of the Federation of American Societies for Experimental Biology 36: e22170
746 Kim TS, Jin YB, Kim YS, Kim S, Kim JK, Lee HM, Suh HW, Choe JH, Kim YJ, Koo BS, Kim HN, Jung M, Lee
747 SH, Kim DK, Chung C, Son JW, Min JJ, Kim JM, Deng CX, Kim HS et al. (2019) SIRT3 promotes
748 antimycobacterial defenses by coordinating mitochondrial and autophagic functions. Autophagy 15:
749 1356-1375
750 Kirienko NV, Ausubel FM, Ruvkun G (2015) Mitophagy confers resistance to siderophore-mediated
751 killing by Pseudomonas aeruginosa. Proceedings of the National Academy of Sciences of the United
752 States of America 112: 1821-6
753 Knodler LA, Elfenbein JR (2019) Salmonella enterica. Trends in microbiology 27: 964-965
754 Koterski JF, Nahvi M, Venkatesan MM, Haimovich B (2005) Virulent Shigella flexneri causes damage
755 to mitochondria and triggers necrosis in infected human monocyte-derived macrophages. Infection
756 and immunity 73: 504-13
757 Kurihara Y, Itoh R, Shimizu A, Walenna NF, Chou B, Ishii K, Soejima T, Fujikane A, Hiromatsu K (2019)
758 Chlamydia trachomatis targets mitochondrial dynamics to promote intracellular survival and
759 proliferation. Cellular microbiology 21: e12962
760 Lee HJ, Kang SJ, Woo Y, Hahn TW, Ko HJ, Jung YJ (2020) TLR7 Stimulation With Imiquimod Induces
761 Selective Autophagy and Controls Mycobacterium tuberculosis Growth in Mouse Macrophages.
762 Frontiers in microbiology 11: 1684
763 Li P, Meng X, Bian H, Burns N, Zhao KS, Song R (2015) Activation of sirtuin 1/3 improves vascular
764 hyporeactivity in severe hemorrhagic shock by alleviation of mitochondrial damage. Oncotarget 6:
765 36998-7011
766 Lum M, Morona R (2014) Dynamin-related protein Drp1 and mitochondria are important for Shigella
767 flexneri infection. International journal of medical microbiology : IJMM 304: 530-41
768 Menzies KJ, Hood DA (2012) The role of SirT1 in muscle mitochondrial turnover. Mitochondrion 12:
769 5-13
770 Morató L, Astori S, Zalachoras I, Rodrigues J, Ghosal S, Huang W, Guillot de Suduiraut I, Grosse J,
771 Zanoletti O, Cao L, Auwerx J, Sandi C (2022) eNAMPT actions through nucleus accumbens
772 NAD(+)/SIRT1 link increased adiposity with sociability deficits programmed by peripuberty stress.
773 Science advances 8: eabj9109
774 Murphy MP (1989) Slip and leak in mitochondrial oxidative phosphorylation. Biochimica et
775 biophysica acta 977: 123-41
776 Nemoto S, Fergusson MM, Finkel T (2005) SIRT1 Functionally Interacts with the Metabolic Regulator
777 and Transcriptional Coactivator PGC-1α*. Journal of Biological Chemistry 280: 16456-16460

Park WH, Han YW, Kim SH, Kim SZ (2007) An ROS generator, antimycin A, inhibits the growth of HeLa cells via apoptosis. Journal of cellular biochemistry 102: 98-109

Poburko D, Santo-Domingo J, Demaurex N (2011) Dynamic regulation of the mitochondrial proton gradient during cytosolic calcium elevations. The Journal of biological chemistry 286: 11672-84

Powell RD, Swet JH, Kennedy KL, Huynh TT, McKillop IH, Evans SL (2014) Resveratrol attenuates hypoxic injury in a primary hepatocyte model of hemorrhagic shock and resuscitation. The journal of trauma and acute care surgery 76: 409-17

Qiu X, Brown K, Hirschey MD, Verdin E, Chen D (2010) Calorie Restriction Reduces Oxidative Stress by SIRT3-Mediated SOD2 Activation. Cell Metabolism 12: 662-667

Ramond E, Jamet A, Coureuil M, Charbit A (2019) Pivotal Role of Mitochondria in Macrophage Response to Bacterial Pathogens. Frontiers in immunology 10

Roy Chowdhury A, Sah S, Varshney U, Chakravortty D (2022) Salmonella Typhimurium outer membrane protein A (OmpA) renders protection from nitrosative stress of macrophages by maintaining the stability of bacterial outer membrane. PLoS pathogens 18: e1010708

Samant SA, Zhang HJ, Hong Z, Pillai VB, Sundaresan NR, Wolfgeher D, Archer SL, Chan DC, Gupta MP (2014) SIRT3 deacetylates and activates OPA1 to regulate mitochondrial dynamics during stress. Molecular and cellular biology 34: 807-819

Shchepina LA, Pletjushkina OY, Avetisyan AV, Bakeeva LE, Fetisova EK, Izyumov DS, Saprunova VB, Vyssokikh MY, Chernyak BV, Skulachev VP (2002) Oligomycin, inhibitor of the F0 part of H+-ATP-synthase, suppresses the TNF-induced apoptosis. Oncogene 21: 8149-57

Shen Y, Rosendale M, Campbell RE, Perrais D (2014) pHuji, a pH-sensitive red fluorescent protein for imaging of exo- and endocytosis. The Journal of cell biology 207: 419-32

Shi L, Jiang Q, Bushkin Y, Subbian S, Tyagi S (2019) Biphasic Dynamics of Macrophage Immunometabolism during Mycobacterium tuberculosis Infection. mBio 10

Shi L, Salamon H, Eugenin EA, Pine R, Cooper A, Gennaro ML (2015) Infection with Mycobacterium tuberculosis induces the Warburg effect in mouse lungs. Sci Rep 5: 18176

Siegl C, Prusty BK, Karunakaran K, Wischhusen J, Rudel T (2014) Tumor suppressor p53 alters host cell metabolism to limit Chlamydia trachomatis infection. Cell reports 9: 918-29

Smulan LJ, Martinez N, Kiritsy MC, Kativhu C, Cavallo K, Sassetti CM, Singhal A, Remold HG, Kornfeld H (2021) Sirtuin 3 Downregulation in Mycobacterium tuberculosis-Infected Macrophages Reprograms Mitochondrial Metabolism and Promotes Cell Death. mBio 12

Stavru F, Bouillaud F, Sartori A, Ricquier D, Cossart P (2011) Listeria monocytogenes transiently alters mitochondrial dynamics during infection. Proc Natl Acad Sci U S A 108: 3612-7

Sun LL, Shao YN, You MX, Li CH (2022) ROS-mediated BNIP3-dependent mitophagy promotes coelomocyte survival in Apostichopus japonicus in response to Vibrio splendidus infection. Zoological research 43: 285-300

Sundaresan NR, Gupta M, Kim G, Rajamohan SB, Isbatan A, Gupta MP (2009) Sirt3 blocks the cardiac hypertrophic response by augmenting Foxo3a-dependent antioxidant defense mechanisms in mice. The Journal of clinical investigation 119: 2758-71

Suzuki M, Danilchanka O, Mekalanos JJ (2014) Vibrio cholerae T3SS effector VopE modulates mitochondrial dynamics and innate immune signaling by targeting Miro GTPases. Cell host & microbe 16: 581-91

Tiku V, Tan MW, Dikic I (2020) Mitochondrial Functions in Infection and Immunity. Trends in cell biology 30: 263-275

Totzke G, Essmann F, Pohlmann S, Lindenblatt C, Jänicke RU, Schulze-Osthoff K (2006) A novel member of the IkappaB family, human IkappaB-zeta, inhibits transactivation of p65 and its DNA binding. The Journal of biological chemistry 281: 12645-54

Verbeke J, De Bolle X, Arnould T (2023) To eat or not to eat mitochondria? How do host cells cope with mitophagy upon bacterial infection? PLoS pathogens 19: e1011471

Verbeke J, Fayt Y, Martin L, Yilmaz O, Sedzicki J, Reboul A, Jadot M, Renard P, Dehio C, Renard HF, Letesson JJ, De Bolle X, Arnould T (2023) Host cell egress of Brucella abortus requires BNIP3L-mediated mitophagy. The EMBO journal 42: e112817

Wang LC, Morgan LK, Godakumbura P, Kenney LJ, Anand GS (2012) The inner membrane histidine kinase EnvZ senses osmolality via helix-coil transitions in the cytoplasm. The EMBO journal 31: 2648-59

Wu Z, Puigserver P, Andersson U, Zhang C, Adelmant G, Mootha V, Troy A, Cinti S, Lowell B, Scarpulla RC, Spiegelman BM (1999) Mechanisms Controlling Mitochondrial Biogenesis and Respiration through the Thermogenic Coactivator PGC-1. Cell 98: 115-124

Yang M, Darwish T, Larraufie P, Rimmington D, Cimino I, Goldspink DA, Jenkins B, Koulman A, Brighton CA, Ma M, Lam BYH, Coll AP, O'Rahilly S, Reimann F, Gribble FM (2021) Inhibition of mitochondrial function by metformin increases glucose uptake, glycolysis and GDF-15 release from intestinal cells. Scientific Reports 11: 2529

Yang R, Song C, Chen J, Zhou L, Jiang X, Cao X, Sun Y, Zhang Q (2020) Limonin ameliorates acetaminophen-induced hepatotoxicity by activating Nrf2 antioxidative pathway and inhibiting NF-κB inflammatory response via upregulating Sirt1. Phytomedicine : international journal of phytotherapy and phytopharmacology 69: 153211

Yang W, Nagasawa K, Münch C, Xu Y, Satterstrom K, Jeong S, Hayes SD, Jedrychowski MP, Vyas FS, Zaganjor E, Guarani V, Ringel AE, Gygi SP, Harper JW, Haigis MC (2016) Mitochondrial Sirtuin Network Reveals Dynamic SIRT3-Dependent Deacetylation in Response to Membrane Depolarization. Cell 167: 985-1000.e21

Yao Y, Chen T, Wu H, Yang N, Xu S (2023) Melatonin attenuates bisphenol A-induced colon injury by dual targeting mitochondrial dynamics and Nrf2 antioxidant system via activation of SIRT1/PGC-1α signaling pathway. Free radical biology & medicine 195: 13-22

Yu XJ, McGourty K, Liu M, Unsworth KE, Holden DW (2010) pH sensing by intracellular Salmonella induces effector translocation. Science (New York, NY) 328: 1040-3

Zhang Y, Yao Y, Qiu X, Wang G, Hu Z, Chen S, Wu Z, Yuan N, Gao H, Wang J (2019) Listeria hijacks host mitophagy through a novel mitophagy receptor to evade killing. Nature immunology 20: 433-446

Zhou W, Faraldo-Gómez JD (2018) Membrane plasticity facilitates recognition of the inhibitor oligomycin by the mitochondrial ATP synthase rotor. Biochimica et biophysica acta Bioenergetics 1859: 789-796

MAIN FIGURE LEGENDS

Fig.1- SIRT3 inhibition leads to enhanced mitochondrial ROS generation in infected macrophages.

A-Mitochondrial ROS estimation via flow cytometry in *S.* Typhimurium infected RAW264.7 macrophages at 16hr post infection under SIRT1 or SIRT3 knockdown condition. Data is representative of N=4, n=2. 10µM antimycin A-treated (ROS inducer) uninfected and infected cells served as positive control. Unpaired two-tailed Student's t test was performed to obtain the p values. *** $p < 0.001$, ** $p<0.01$, * $p<0.05$

B-Mitochondrial ROS estimation via flow cytometry in *S.* Typhimurium infected peritoneal macrophages (isolated post 5th day of thioglycolate injection) at 16hr post infection in presence of SIRT1 (EX-527,1µM) or SIRT3 (3TYP, 1µM) inhibitor treatment. Data is representative of N=3, n=2. Unpaired two-tailed Student's t test was performed to obtain the p values. *** p < 0.001, ** p<0.01, * p<0.05

C-Representative confocal images of SIRT3 knockdown RAW264.7 macrophages exhibiting Mean Fluorescence Intensity (MFI) of mitoSox Red detecting mitochondrial ROS upon *S.* Typhimurium infection at indicated time points post infection. Data is representative of N=3, n>50 (microscopic field). Unpaired two-tailed Student's t test was performed to obtain the p values. *** p < 0.001, ** p<0.01, * p<0.05

D- Representative confocal images of SIRT3 knockdown RAW264.7 macrophages exhibiting co-localization coefficient of mitoSox Red detecting mitochondrial ROS with mitochondria (mitoBFP) upon *S.* Typhimurium infection at indicated time points post infection. Data is representative of N=3, n>50 (microscopic field). Unpaired two-tailed Student's t test was performed to obtain the p values. *** p < 0.001, ** p<0.01, * p<0.05

Fig.2- Increased mtROS production attenuates intracellular proliferation of *Salmonella* Typhimurium within SIRT3 knockdown macrophages and alleviation of the mtROS with mitoTEMPO restores the intracellular replication of the pathogen.

A- Intracellular proliferation assay of *S*. Typhimurium within scrambled control or SIRT3 knockdown macrophages in presence or absence of mitoTEMPO treatment. Data is representative of N=3, n=2. Unpaired two-tailed Student's t test was performed to obtain the p values. *** p < 0.001, ** p<0.01, * p<0.05

Fig.3 Effect of SIRT1 or SIRT3 inhibition on host mitochondrial antioxidant defense in *Salmonella* Typhimurium infection scenario.

A-Quantitative gene expression studies of several host mitochondrial antioxidant genes such as *Gpx*, *Sod2*, *Cat*, and *Ho-1* in RAW264.7 macrophages upon knockdown of SIRT1 and SIRT3 in *S.* Typhimurium infection scenario. Data is representative of N=3, n=2. Unpaired two-tailed Student's t test was performed to obtain the p values. *** p < 0.001, ** p<0.01, * p<0.05

B-Quantitative gene expression studies of several host mitochondrial antioxidant genes such as *Gpx*, *Sod2*, *Cat*, and *Ho-1* in peritoneal macrophages (isolated from 6–8-week-old adult male mice post 5th day of thioglycolate injection) after 16h of *S.* Typhimurium infection upon SIRT1 (EX-527,1µM) or SIRT3 (3TYP, 1µM) inhibitor treatment. Data is representative of N=3, n=2. Unpaired two-tailed Student's t test was performed to obtain the p values. *** p < 0.001, ** p<0.01, * p<0.05

C- Immunoprecipitation studies depicting SOD2 interaction with SIRT3 upon immunoprecipitation of SOD2 in uninfected (UI) or *S.* Typhimurium (STM) infected SIRT3 knockdown RAW264.7 macrophages at 16hr post-infection . Data is representative of N=2, n=1. *** p < 0.001, ** p<0.01, * p<0.05

D- Immunoprecipitation studies depicting SOD2 interaction with SIRT3 upon immunoprecipitation of SOD2 in uninfected (UI) or *S.* Typhimurium (STM) infected RAW264.7 macrophages at 16hr post-infection upon inhibitor treatment of SIRT3 . Data is representative of N=2, n=1. *** p < 0.001, ** p<0.01, * p<0.05

E- Mitochondrial SOD2 activity assay in uninfected and *S*. Typhimurium infected RAW264.7 macrophages in the knockdown condition of SIRT3. Data is representative of N=2, n=2. Unpaired two-tailed Student's t test was performed to obtain the p values. *** p < 0.001, ** p<0.01, * p<0.05

F- Mitochondrial SOD2 activity assay in uninfected and *S*. Typhimurium infected RAW264.7 macrophages upon SIRT3 inhibitor treatment. Data is representative of N=2, n=2. Unpaired two-tailed Student's t test was performed to obtain the p values. *** p < 0.001, ** p<0.01, * p<0.05

Fig.4 Inhibition of SIRT1 or SIRT3 leads to disruption of mitochondrial bioenergetics in *S*. Typhimurium-infected macrophages.

A-ATP estimation assay in SIRT1 or SIRT3 knockdown RAW264.7 macrophages in the presence or absence of *S*. Typhimurium infection at specified time points post-infection. Data is representative of N=3, n=2. 10µM oligomycin-treated (ATP synthase inhibitor) uninfected and infected cells served as negative control. Unpaired two-tailed Student's t test was performed to obtain the p values. *** p < 0.001, ** p<0.01, * p<0.05

B-qRTPCR mediated expression analysis of several Complex I, Complex II, Complex III, Complex IV, and Complex V genes of the Electron Transport Chain in *S*. Typhimurium infected RAW264.7 macrophages at 16hr post infection under the knockdown condition of either SIRT1 or SIRT3. Data is representative of N=3, n=2. Unpaired two-tailed Student's t test was performed to obtain the p values. *** p < 0.001, ** p<0.01, * p<0.05

C-qRTPCR mediated expression analysis of several Complex I, Complex II, Complex III, Complex IV, and Complex V genes of the Electron Transport Chain in *S*. Typhimurium infected peritoneal macrophages at 16hr post-infection in the presence or absence of SIRT1 (EX-527) or SIRT3 (3TYP) inhibitor treatment at a concentration of 1µM. Data is representative of N=3, n=2. Unpaired two-tailed Student's t test was performed to obtain the p values. *** p < 0.001, ** p<0.01, * p<0.05

Fig.5- SIRT3 inhibition mediates mitochondrial membrane hyperpolarization

A- Mitochondrial membrane potential determination using MitoTracker Red CMxRos dye via flow cytometry in RAW264.7 macrophages under knockdown condition of SIRT1 or SIRT3 at 16hr post infection. Data is representative of N=3, n=2. Unpaired two-tailed Student's t test was performed to obtain the p values. *** p < 0.001, ** p<0.01, * p<0.05

B- Mitochondrial membrane potential determination using TMRM dye via flow cytometry in RAW264.7 macrophages under knockdown condition of SIRT1 or SIRT3 at 16hr post infection. Data is representative of N=3, n=2. Unpaired two-tailed Student's t test was performed to obtain the p values. *** p < 0.001, ** p<0.01, * p<0.05

C- Mitochondrial membrane potential determination using TMRM dye via flow cytometry in peritoneal macrophages under SIRT1 or SIRT3 inhibitor treatment at 16hr post-infection. Data is representative of N=2, n=3. Unpaired two-tailed Student's t test was performed to obtain the p values. *** p < 0.001, ** p<0.01, * p<0.05

Fig.5- SIRT3 inhibition mediates mitochondrial membrane hyperpolarization

A- Mitochondrial membrane potential determination using MitoTracker Red CMxRos dye via flow cytometry in RAW264.7 macrophages under knockdown condition of SIRT1 or SIRT3 at 16hr post infection. Data is representative of N=3, n=2. Unpaired two-tailed Student's t test was performed to obtain the p values. *** p < 0.001, ** p<0.01, * p<0.05

B- Mitochondrial membrane potential determination using TMRM dye via flow cytometry in RAW264.7 macrophages under knockdown condition of SIRT1 or SIRT3 at 16hr post infection. Data is representative of N=3, n=2. Unpaired two-tailed Student's t test was performed to obtain the p values. *** p < 0.001, ** p<0.01, * p<0.05

Fig.7 – SIRT3 knockdown causes alteration in the intracellular cytosolic pH of the infected macrophages.

A-B-Flow cytometric analysis of cytosolic pH of *S.* Typhimurium infected RAW264.7 macrophages using BCECF-AM dye under knockdown conditions of SIRT1 and SIRT3 or 50µg/ml of chloroquine treatment. Data is representative of N=4, n=3. Unpaired two-tailed Student's t test was performed to obtain the p values. *** p < 0.001, ** p<0.01, * p<0.05

C-D-Flow cytometric analysis of cytosolic pH of *S.* Typhimurium infected peritoneal macrophages using BCECF-AM dye under inhibitor treatment of SIRT1 (EX-527) and SIRT3 (3TYP) inhibitor at the concentration of 1µM or 50µg/ml of chloroquine treatment. Data is representative of N=4, n=3. Unpaired two-tailed Student's t test was performed to obtain the p values. *** p < 0.001, ** p<0.01, * p<0.05

Fig.8 – SIRT1 and SIRT3 knockdown or inhibition trigger loss in acidification of bacterial pH and subsequently its SPI-2 secretion within infected macrophages

A-C- Flow cytometric analysis of SCV pH of infected RAW264.7 macrophages under knockdown condition of SIRT1 or SIRT3 at 16h post-infection. Data is representative of N=2,n=3. Unpaired two-tailed Student's t-test was performed to obtain the p-values. *** p < 0.001, ** p<0.01, * p<0.05

D-F- Flow cytometric analysis of SCV pH of infected RAW264.7 macrophages under inhibitor treatment of SIRT1 or SIRT3 at 16h post-infection. Data is representative of N=2,n=3. Unpaired two-tailed Student's t-test was performed to obtain the p-values. *** p < 0.001, ** p<0.01, * p<0.05

G-Intra-bacterial pH of *S.* Typhimurium expressing pH-sensitive plasmid pHUji was measured from infected RAW264.7 macrophages using flow cytometry under knockdown conditions of SIRT1 and SIRT3. Data is representative of N=3, n=4. Unpaired

two-tailed Student's t-test was performed to obtain the p values. *** p < 0.001, ** p<0.01, * p<0.05

H-Intra-bacterial pH of *S.* Typhimurium expressing pH-sensitive plasmid pHUji was measured from infected peritoneal macrophages using flow cytometry under inhibitor treatment of SIRT1 (EX-527) and SIRT3 (3TYP) inhibitor at the concentration of 1µM. Data is representative of N=3, n=2. Unpaired two-tailed Student's t-test was performed to obtain the p values. *** p < 0.001, ** p<0.01, * p<0.05

I-Intra-bacterial pH of *S.* Typhimurium WT (STM WT) and STMΔ*ompR* expressing pH-sensitive plasmid pHUji was measured from infected RAW264.7 macrophages using flow cytometry under knockdown conditions of SIRT1 and SIRT3. Data is representative of N=3, n=4. Unpaired two-tailed Student's t-test was performed to obtain the p values. *** p < 0.001, ** p<0.01, * p<0.05

J-Intra-bacterial pH of *S.* Typhimurium WT (STM WT) and STMΔ*ompR* expressing pH-sensitive plasmid pHUji was measured from infected RAW264.7 macrophages using flow cytometry under inhibitor treatment of SIRT1 (EX-527) and SIRT3 (3TYP) inhibitor at the concentration of 1µM. Data is representative of N=3, n=4. Unpaired two-tailed Student's t-test was performed to obtain the p values. *** p < 0.001, ** p<0.01, * p<0.05

K- Quantitative PCR-mediated expression studies of SPI-2 genes within infected RAW264.7 macrophages under the knockdown condition of SIRT1 and SIRT3. Data is representative of N=3, n=4. Unpaired two-tailed Student's t-test was performed to obtain the p values. *** p < 0.001, ** p<0.01, * p<0.05

L- Quantitative PCR-mediated expression studies of SPI-2 genes within infected peritoneal macrophages under the inhibitor treatment of SIRT1 (EX-527) and SIRT3

(3TYP) inhibitors. Data is representative of N=3, n=4. Unpaired two-tailed Student's t-test was performed to obtain the p values. *** p < 0.001, ** p<0.01, * p<0.05

M- Quantitative PCR-mediated expression studies of *cadA*, *cadB*, and *cadC* genes within infected peritoneal macrophages under the inhibitor treatment of SIRT1 (EX-527) and SIRT3 (3TYP) inhibitors. Data is representative of N=3, n=4. Unpaired two-tailed Student's t-test was performed to obtain the p values. *** p < 0.001, ** p<0.01, * p<0.05

Fig. 9- SIRT1 and SIRT3 inhibition triggers mitophagy in the *S.* Typhimurium-infected macrophages by regulating fusion-fission dynamics

A-Representative confocal images of RAW264.7 macrophages (transfected with mito-eGFP-mCherry) exhibiting mitophagy flux upon *S.* Typhimurium infection at 16h points post-infection. Data is representative of N=2, n=50 (microscopic field).

B- Quantitative representation of the MFI of mitochondrial eGFP as shown in the confocal images (A). Unpaired two-tailed Student's t-test was performed to obtain the p values. *** p < 0.001, ** p<0.01, * p<0.05

C- Immunoblotting of LC3B and TOM20 in uninfected and infected RAW264.7 macrophages under knockdown condition of SIRT3 at 2hr post-infection. UI-Uninfected, STM-*S.* Typhimurium infected, Scrambled shRNA control

D-Densitometric analysis of TOM20 with respect to βactin LC3BII with respect to TOM20 and of the immunoblot A to detect mitophagy.

E-F- qRTPCR mediated expression analysis of mitochondrial fusion (E) and fission (F) genes in *S.* Typhimurium infected RAW264.7 macrophages at 16hr post infection under knockdown of SIRT1 or SIRT3.

G- Immunoprecipitation of SIRT3 in uninfected or *S.* Typhimurium infected RAW264.7 macrophages at 16hr post infection to detect interaction of SIRT3 with OPA-1.

H- Immunoblotting of SIRT3 knockdown RAW 264.7 cells in *S.* Typhimurium infected and uninfected upon immunoprecipitation of OPA-1 to check the acetylation status of OPA-1.

I- Immunoprecipitation of OPA-1 in uninfected or *S.* Typhimurium infected RAW264.7 macrophages at 16hr post infection under the knockdown condition of SIRT3 to assess the interaction of OPA-1 with SIRT3 in knockdown condition.

J- Immunoprecipitation of OPA-1 in uninfected or *S.* Typhimurium infected RAW264.7 macrophages at 16hr post infection under the catalytic inhibitor treatment of SIRT3.

SUPPLEMENTARY FIGURE LEGENDS

Fig. S1- SIRT1 and SIRT3 knockdown confirmation in RAW264.7 cells using shRNA constructs

A- Immunoblotting of SIRT3 for knockdown validation. (SCR=Scrambled, Mix=transfection with equimolar concentration of both SIRT3 shRNA construct E8 and E12)

B- Immunoblotting of SIRT1 for knockdown confirmation. (SCR=Scrambled, Mix=transfection with equimolar concentration of both SIRT3 shRNA construct C4 and C12)

C- Densitometric analysis of the immunoblot represented in A.

D- Densitometric analysis of the immunoblot represented in B.

Fig. S2- Validation of action of mitoTEMPO as a mitochondrial ROS scavenger

A-Flow cytometric estimation of mitochondrial ROS generation using mitoSOX dye in presence or absence of mtROS scavenger, mitoTEMPO (10µM) in infected RAW264.7 macrophages.

Fig. S3- SIRT1 and SIRT3 knockdown lead to alteration in bacterial antioxidant gene expression

A-qRT-PCR mediated expression analysis of bacterial antioxidant genes in *S.* Typhimurium infected RAW264.7 macrophages at 16hr post infection under knockdown condition of SIRT1 or SIRT3. Data is representative of N=3, n=2. Unpaired two-tailed Student's t test was performed to obtain the p values. *** p < 0.001, ** p<0.01, * p<0.05

Fig. S4- SIRT1 and SIRT3 knockdown or inhibition leads to loss of acidification of SCV

A-C- Flow cytometric analysis of SCV pH of infected RAW264.7 macrophages under knockdown condition of SIRT1 or SIRT3 at 6h post-infection. Data is representative of N=2, n=3. Unpaired two-tailed Student's t-test was performed to obtain the p-values. *** p < 0.001, ** p<0.01, * p<0.05

D-F- Flow cytometric analysis of SCV pH of infected RAW264.7 macrophages under inhibitor treatment of SIRT1 or SIRT3 at 6h post-infection. Data is representative of N=2,n=3. Unpaired two-tailed Student's t-test was performed to obtain the p-values. *** p < 0.001, ** p<0.01, * p<0.05

Fig. S5- SIRT1 or SIRT3 knockdown triggers mitophagy in the *S.* Typhimurium-infected macrophages

A-B-Representative confocal images of SIRT1 or SIRT3 knockdown RAW264.7 macrophages exhibiting colocalization of LC3B with mitotracker Red to detect

mitophagy upon *S.* Typhimurium infection at 6hr (A) and 16hr (B) post-infection. Data is representative of N=2, n=80 (microscopic field).

C-D-Quantitative representation of the colocalization co-efficient of LC3B with that of mitotracker Red as shown in the confocal images (A-B). Unpaired two-tailed Student's t test was performed to obtain the p values. *** p < 0.001, ** p<0.01, * p<0.05

Fig. S6- SIRT3 knockdown triggers mitophagy in the *S.* Typhimurium-RAW264.7 infected macrophages at early time points of 2hr post-infection

A-Representative confocal images of SIRT1 or SIRT3 knockdown RAW264.7 macrophages exhibiting colocalization of LC3B with mitotracker Red to detect mitophagy upon *S.* Typhimurium infection at 2hr post-infection. Data is representative of N=2, n=80 (microscopic field).

B-Quantitative representation of the colocalization co-efficient of LC3B with that of mitotracker Red as shown in the confocal images A. Unpaired two-tailed Student's t test was performed to obtain the p values. *** p < 0.001, ** p<0.01, * p<0.05

Fig. S7- SIRT1 and SIRT3 inhibition causes alteration in mitochondrial fusion-fission dynamics in STM-infected peritoneal macrophages

A-qRTPCR mediated expression analysis of mitochondrial fusion genes in *S.* Typhimurium infected peritoneal macrophages at 16hr post infection under inhibitor treatment of SIRT1 or SIRT3 at a concentration of 1μM. Data is representative of N=3,n=2. Unpaired two-tailed Student's t test was performed to obtain the p values. *** p < 0.001, ** p<0.01, * p<0.05

B-qRTPCR mediated expression analysis of mitochondrial fission genes in *S.* Typhimurium infected peritoneal macrophages at 16hr post infection under inhibitor

treatment of SIRT1 or SIRT3 at a concentration of 1μM. Data is representative of N=3,n=2. Unpaired two-tailed Student's t test was performed to obtain the p values. *** $p < 0.001$, ** $p<0.01$, * $p<0.05$

Title: SIRT1 and SIRT3 impact host mitochondrial function and host- *Salmonella* pH balance during infection

MAIN FIGURES

FIGURE 1

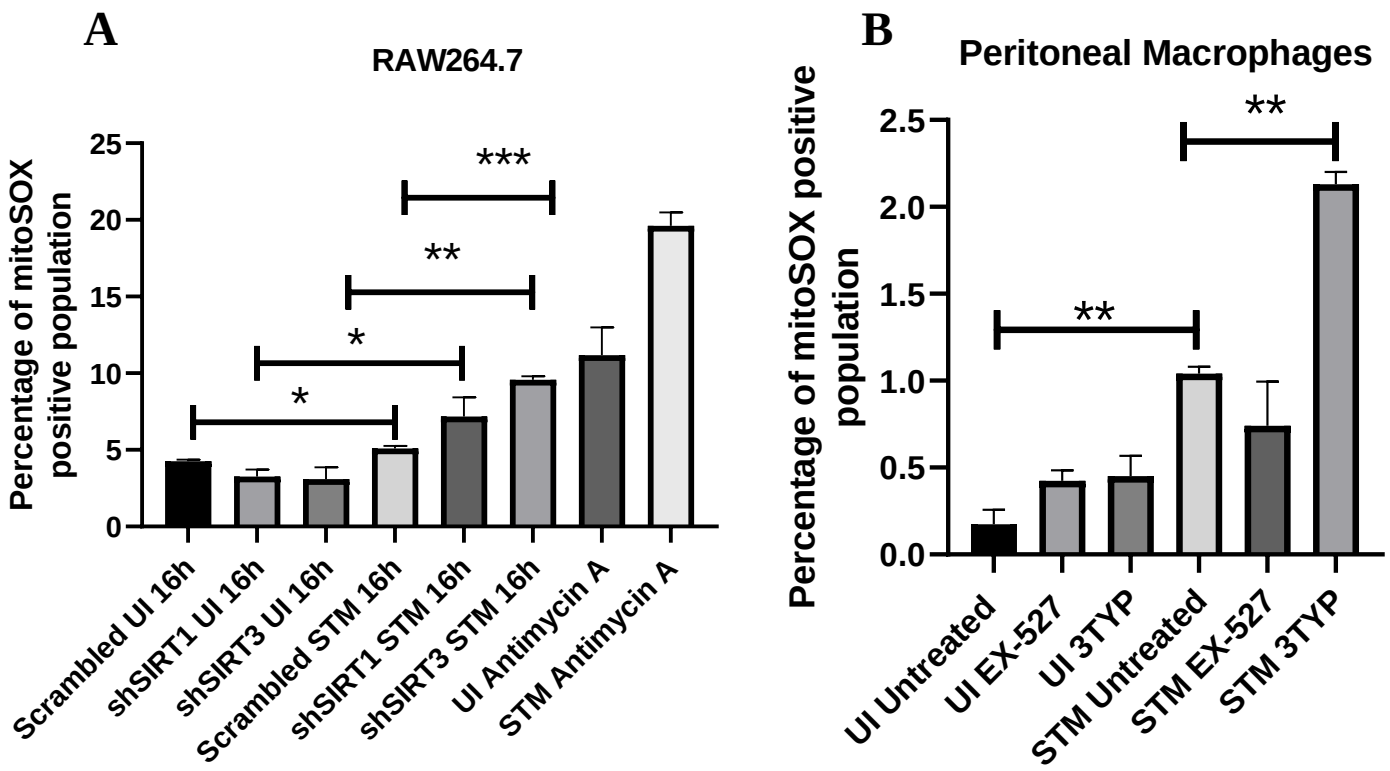
A
RAW264.7
Percentage of mitoSOX positive population
25
20
15
10
5
0
***
**
*
*
Scrambled UI 16h
shSIRT1 UI 16h
shSIRT3 UI 16h
Scrambled STM 16h
shSIRT1 STM 16h
shSIRT3 STM 16h
UI Antimycin A
STM Antimycin A
B
Peritoneal Macrophages
Percentage of mitoSOX positive population
2.5
2.0
1.5
1.0
0.5
0.0
**
**
UI Untreated
UI EX-527
UI 3TYP
STM Untreated
STM EX-527
STM 3TYP

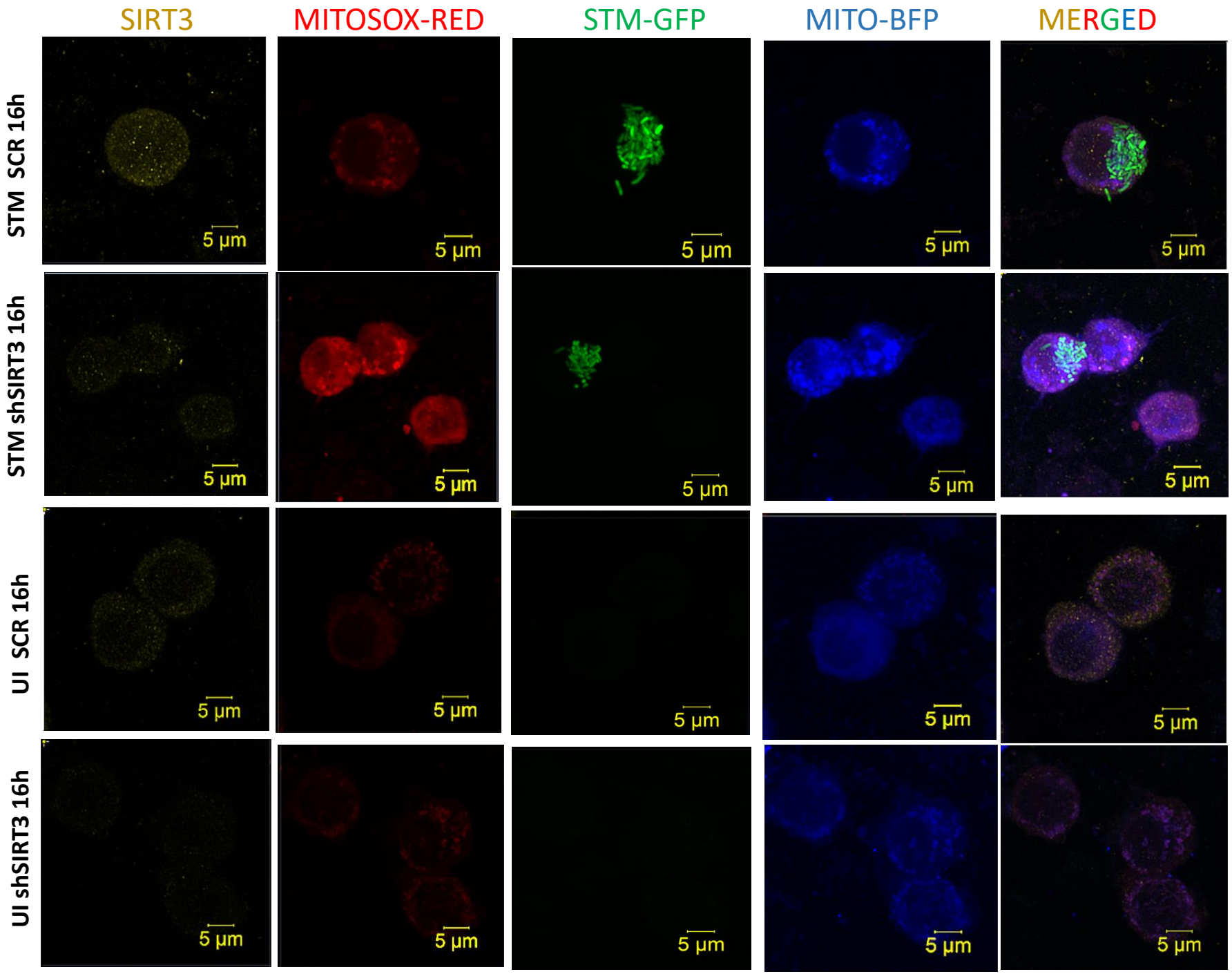
SIRT3
MITOSOX-RED
STM-GFP
MITO-BFP
MERGED
STM SCR 16h
STM shSIRT3 16h
UI SCR 16h
UI shSIRT3 16h
5 µm

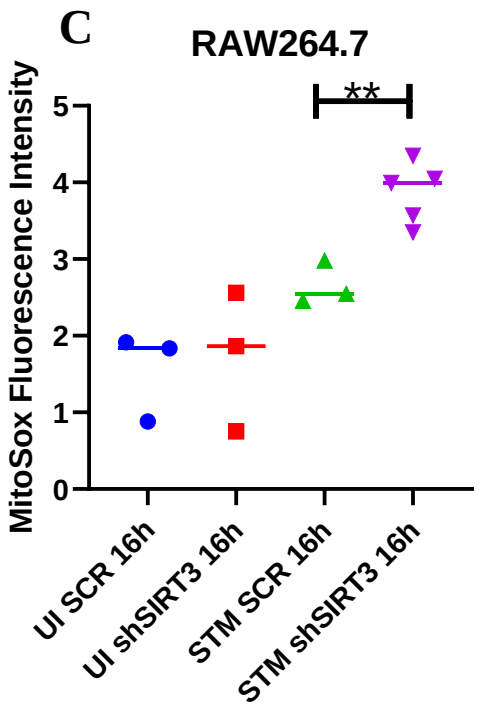
C
RAW264.7
**
MitoSox Fluorescence Intensity
0
1
2
3
4
5
UI SCR 16h
UI shSIRT3 16h
STM SCR 16h
STM shSIRT3 16h

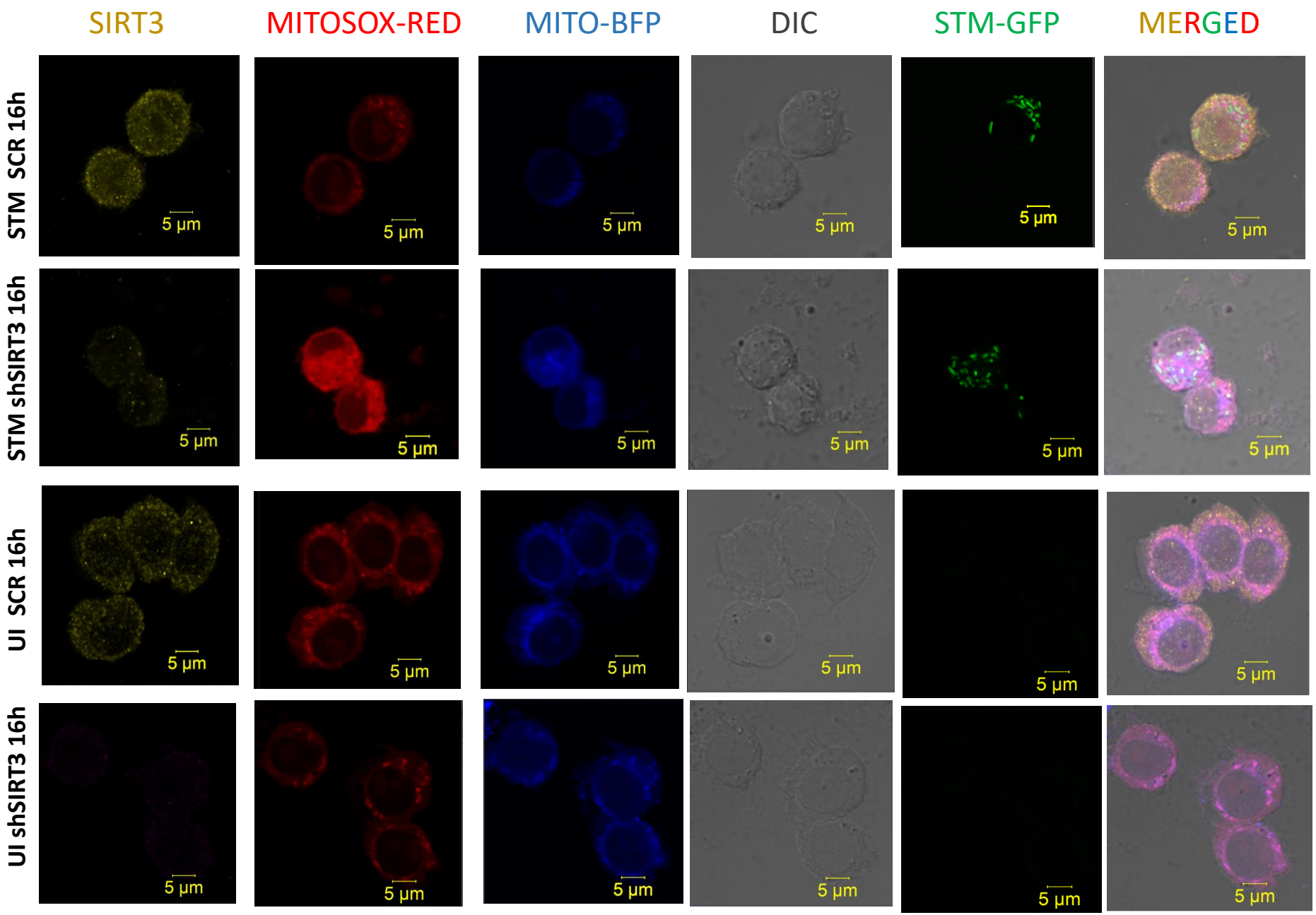
SIRT3
MITOSOX-RED
MITO-BFP
DIC
STM-GFP
MERGED
STM SCR 16h
STM shSIRT3 16h
UI SCR 16h
UI shSIRT3 16h
5 µm

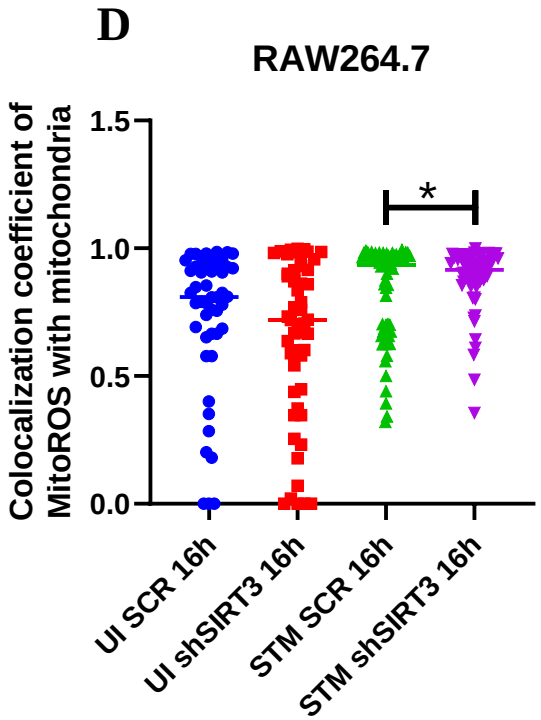
D
RAW264.7
Colocalization coefficient of MitoROS with mitochondria
1.5
1.0
0.5
0.0
*
UI SCR 16h
UI shSIRT3 16h
STM SCR 16h
STM shSIRT3 16h

Fig.1- SIRT3 inhibition leads to enhanced mitochondrial ROS generation in infected macrophages.

A-Mitochondrial ROS estimation via flow cytometry in *S.* Typhimurium infected RAW264.7 macrophages at 16hr post infection under SIRT1 or SIRT3 knockdown condition. Data is representative of N=4, n=2. 10µM antimycin A-treated (ROS inducer) uninfected and infected cells served as positive control. Unpaired two-tailed Student's t-test was performed to obtain the p values. ***** $p < 0.001$, ** $p<0.01$, * $p<0.05$**

B-Mitochondrial ROS estimation via flow cytometry in *S.* Typhimurium infected peritoneal macrophages (isolated post 5th day of thioglycolate injection, intraperitoneally) at 16hr post-infection in the presence of SIRT1 (EX-527,1µM) or SIRT3 (3TYP,1µM) inhibitor treatment. Data is representative of N=3, n=2. Unpaired two-tailed Student's t-test was performed to obtain the p values. ***** $p < 0.001$, ** $p<0.01$, * $p<0.05$**

C-Representative confocal images of SIRT3 knockdown RAW264.7 macrophages exhibiting Mean Fluorescence Intensity (MFI) of mitoSox Red detecting mitochondrial ROS upon *S.* Typhimurium infection at indicated time points post-infection. Data is representative of N=3, n>50 (microscopic field). Unpaired two-tailed Student's t test was performed to obtain the p values. ***** $p < 0.001$, ** $p<0.01$, * $p<0.05$**

D- Representative confocal images of SIRT3 knockdown RAW264.7 macrophages exhibiting co-localization coefficient of mitoSox Red detecting mitochondrial ROS with mitochondria (mitoBFP) upon *S.* Typhimurium infection at indicated time points post infection. Data is representative of N=3, n>50 (microscopic field). Unpaired two-tailed Student's t test was performed to obtain the p values. ***** $p < 0.001$, ** $p<0.01$, * $p<0.05$**

FIGURE 2

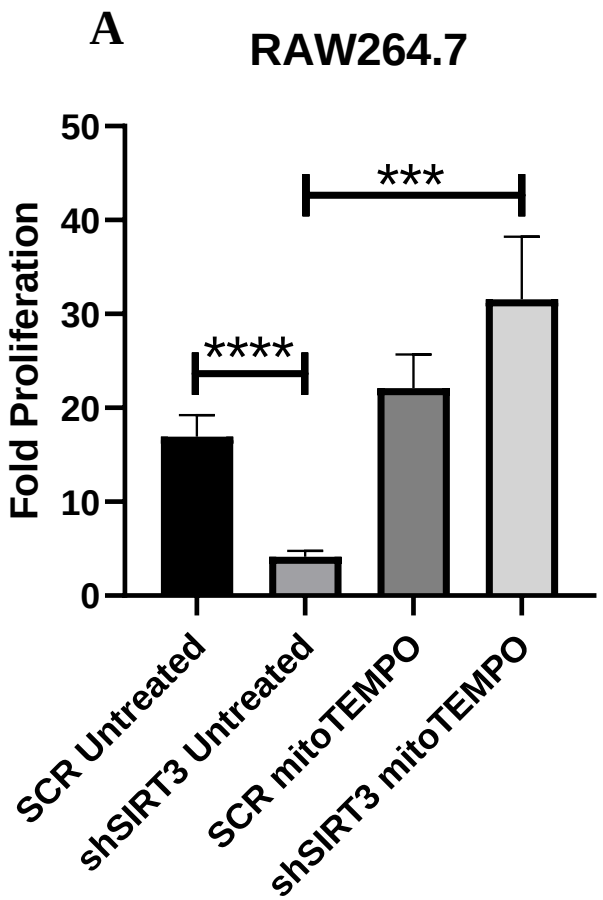

Fig.2- Increased mtROS production attenuates intracellular proliferation of *Salmonella* Typhimurium within SIRT3 knockdown macrophages and alleviation of the mtROS with mitoTEMPO restores the intracellular replication of the pathogen.

A- Intracellular proliferation assay of *S*. Typhimurium within scrambled control or SIRT3 knockdown macrophages in presence or absence of mitoTEMPO treatment. Data is representative of N=3, n=2. Unpaired two-tailed Student's t test was performed to obtain the p values. ***** p < 0.001, ** p<0.01, * p<0.05**

FIGURE 3

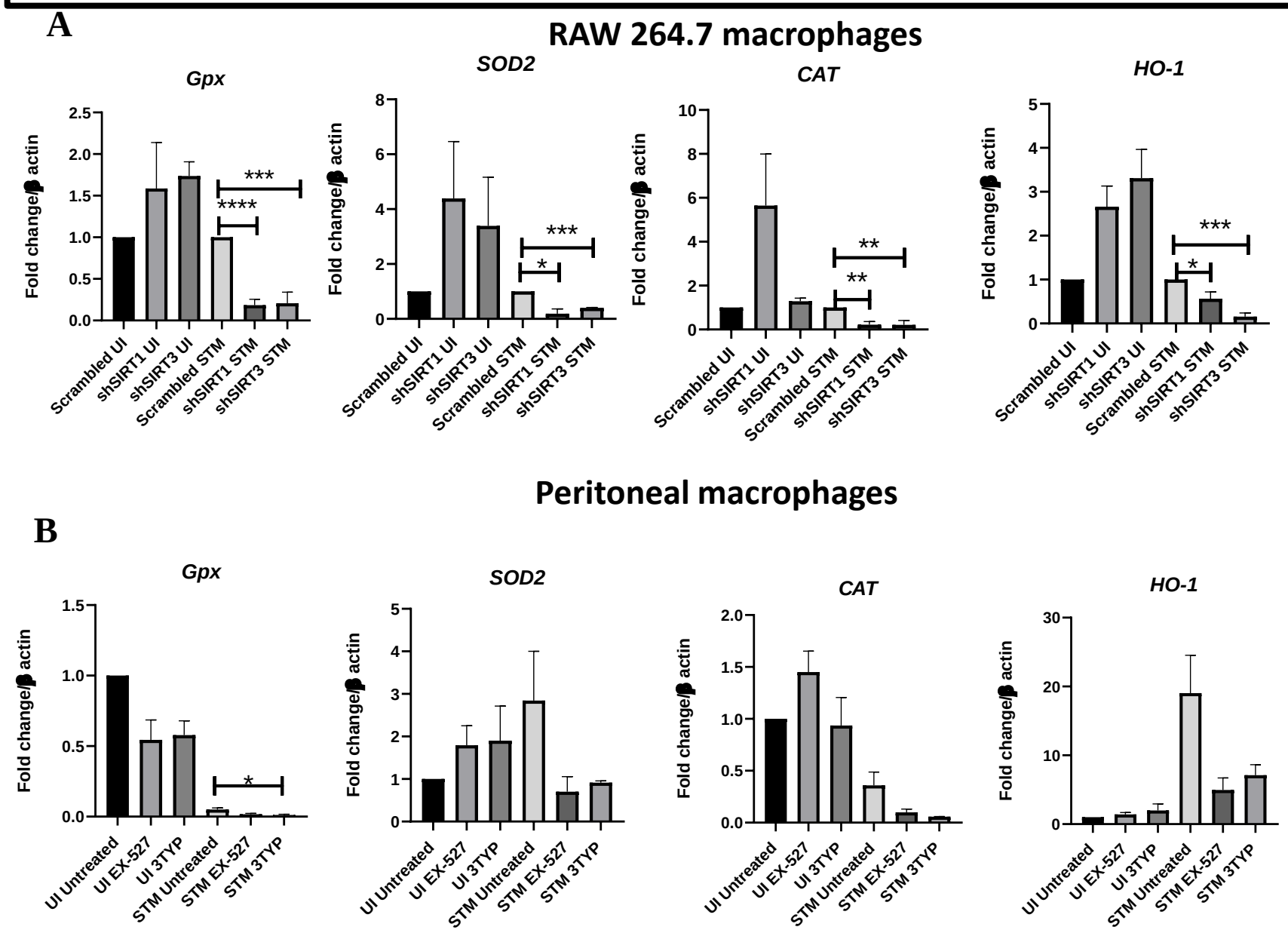
A
RAW 264.7 macrophages
Gpx
SOD2
CAT
HO-1
Fold change/β actin
Scrambled UI
shSIRT1 UI
shSIRT3 UI
Scrambled STM
shSIRT1 STM
shSIRT3 STM
***
****
*
**
B
Peritoneal macrophages
UI Untreated
UI EX-527
UI 3TYP
STM Untreated
STM EX-527
STM 3TYP

C

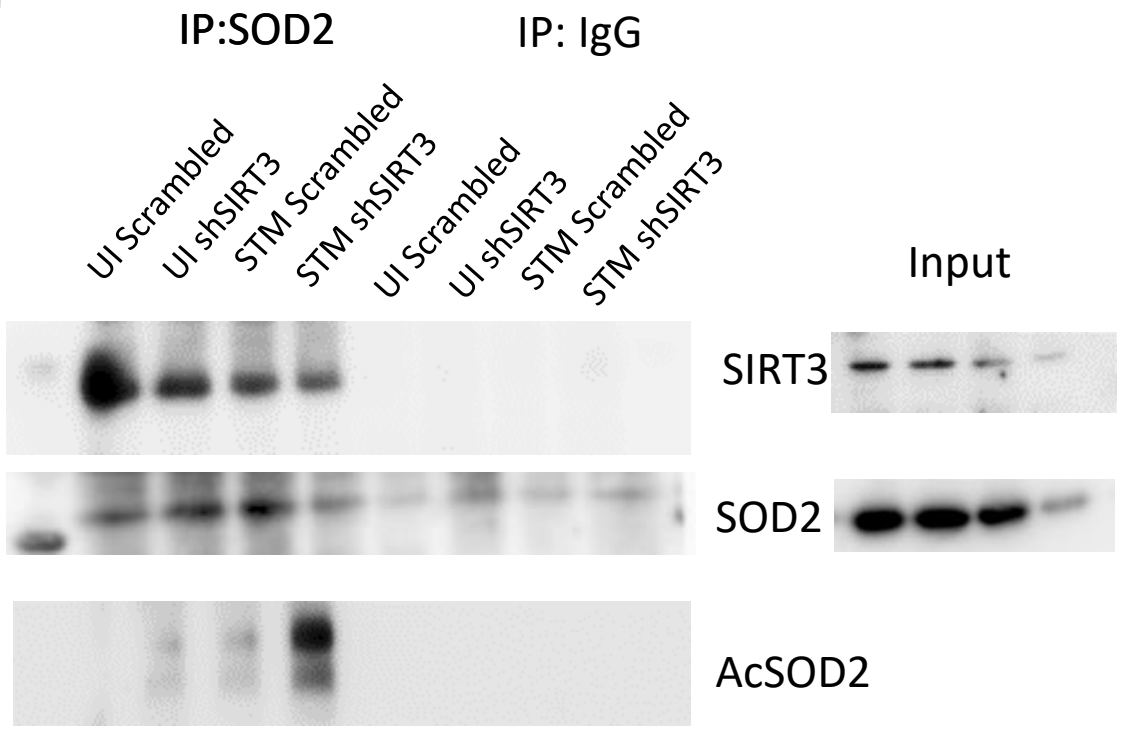
IP:SOD2
IP: IgG
UI Scrambled
UI shSIRT3
STM Scrambled
STM shSIRT3
UI Scrambled
UI shSIRT3
STM Scrambled
STM shSIRT3
Input
SIRT3
SOD2
AcSOD2

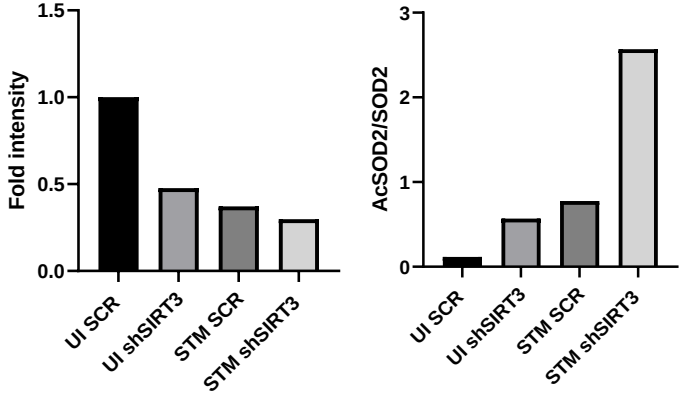
Fold intensity
1.5
1.0
0.5
0.0
UI SCR
UI shSIRT3
STM SCR
STM shSIRT3
AcSOD2/SOD2
3
2
1
0
UI SCR
UI shSIRT3
STM SCR
STM shSIRT3

D

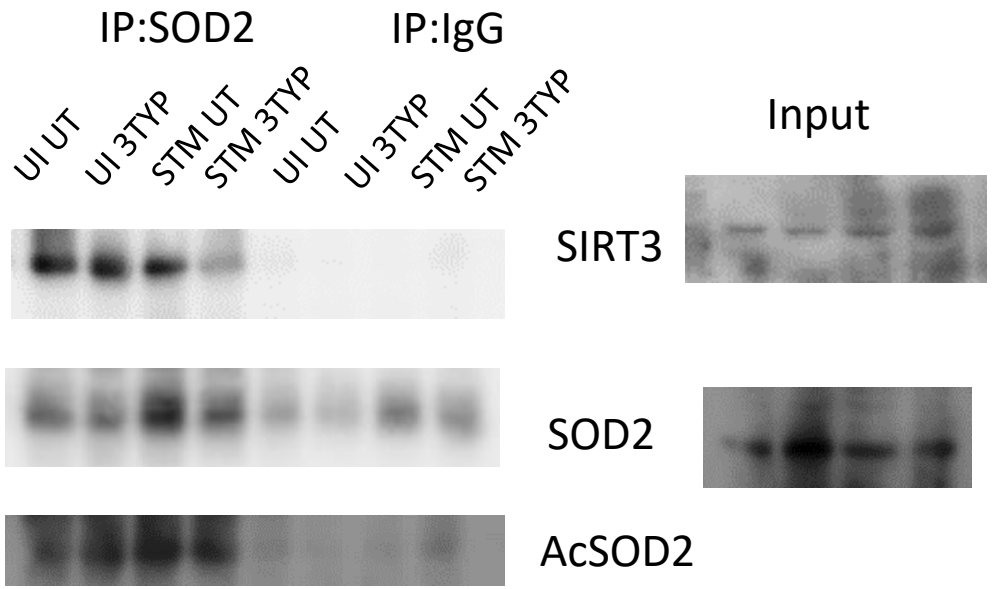
IP:SOD2
IP:IgG
UI UT
UI 3TYP
STM UT
STM 3TYP
UI UT
UI 3TYP
STM UT
STM 3TYP
Input
SIRT3
SOD2
AcSOD2

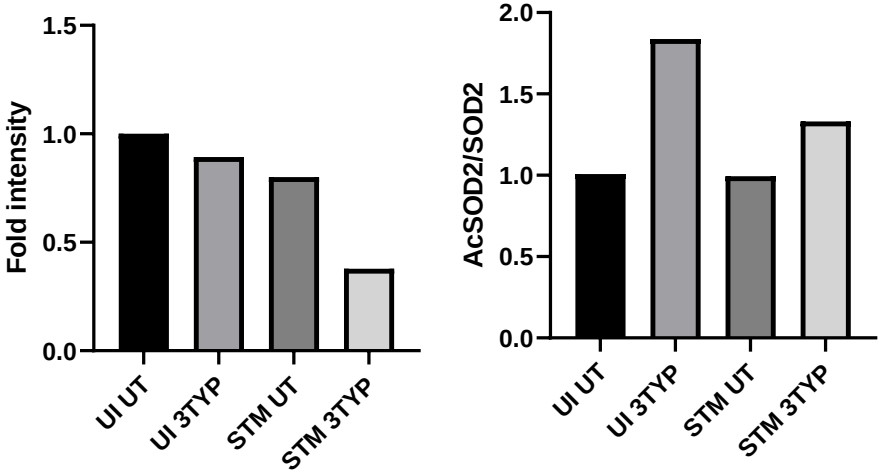
Fold intensity
1.5
1.0
0.5
0.0
UI UT
UI 3TYP
STM UT
STM 3TYP
AcSOD2/SOD2
2.0
1.5
1.0
0.5
0.0
UI UT
UI 3TYP
STM UT
STM 3TYP

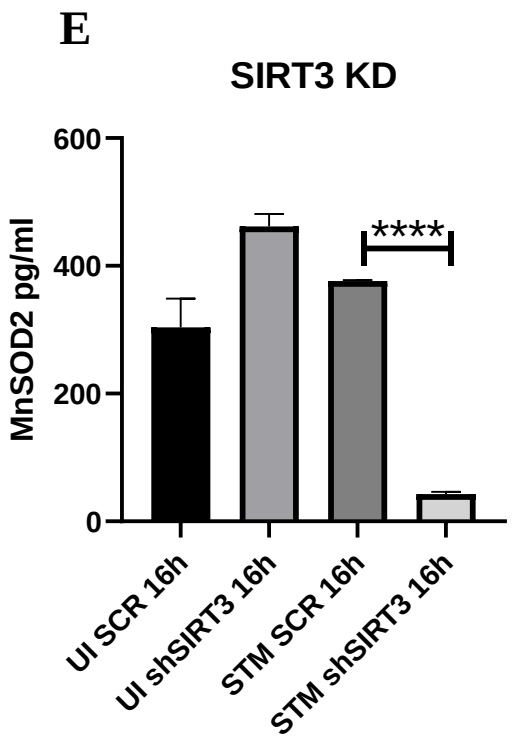
E
SIRT3 KD
MnSOD2 pg/ml
600
400
200
0
****
UI SCR 16h
UI shSIRT3 16h
STM SCR 16h
STM shSIRT3 16h

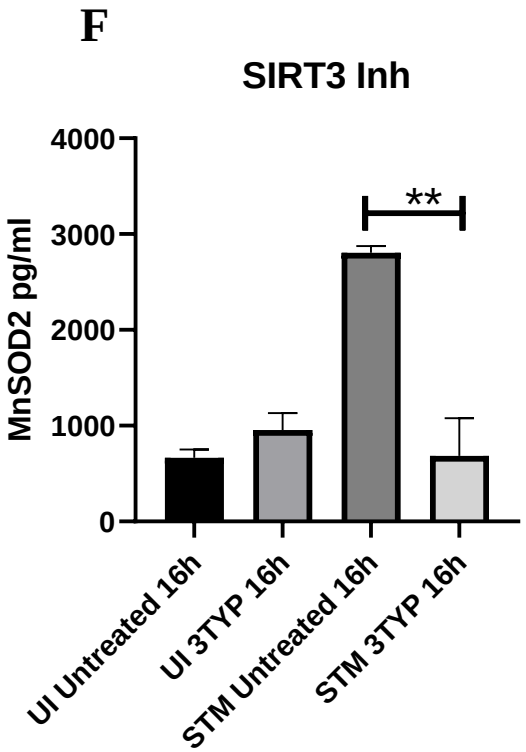
F
SIRT3 Inh
MnSOD2 pg/ml
4000
3000
2000
1000
0
**
UI Untreated 16h
UI 3TYP 16h
STM Untreated 16h
STM 3TYP 16h

Fig.3 Effect of SIRT1 or SIRT3 inhibition on host mitochondrial antioxidant defense in *Salmonella* Typhimurium infection scenario.

A-Quantitative gene expression studies of several host mitochondrial antioxidant genes such as *Gpx*, *Sod2*, *Cat*, and *Ho-1* in RAW264.7 macrophages upon knockdown of SIRT1 and SIRT3 in *S.* Typhimurium infection scenario. Data is representative of N=3, n=2. Unpaired two-tailed Student's t test was performed to obtain the p values. ***** p < 0.001, ** p<0.01, * p<0.05**

B-Quantitative gene expression studies of several host mitochondrial antioxidant genes such as *Gpx*, *Sod2*, *Cat*, and *Ho-1* in peritoneal macrophages (isolated from 6–8-week-old adult male mice post 5th day of thioglycolate injection) after 16h of *S.* Typhimurium infection upon SIRT1 (EX-527,1µM) or SIRT3 (3TYP, 1µM) inhibitor treatment. Data is representative of N=3, n=2. Unpaired two-tailed Student's t test was performed to obtain the p values. ***** p < 0.001, ** p<0.01, * p<0.05, no stars-non-significant**

C- Immunoprecipitation studies depicting SOD2 interaction with SIRT3 upon immunoprecipitation of SOD2 in uninfected (UI) or *S.* Typhimurium (STM) infected SIRT3 knockdown RAW264.7 macrophages at 16hr post-infection . Data is representative of N=2, n=1. ***** p < 0.001, ** p<0.01, * p<0.05**

D- Immunoprecipitation studies depicting SOD2 interaction with SIRT3 upon immunoprecipitation of SOD2 in uninfected (UI) or *S.* Typhimurium (STM) infected RAW264.7 macrophages at 16hr post-infection upon inhibitor treatment of SIRT3 . Data is representative of N=2, n=1. ***** p < 0.001, ** p<0.01, * p<0.05**

E- Mitochondrial SOD2 activity assay in uninfected and *S.* Typhimurium infected RAW264.7 macrophages in the knockdown condition of SIRT3. Data is representative of N=3, n=2. Unpaired two-tailed Student's t test was performed to obtain the p values. ***** p < 0.001, ** p<0.01, * p<0.05**

F- Mitochondrial SOD2 activity assay in uninfected and *S.* Typhimurium infected RAW264.7 macrophages upon SIRT3 inhibitor treatment. Data is representative of N=3, n=2. Unpaired two-tailed Student's t test was performed to obtain the p values. ***** p < 0.001, ** p<0.01, * p<0.05**

FIGURE 4

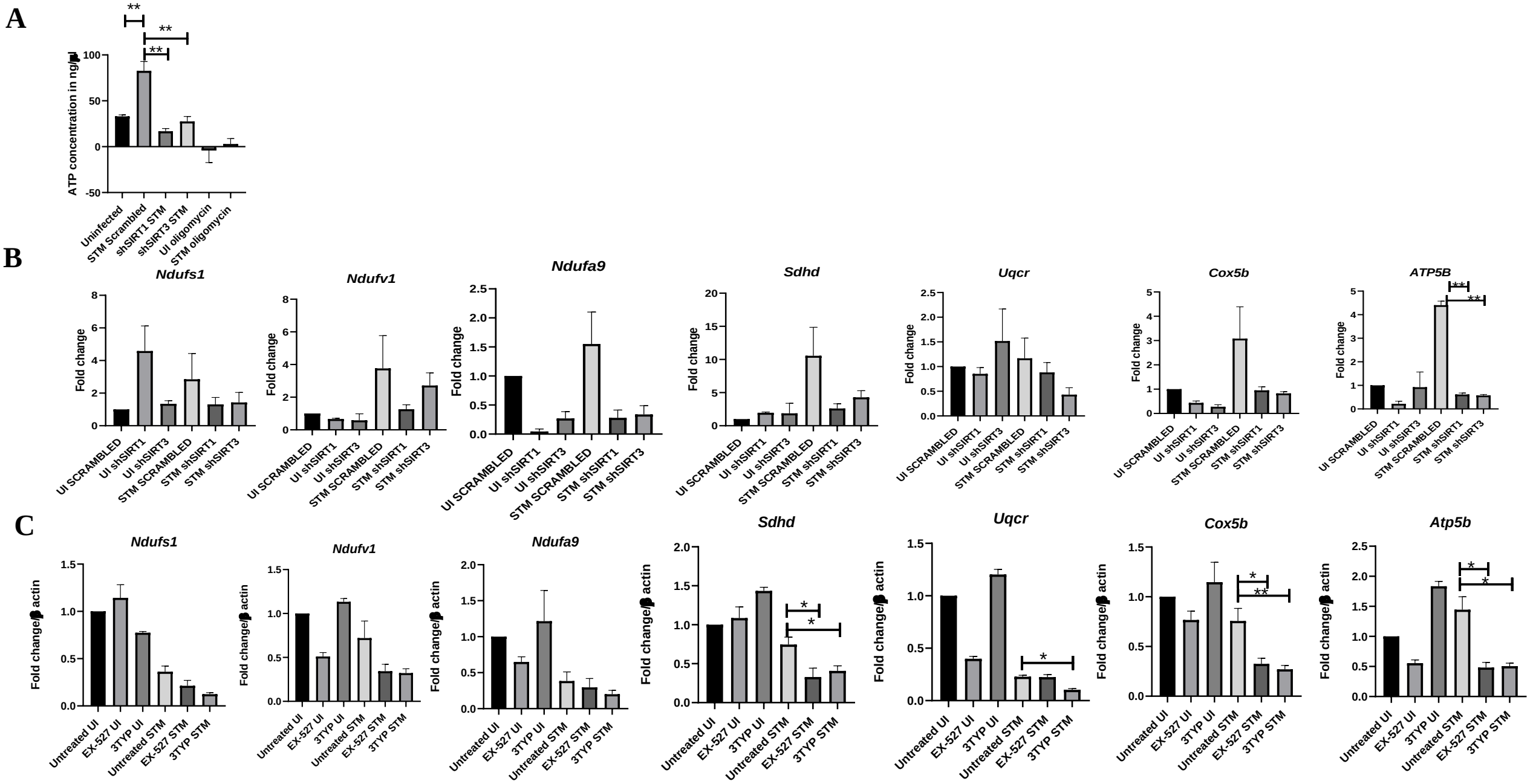
A
ATP concentration in ng/ml
Uninfected
STM Scrambled
shSIRT1 STM
shSIRT3 STM
UI oligomycin
STM oligomycin
B
Ndufs1
Ndufv1
Ndufa9
Sdhd
Uqcr
Cox5b
ATP5B
Fold change
UI SCRAMBLED
UI shSIRT1
UI shSIRT3
STM SCRAMBLED
STM shSIRT1
STM shSIRT3
C
Ndufs1
Ndufv1
Ndufa9
Sdhd
Uqcr
Cox5b
Atp5b
Fold change/β actin
Untreated UI
EX-527 UI
3TYP UI
Untreated STM
EX-527 STM
3TYP STM

Fig.4 Inhibition of SIRT1 or SIRT3 leads to disruption of mitochondrial bioenergetics in *S.* Typhimurium-infected macrophages.

A-ATP estimation assay in SIRT1 or SIRT3 knockdown RAW264.7 macrophages in the presence or absence of *S.* Typhimurium infection at time 16h post-infection. Data is representative of N=3,n=2. 10µM oligomycin-treated (ATP synthase inhibitor) uninfected and infected cells served as negative control. Unpaired two-tailed Student's t-test was performed to obtain the p values. ***** p < 0.001, ** p<0.01, * p<0.05**

B-q RT-PCR mediated expression analysis of several Complex I, Complex II, Complex III, Complex IV, and Complex V genes of the Electron Transport Chain in *S.* Typhimurium infected RAW264.7 macrophages at 16hr post infection under the knockdown condition of either SIRT1 or SIRT3. Data is representative of N=3, n=2. Unpaired two-tailed Student's t test was performed to obtain the p values. ***** p < 0.001, ** p<0.01, * p<0.05**

C-q RT-PCR mediated expression analysis of several Complex I, Complex II, Complex III, Complex IV, and Complex V genes of the Electron Transport Chain in *S.* Typhimurium infected peritoneal macrophages at 16hr post-infection in the presence or absence of SIRT1 (EX-527) or SIRT3 (3TYP) inhibitor treatment at a concentration of 1µM. Data is representative of N=3, n=2. Unpaired two-tailed Student's t-test was performed to obtain the p values. ***** p < 0.001, ** p<0.01, * p<0.05**

FIGURE 5

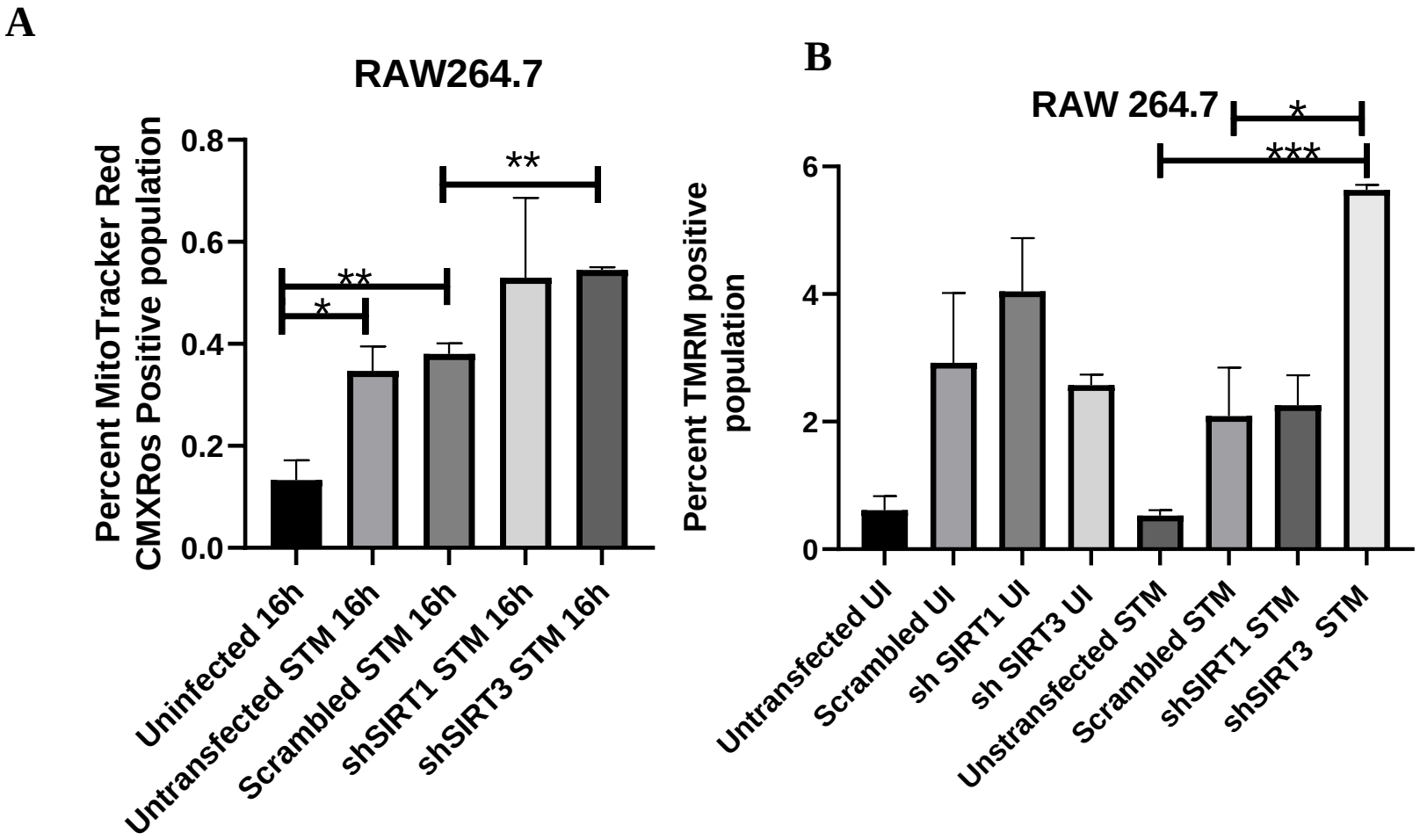
A
RAW264.7
Percent MitoTracker Red CMXRos Positive population
0.8
0.6
0.4
0.2
0.0
**
**
*
Uninfected 16h
Untransfected STM 16h
Scrambled STM 16h
shSIRT1 STM 16h
shSIRT3 STM 16h
B
RAW 264.7
Percent TMRM positive population
6
4
2
0
*
***
Untransfected UI
Scrambled UI
sh SIRT1 UI
sh SIRT3 UI
Unstransfected STM
Scrambled STM
shSIRT1 STM
shSIRT3 STM

Fig.5- SIRT3 inhibition mediates mitochondrial membrane hyperpolarization

A- Mitochondrial membrane potential determination using MitoTracker Red CMxRos dye via flow cytometry in RAW264.7 macrophages under knockdown condition of SIRT1 or SIRT3 at 16hr post infection. Data is representative of N=3, n=2. Unpaired two-tailed Student's t test was performed to obtain the p values. ***** $p < 0.001$, ** $p<0.01$, * $p<0.05$**

B- Mitochondrial membrane potential determination using TMRM dye via flow cytometry in RAW264.7 macrophages under knockdown condition of SIRT1 or SIRT3 at 16hr post infection. Data is representative of N=3, n=2. Unpaired two-tailed Student's t test was performed to obtain the p values. ***** $p < 0.001$, ** $p<0.01$, * $p<0.05$**

C- Mitochondrial membrane potential determination using TMRM dye via flow cytometry in peritoneal macrophages under SIRT1 or SIRT3 inhibitor treatment at 16hr post-infection. Data is representative of N=2, n=3. Unpaired two-tailed Student's t test was performed to obtain the p values. ***** $p < 0.001$, ** $p<0.01$, * $p<0.05$**

FIGURE 6

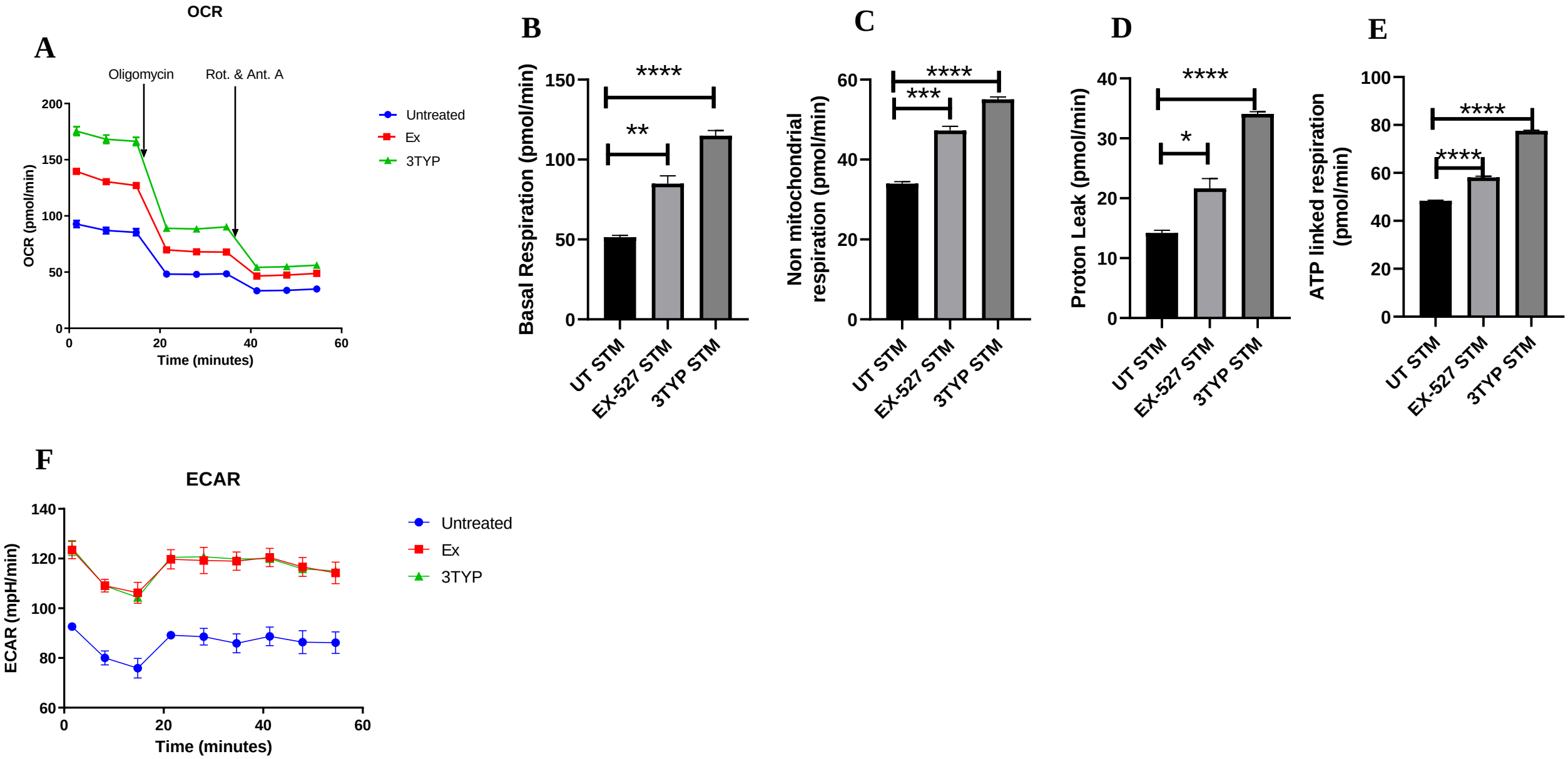
A
OCR
Oligomycin
Rot. & Ant. A
OCR (pmol/min)
Time (minutes)
Untreated
Ex
3TYP
B
Basal Respiration (pmol/min)
C
Non mitochondrial respiration (pmol/min)
D
Proton Leak (pmol/min)
E
ATP linked respiration (pmol/min)
UT STM
EX-527 STM
3TYP STM
F
ECAR
ECAR (mpH/min)
Time (minutes)
Untreated
Ex
3TYP

Fig.6 – Mito stress test of *S.* Typhimurium infected peritoneal macrophages under SIRT3 inhibitor treatment

A-Mitochondrial Oxygen Consumption Rate (OCR) curve of infected peritoneal macrophages isolated from 6-8 week old adult male mice post 5th day of thioglycolate injection in the presence or absence of SIRT1 (EX-527) or SIRT3 inhibitor (3TYP,1µM) treatment. Data is representative of N=3, n=2. Unpaired two-tailed Student's t test was performed to obtain the p values. ***** p < 0.001, ** p<0.01, * p<0.05**

B- Basal mitochondrial respiration of infected peritoneal macrophages isolated from 6–8-week-old adult male mice post 5th day of thioglycolate injection in the presence or absence of SIRT3 inhibitor (3TYP,1µM) treatment as calculated from A. Data is representative of N=3, n=2. Unpaired two-tailed Student's t test was performed to obtain the p values. ***** p < 0.001, ** p<0.01, * p<0.05**

C- Non-mitochondrial respiration of infected peritoneal macrophages upon SIRT1 and SIRT3 inhibitor treatment post 6h of *S*. Typhimurium infection as shown in A. Data is representative of N=3, n=2. Unpaired two-tailed Student's t test was performed to obtain the p values. ***** p < 0.001, ** p<0.01, * p<0.05**

D-Proton leak of infected peritoneal macrophages upon SIRT1 and SIRT3 inhibitor treatment post 6h of *S*. Typhimurium infection as obtained from A. Data is representative of N=3, n=2. Unpaired two-tailed Student's t test was performed to obtain the p values. ***** p < 0.001, ** p<0.01, * p<0.05**

E-ATP-linked respiration infected peritoneal macrophages upon SIRT1 and SIRT3 inhibitor treatment post 6h of *S*. Typhimurium infection as obtained from A. Data is representative of N=3, n=2. Unpaired two-tailed Student's t test was performed to obtain the p values. ***** p < 0.001, ** p<0.01, * p<0.05**

F-Extracellular Acidification Rate (ECAR) profile of infected peritoneal macrophages upon SIRT1 and SIRT3 inhibitor treatment post 6h of *S*. Typhimurium infection. Data is representative of N=3, n=2. Unpaired two-tailed Student's t test was performed to obtain the p values. ***** p < 0.001, ** p<0.01, * p<0.05**

FIGURE 7

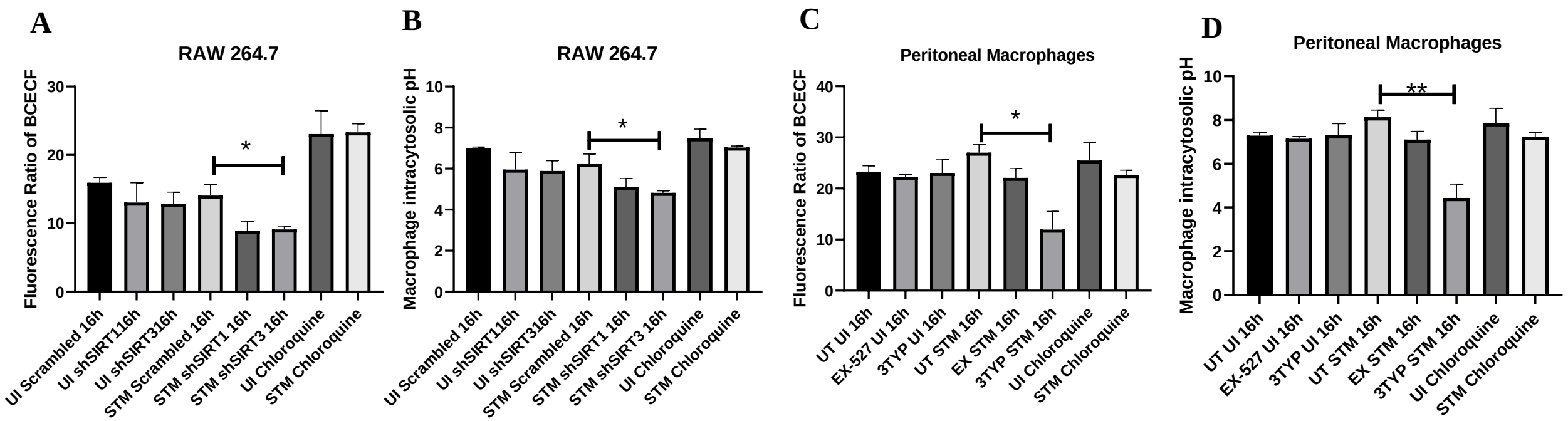
A
RAW 264.7
Fluorescence Ratio of BCECF
30
20
10
0
*
UI Scrambled 16h
UI shSIRT116h
UI shSIRT316h
STM Scrambled 16h
STM shSIRT1 16h
STM shSIRT3 16h
UI Chloroquine
STM Chloroquine
B
RAW 264.7
Macrophage intracytosolic pH
10
8
6
4
2
0
*
UI Scrambled 16h
UI shSIRT116h
UI shSIRT316h
STM Scrambled 16h
STM shSIRT1 16h
STM shSIRT3 16h
UI Chloroquine
STM Chloroquine
C
Peritoneal Macrophages
Fluorescence Ratio of BCECF
40
30
20
10
0
*
UT UI 16h
EX-527 UI 16h
3TYP UI 16h
UT STM 16h
EX STM 16h
3TYP STM 16h
UI Chloroquine
STM Chloroquine
D
Peritoneal Macrophages
Macrophage intracytosolic pH
10
8
6
4
2
0
**
UT UI 16h
EX-527 UI 16h
3TYP UI 16h
UT STM 16h
EX STM 16h
3TYP STM 16h
UI Chloroquine
STM Chloroquine

Fig.7 – SIRT3 knockdown causes alteration in the intracellular cytosolic pH of the infected macrophages.

A-B-Flow cytometric analysis of cytosolic pH of *S.* Typhimurium infected RAW264.7 macrophages using BCECF-AM dye under knockdown conditions of SIRT1 and SIRT3 or 50µg/ml of chloroquine treatment. Data is representative of N=4, n=3. Unpaired two-tailed Student's t test was performed to obtain the p values. ***** p < 0.001, ** p<0.01, * p<0.05**

C-D-Flow cytometric analysis of cytosolic pH of *S.* Typhimurium infected peritoneal macrophages using BCECF-AM dye under inhibitor treatment of SIRT1 (EX-527) and SIRT3 (3TYP) inhibitor at the concentration of 1µM or 50µg/ml of chloroquine treatment. Data is representative of N=4, n=3. Unpaired two-tailed Student's t test was performed to obtain the p values. ***** p < 0.001, ** p<0.01, * p<0.05**

FIGURE 8

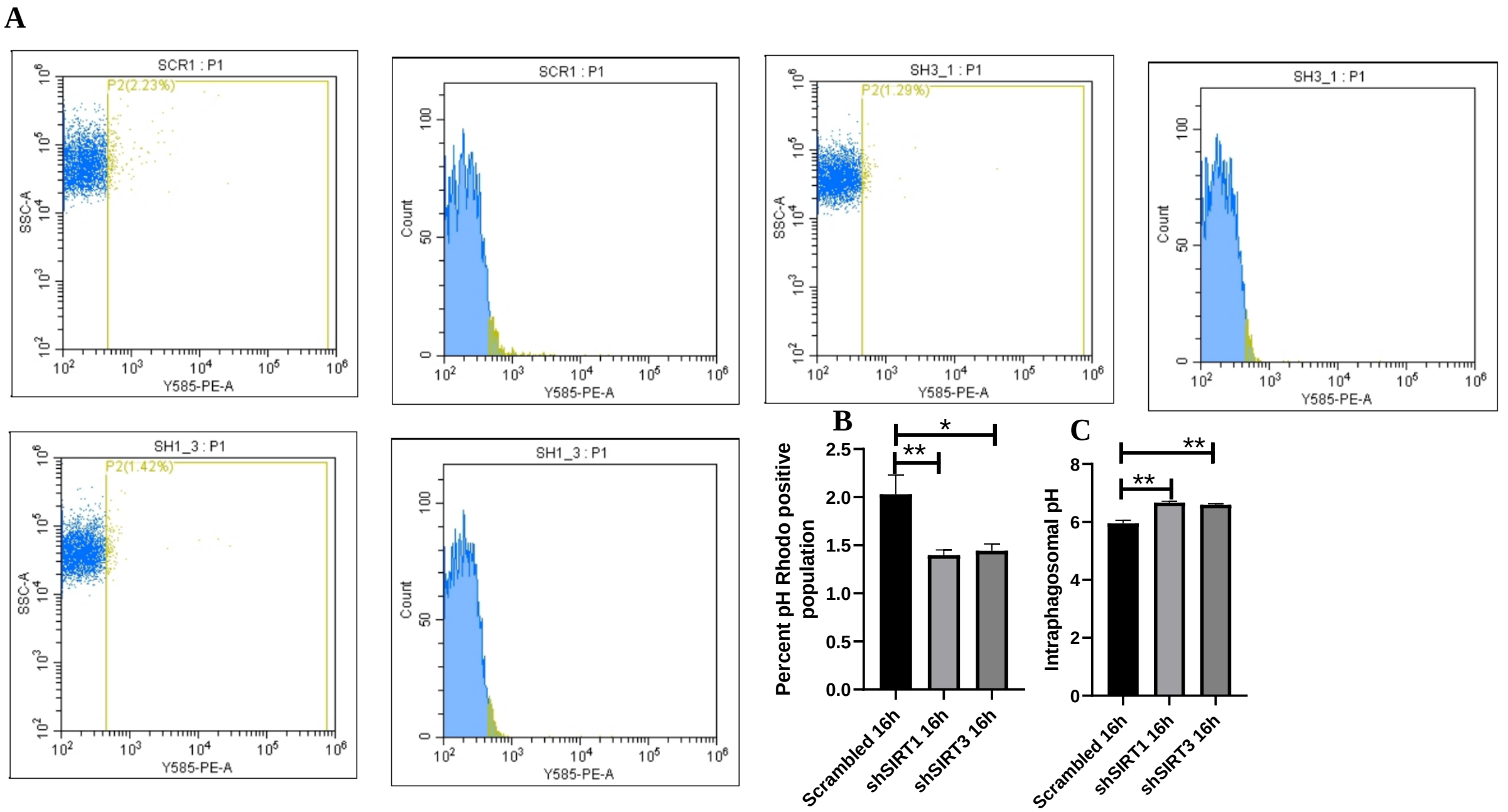
A
SCR1 : P1
P2(2.23%)
SSC-A
Y585-PE-A
Count
SH3_1 : P1
P2(1.29%)
SH1_3 : P1
P2(1.42%)
B
Percent pH Rhodo positive population
Scrambled 16h
shSIRT1 16h
shSIRT3 16h
C
Intraphagosomal pH

D

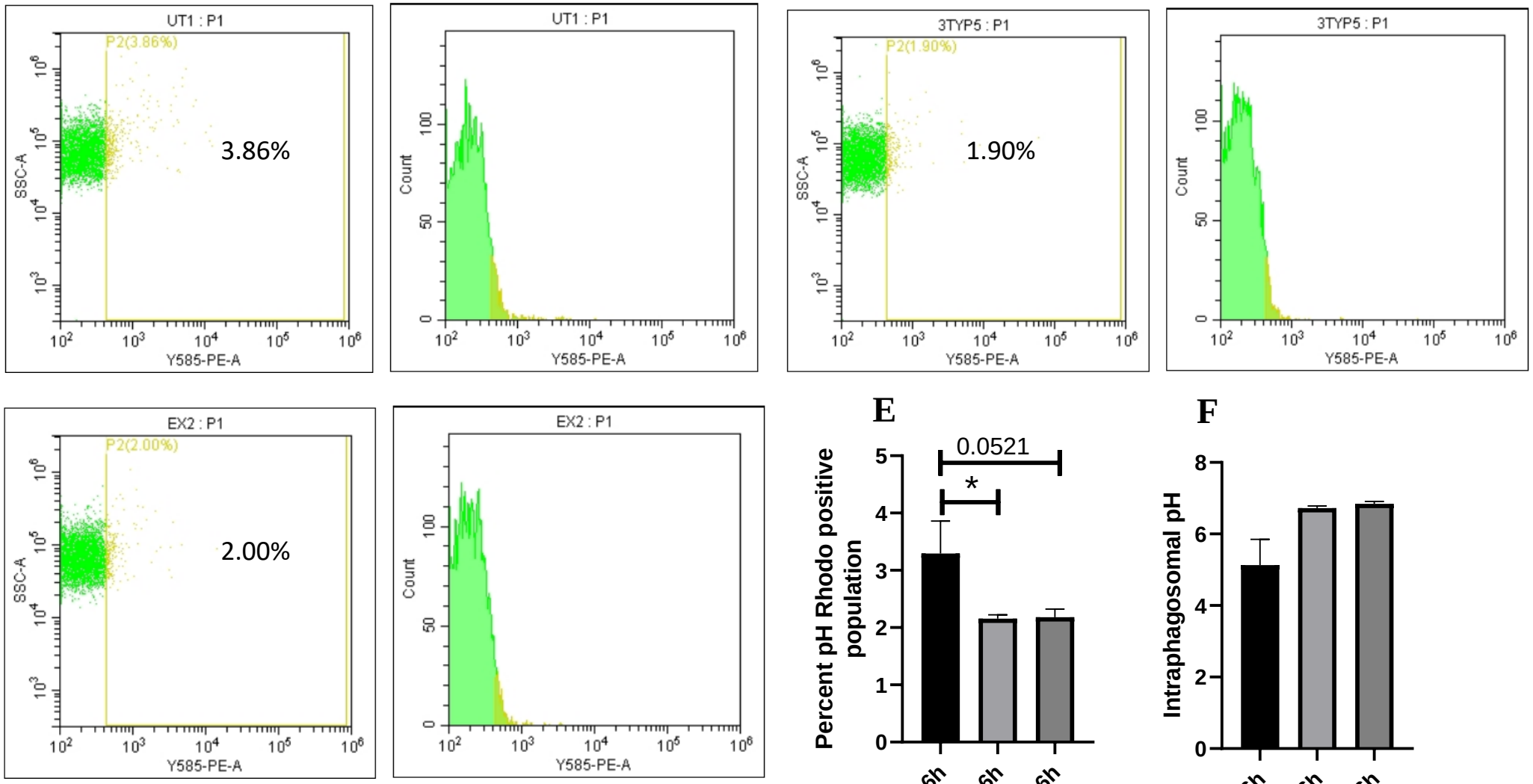
UT1 : P1
P2(3.86%)
3.86%
SSC-A
Y585-PE-A
Count
3TYP5 : P1
P2(1.90%)
1.90%
EX2 : P1
P2(2.00%)
2.00%

E

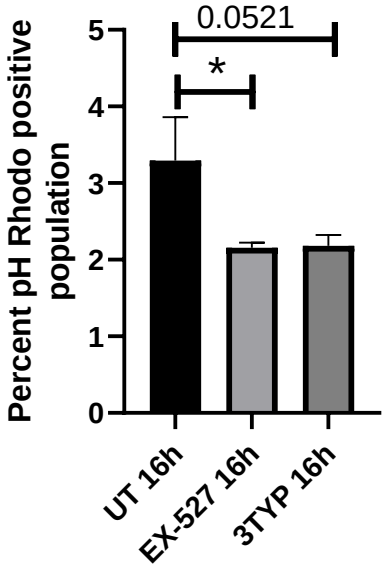
Percent pH Rhodo positive population
0.0521
*
UT 16h
EX-527 16h
3TYP 16h

F

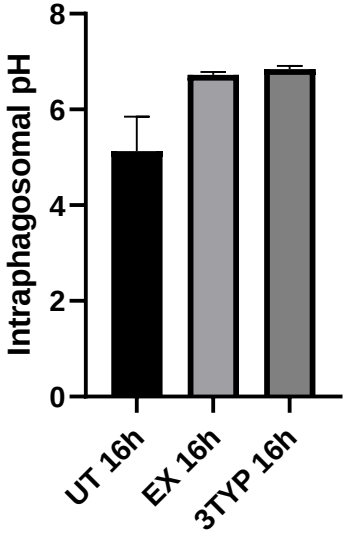
Intraphagosomal pH
UT 16h
EX 16h
3TYP 16h

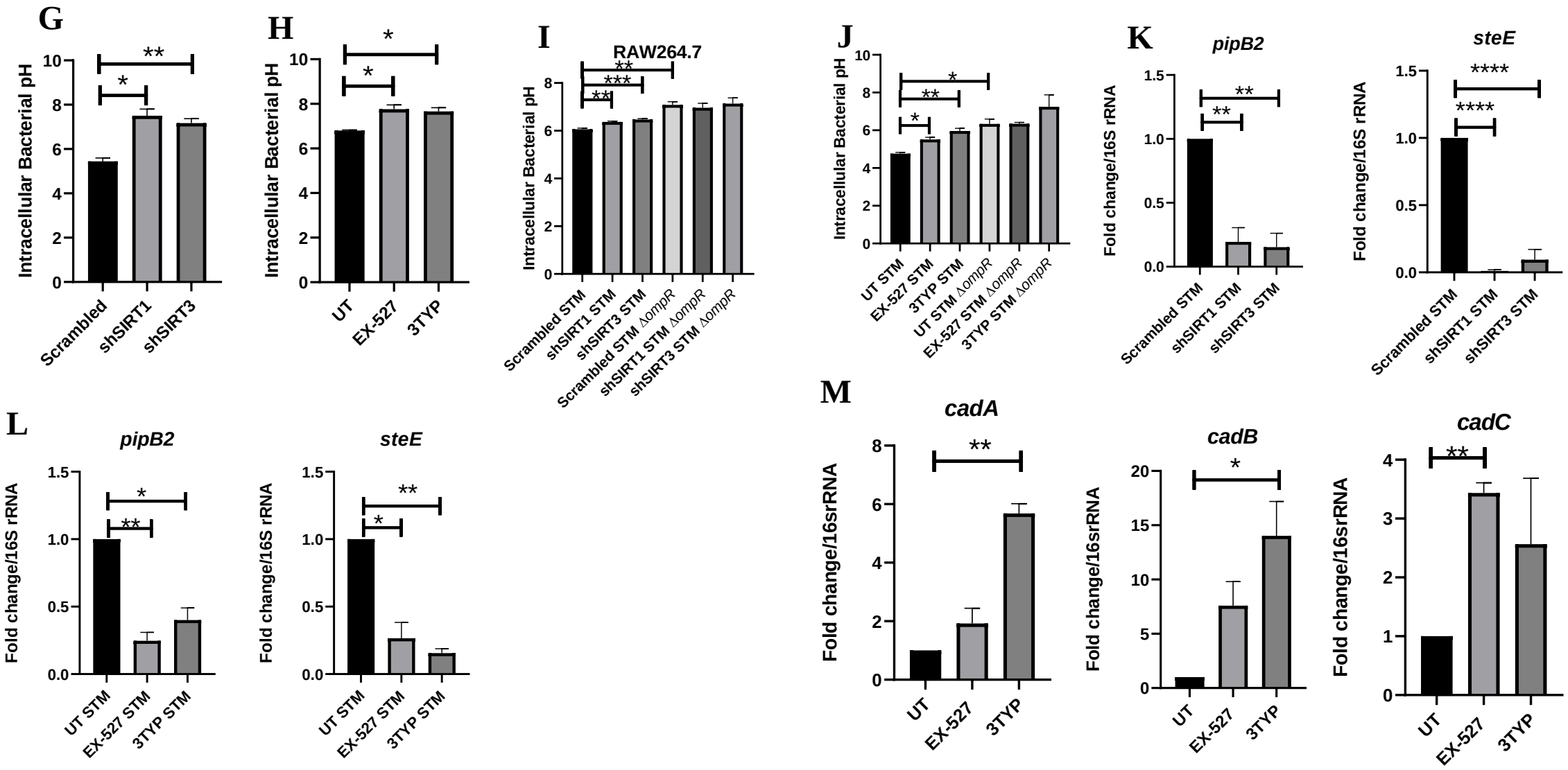
G
Intracellular Bacterial pH
Scrambled
shSIRT1
shSIRT3
H
Intracellular Bacterial pH
UT
EX-527
3TYP
I
RAW264.7
Intracellular Bacterial pH
Scrambled STM
shSIRT1 STM
shSIRT3 STM
Scrambled STM ΔompR
shSIRT1 STM ΔompR
shSIRT3 STM ΔompR
J
Intracellular Bacterial pH
UT STM
EX-527 STM
3TYP STM
UT STM ΔompR
EX-527 STM ΔompR
3TYP STM ΔompR
K
pipB2
steE
Fold change/16S rRNA
Scrambled STM
shSIRT1 STM
shSIRT3 STM
L
pipB2
steE
Fold change/16S rRNA
UT STM
EX-527 STM
3TYP STM
M
cadA
cadB
cadC
Fold change/16srRNA
UT
EX-527
3TYP

Fig.8 – SIRT1 and SIRT3 knockdown or inhibition trigger loss in acidification of bacterial pH and subsequently its SPI-2 secretion within infected macrophages

A-C- Flow cytometric analysis of SCV pH of infected RAW264.7 macrophages under knockdown condition of SIRT1 or SIRT3 at 16h post-infection. Data is representative of N=2,n=3. Unpaired two-tailed Student's t-test was performed to obtain the p-values. ***** p < 0.001, ** p<0.01, * p<0.05**

D-F- Flow cytometric analysis of SCV pH of infected RAW264.7 macrophages under inhibitor treatment of SIRT1 or SIRT3 at 16h post-infection. Data is representative of N=2,n=3. Unpaired two-tailed Student's t-test was performed to obtain the p-values. ***** p < 0.001, ** p<0.01, * p<0.05**

G-Intra-bacterial pH of *S.* Typhimurium expressing pH-sensitive plasmid pHUji was measured from infected RAW264.7 macrophages using flow cytometry under knockdown conditions of SIRT1 and SIRT3. Data is representative of N=3, n=4. Unpaired two-tailed Student's t-test was performed to obtain the p values. ***** p < 0.001, ** p<0.01, * p<0.05**

H-Intra-bacterial pH of *S.* Typhimurium expressing pH-sensitive plasmid pHUji was measured from infected peritoneal macrophages using flow cytometry under inhibitor treatment of SIRT1 (EX-527) and SIRT3 (3TYP) inhibitor at the concentration of 1µM. Data is representative of N=3, n=2. Unpaired two-tailed Student's t-test was performed to obtain the p values. ***** p < 0.001, ** p<0.01, * p<0.05**

I-Intra-bacterial pH of *S.* Typhimurium WT (STM WT) and STMΔ*ompR* expressing pH-sensitive plasmid pHUji was measured from infected RAW264.7 macrophages using flow cytometry under knockdown conditions of SIRT1 and SIRT3. Data is representative of N=3, n=4. Unpaired two-tailed Student's t-test was performed to obtain the p values. ***** p < 0.001, ** p<0.01, * p<0.05**

J-Intra-bacterial pH of *S.* Typhimurium WT (STM WT) and STMΔ*ompR* expressing pH-sensitive plasmid pHUji was measured from infected RAW264.7 macrophages using flow cytometry under inhibitor treatment of SIRT1 (EX-527) and SIRT3 (3TYP) inhibitor at the concentration of 1µM. Data is representative of N=3, n=4. Unpaired two-tailed Student's t-test was performed to obtain the p values. ***** p < 0.001, ** p<0.01, * p<0.05**

K- Quantitative PCR-mediated expression studies of SPI-2 genes within infected RAW264.7 macrophages under the knockdown condition of SIRT1 and SIRT3. Data is representative of N=3, n=4. Unpaired two-tailed Student's t-test was performed to obtain the p values. ***** p < 0.001, ** p<0.01, * p<0.05**

L- Quantitative PCR-mediated expression studies of SPI-2 genes within infected peritoneal macrophages under the inhibitor treatment of SIRT1 (EX-527) and SIRT3 (3TYP) inhibitors. Data is representative of N=3, n=4. Unpaired two-tailed Student's t-test was performed to obtain the p values. ***** p < 0.001, ** p<0.01, * p<0.05**

M- Quantitative PCR-mediated expression studies of *cadA*, *cadB,* and *cadC* genes within infected peritoneal macrophages under the inhibitor treatment of SIRT1 (EX-527) and SIRT3 (3TYP) inhibitors. Data is representative of N=3, n=4. Unpaired two-tailed Student's t-test was performed to obtain the p values. ***** p < 0.001, ** p<0.01, * p<0.05**

FIGURE 9

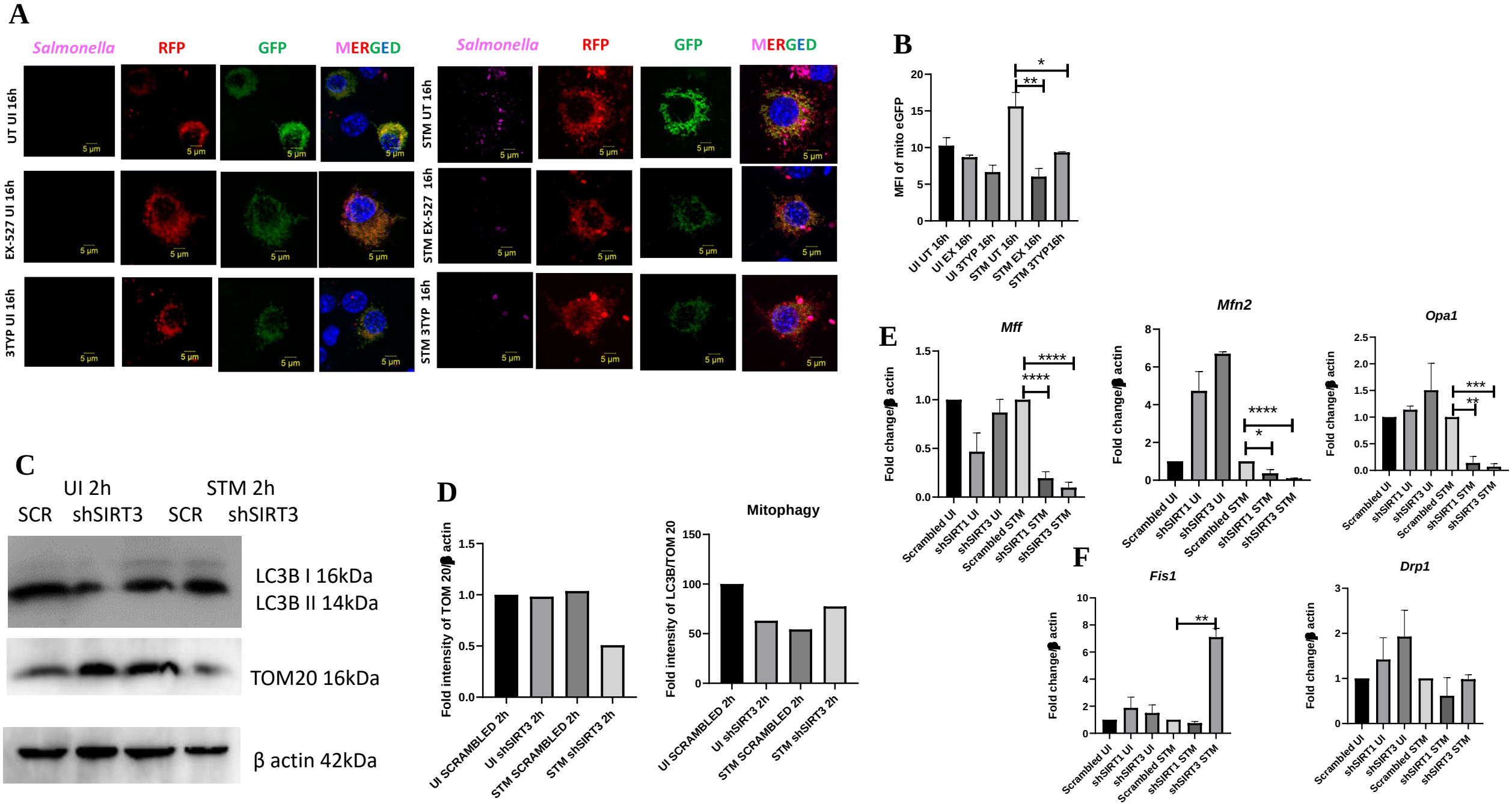
A
Salmonella
RFP
GFP
MERGED
UT UI 16h
EX-527 UI 16h
3TYP UI 16h
STM UT 16h
STM EX-527 16h
STM 3TYP 16h
5 µm
B
MFI of mito eGFP
UI UT 16h
UI EX 16h
UI 3TYP 16h
STM UT 16h
STM EX 16h
STM 3TYP16h
C
UI 2h
STM 2h
SCR
shSIRT3
LC3B I 16kDa
LC3B II 14kDa
TOM20 16kDa
β actin 42kDa
D
Fold intensity of TOM 20/β actin
UI SCRAMBLED 2h
UI shSIRT3 2h
STM SCRAMBLED 2h
STM shSIRT3 2h
Mitophagy
Fold intensity of LC3B/TOM 20
E
Mff
Mfn2
Opa1
Fold change/β actin
Scrambled UI
shSIRT1 UI
shSIRT3 UI
Scrambled STM
shSIRT1 STM
shSIRT3 STM
F
Fis1
Drp1

G

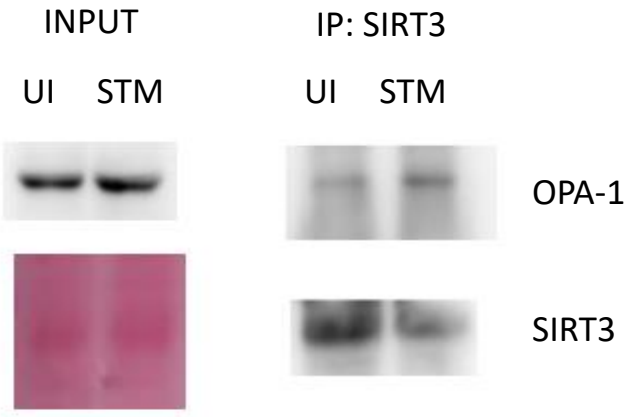
INPUT
UI
STM
IP: SIRT3
UI
STM
OPA-1
SIRT3

H

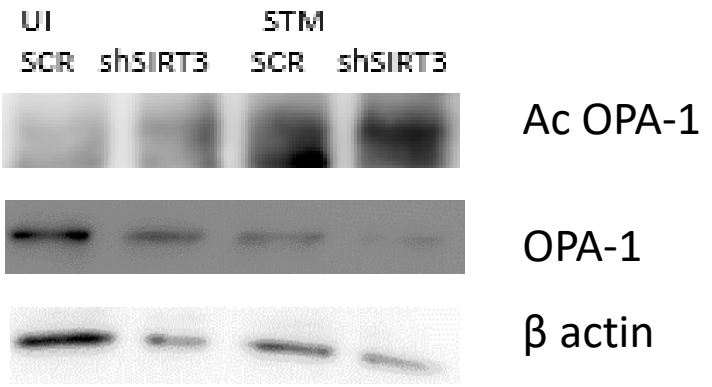
UI
STM
SCR
shSIRT3
SCR
shSIRT3
Ac OPA-1
OPA-1
β actin

I

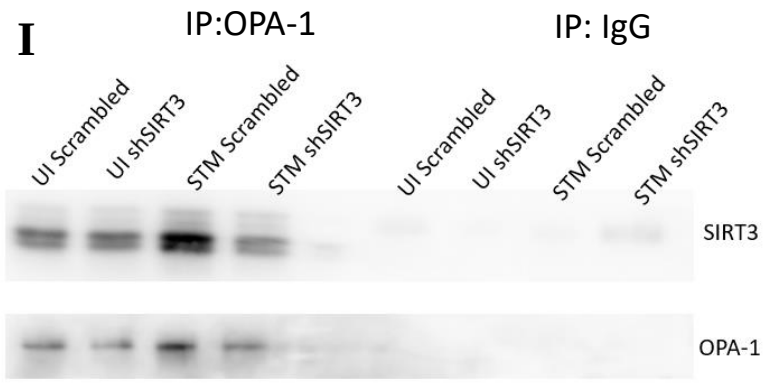
IP:OPA-1
IP: IgG
UI Scrambled
UI shSIRT3
STM Scrambled
STM shSIRT3
UI Scrambled
UI shSIRT3
STM Scrambled
STM shSIRT3
SIRT3
OPA-1

J

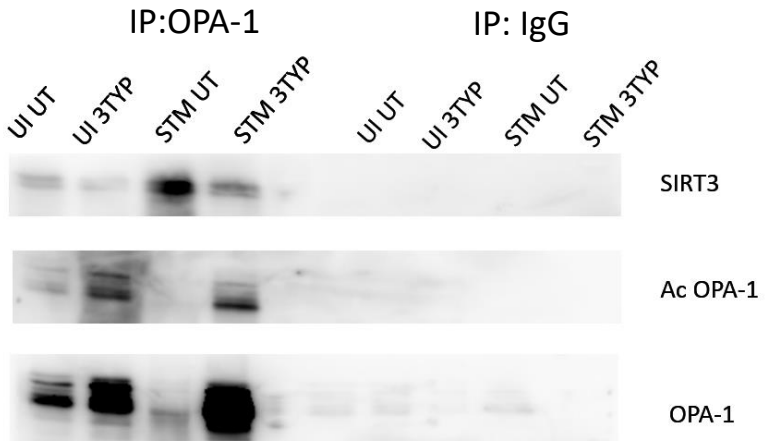
IP:OPA-1
IP: IgG
UI UT
UI 3TYP
STM UT
STM 3TYP
UI UT
UI 3TYP
STM UT
STM 3TYP
SIRT3
Ac OPA-1
OPA-1

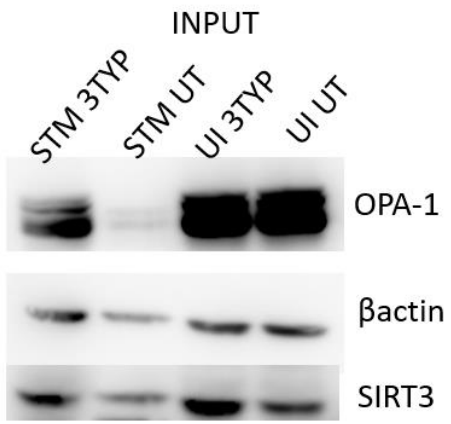
INPUT
STM 3TYP
STM UT
UI 3TYP
UI UT
OPA-1
βactin
SIRT3

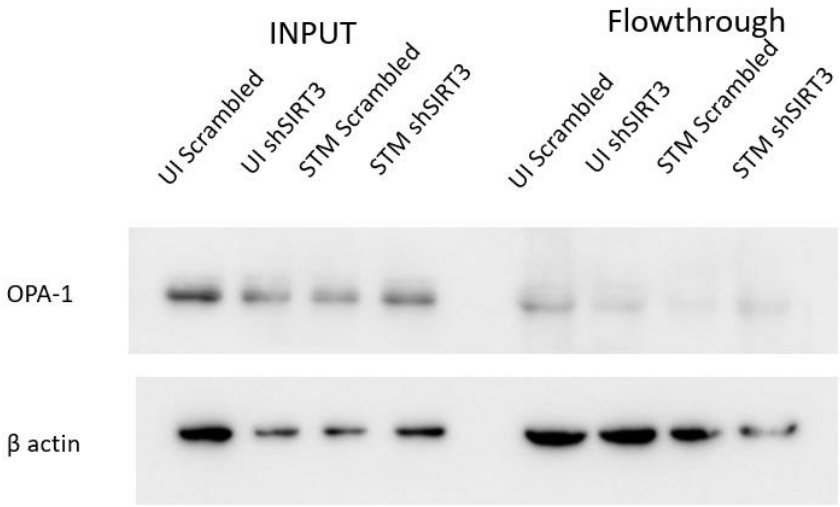
INPUT
Flowthrough
UI Scrambled
UI shSIRT3
STM Scrambled
STM shSIRT3
UI Scrambled
UI shSIRT3
STM Scrambled
STM shSIRT3
OPA-1
β actin

Fig. 9- SIRT1 and SIRT3 inhibition triggers mitophagy in the *S.* Typhimurium-infected macrophages by regulating fusion-fission dynamics

A-Representative confocal images of RAW264.7 macrophages (transfected with mito-eGFP-mCherry) exhibiting mitophagy flux upon *S.* Typhimurium infection at 16h points post-infection. Data is representative of N=2, n=50 (microscopic field).

B- Quantitative representation of the MFI of mitochondrial eGFP as shown in the confocal images (A). Unpaired two-tailed Student's t-test was performed to obtain the p values. ***** p < 0.001, ** p<0.01, * p<0.05**

C- Immunoblotting of LC3B and TOM20 in uninfected and infected RAW264.7 macrophages under knockdown condition of SIRT3 at 2hr post-infection. UI-Uninfected, STM-*S.* Typhimurium infected, Scrambled shRNA control

D-Densitometric analysis of TOM20 with respect to βactin LC3BII with respect to TOM20 and of the immunoblot A to detect mitophagy.

E-F- qRTPCR mediated expression analysis of mitochondrial fusion (E) and fission (F) genes in *S.* Typhimurium infected RAW264.7 macrophages at 16hr post infection under knockdown of SIRT1 or SIRT3.

G- Immunoprecipitation of SIRT3 in uninfected or *S.* Typhimurium infected RAW264.7 macrophages at 16hr post infection to detect interaction of SIRT3 with OPA-1.

H- Immunoblotting of SIRT3 knockdown RAW 264.7 cells in *S.* Typhimurium infected and uninfected condition upon immunoprecipitation of OPA-1 to check the acetylation status of OPA-1.

I- Immunoprecipitation of OPA-1 in uninfected or *S.* Typhimurium infected RAW264.7 macrophages at 16hr post infection under the knockdown condition of SIRT3 to assess the interaction of OPA-1 with SIRT3 in knockdown condition.

J- Immunoprecipitation of OPA-1 in uninfected or *S.* Typhimurium infected RAW264.7 macrophages at 16hr post infection under the catalytic inhibitor treatment of SIRT3.

Title:SIRT1 and SIRT3 impact host mitochondrial function and host- *Salmonella* pH balance during infection

SUPPLEMENTARY FIGURES

SUPPLEMENTARY FIG. S1

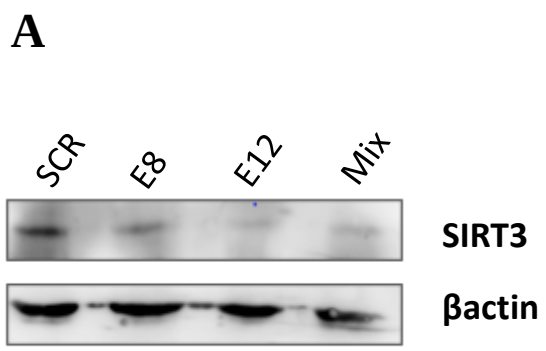

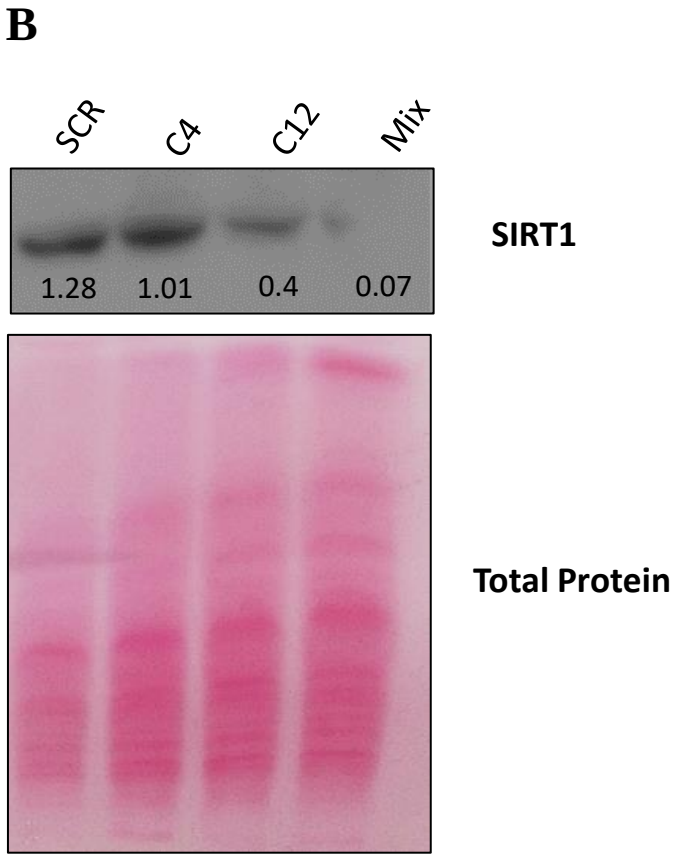

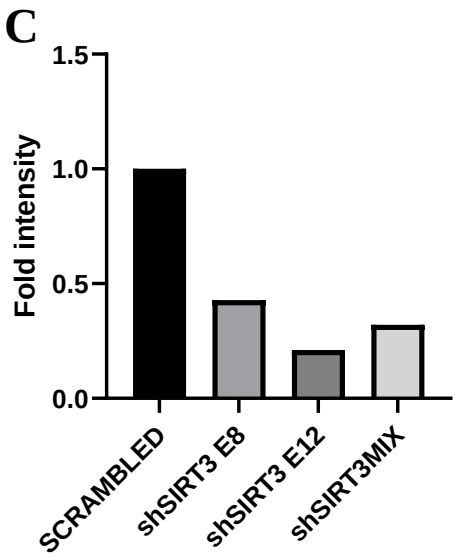

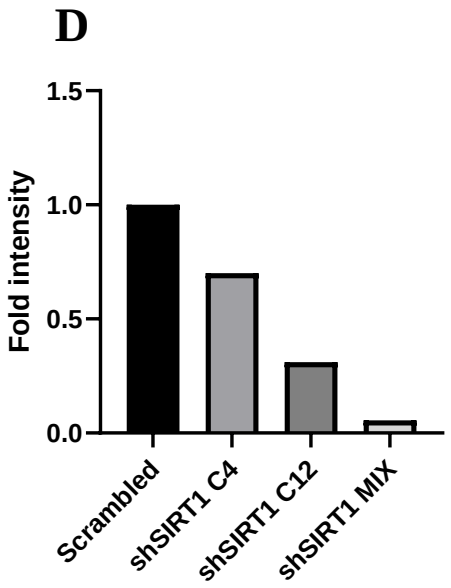

Fig. S1- SIRT1 and SIRT3 knockdown confirmation in RAW264.7 cells using shRNA constructs

A- Immunoblotting of SIRT3 for knockdown validation. (SCR=Scrambled, Mix=transfection with equimolar concentration of both SIRT3 shRNA construct E8 and E12)

B- Immunoblotting of SIRT1 for knockdown confirmation.(SCR=Scrambled, Mix=transfection with equimolar concentration of both SIRT3 shRNA construct C4 and C12)

C- Densitometric analysis of the immunoblot represented in A.

D- Densitometric analysis of the immunoblot represented in B.

SUPPLEMENTARY FIG. S2

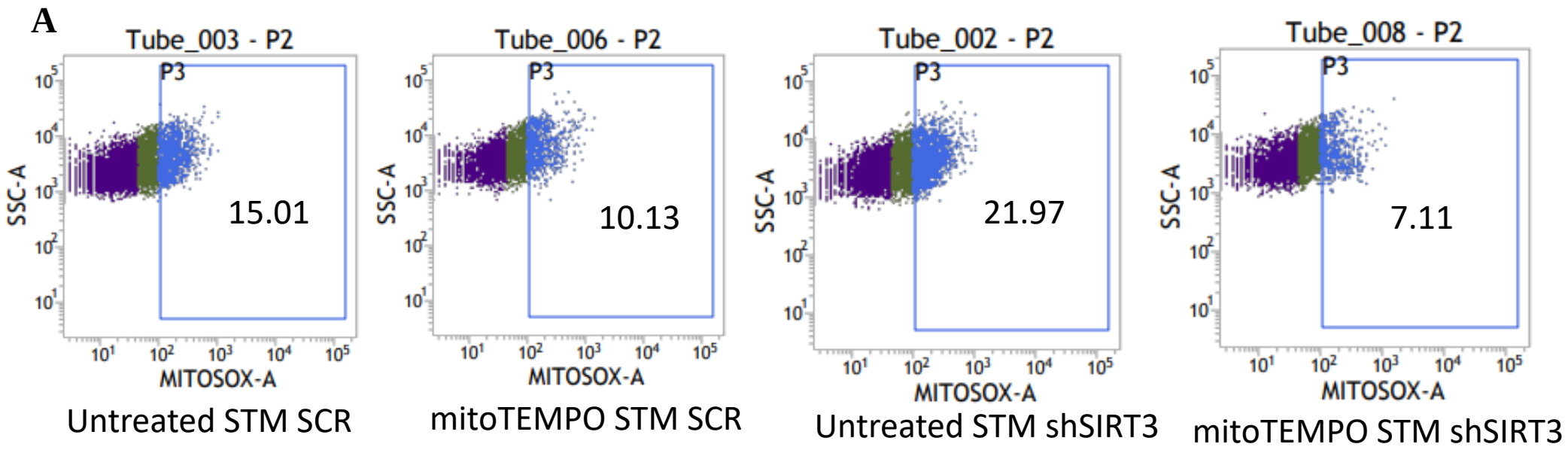

Fig. S2- Validation of action of mitoTEMPO as a mitochondrial ROS scavenger

A-Flow cytometric estimation of mitochondrial ROS generation using mitoSOX dye in presence or absence of mtROS scavenger, mitoTEMPO (10µM) in infected RAW264.7 macrophages.

SUPPLEMENTARY FIG. S3

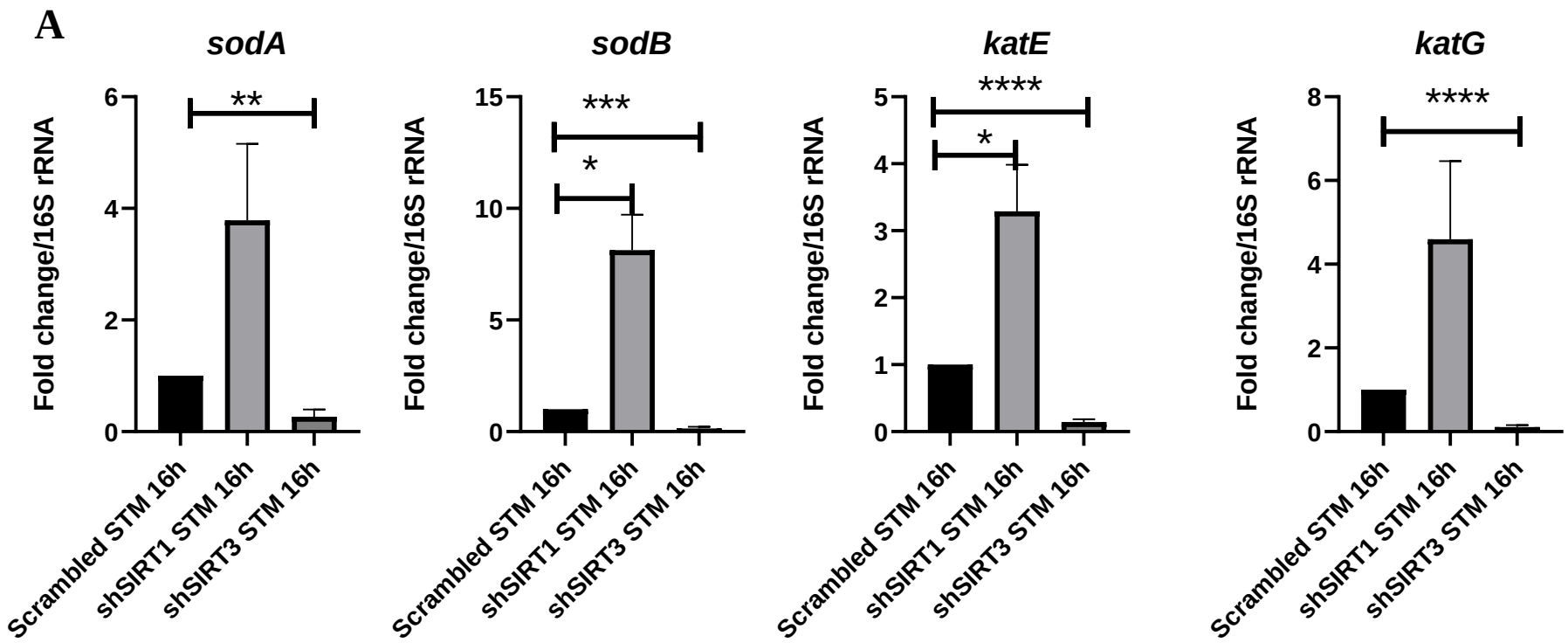

Fig. S3- SIRT1 and SIRT3 knockdown lead to alteration in bacterial antioxidant gene expression

A-qRT-PCR mediated expression analysis of bacterial antioxidant genes in *S.* Typhimurium infected RAW264.7 macrophages at 16hr post infection under knockdown condition of SIRT1 or SIRT3. Data is representative of N=3,n=2. Unpaired two-tailed Student's t test was performed to obtain the p values. ***** p < 0.001, ** p<0.01, * p<0.05**

SUPPLEMENTARY FIG. S4

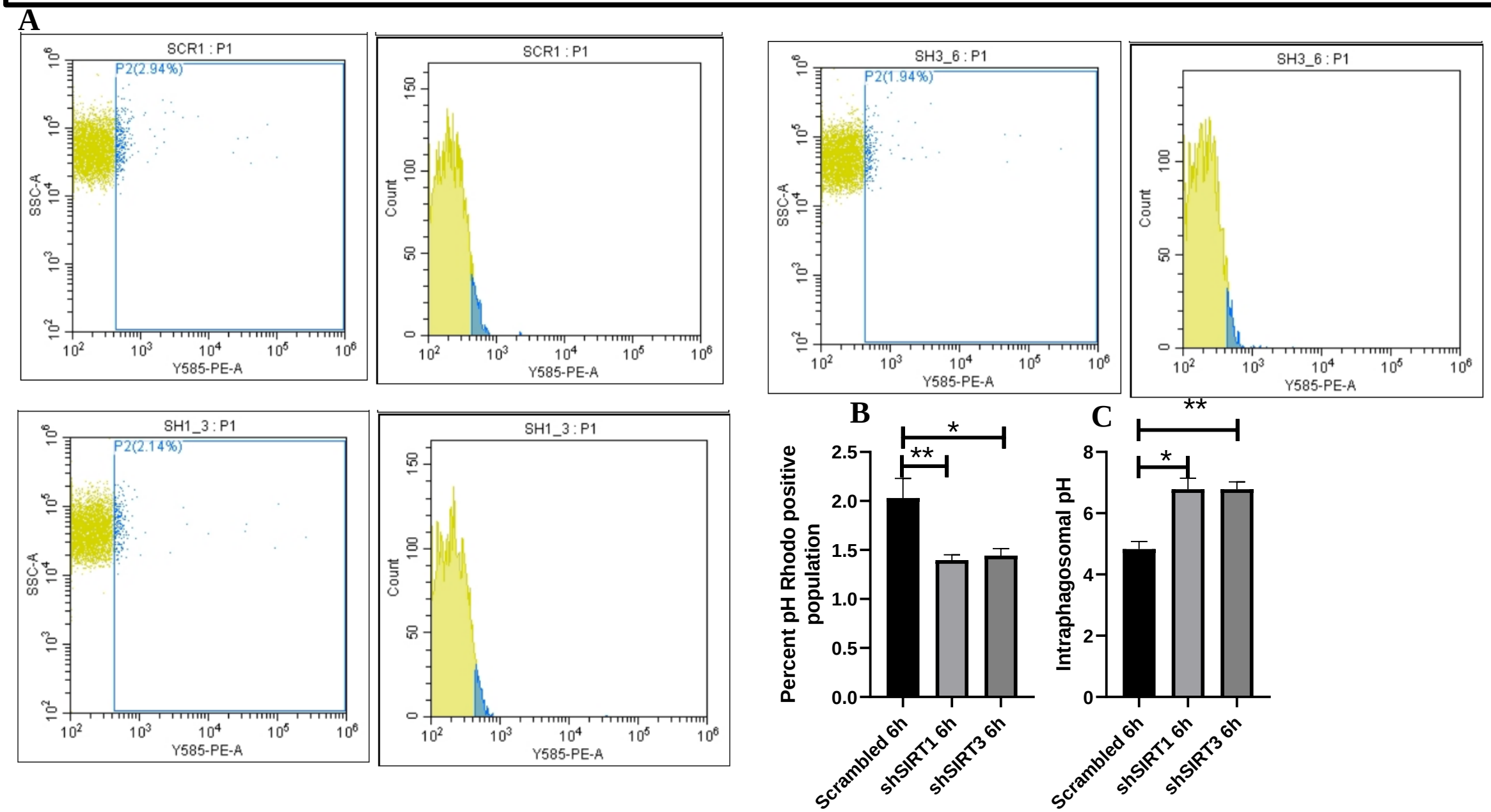

D

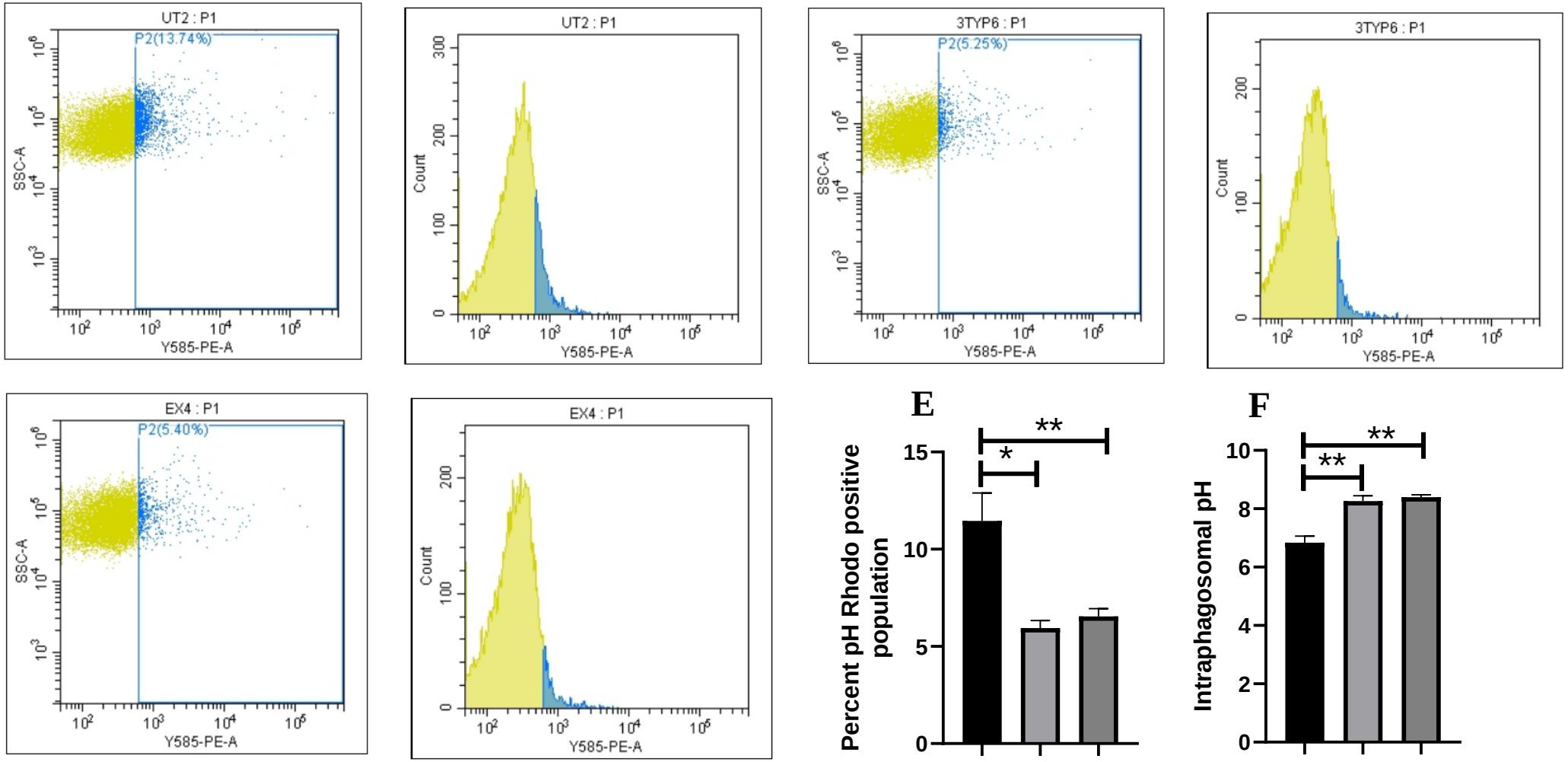
UT2 : P1
P2(13.74%)
SSC-A
Y585-PE-A
UT2 : P1
Count
Y585-PE-A
3TYP6 : P1
P2(5.25%)
SSC-A
Y585-PE-A
3TYP6 : P1
Count
Y585-PE-A
EX4 : P1
P2(5.40%)
SSC-A
Y585-PE-A
EX4 : P1
Count
Y585-PE-A

E

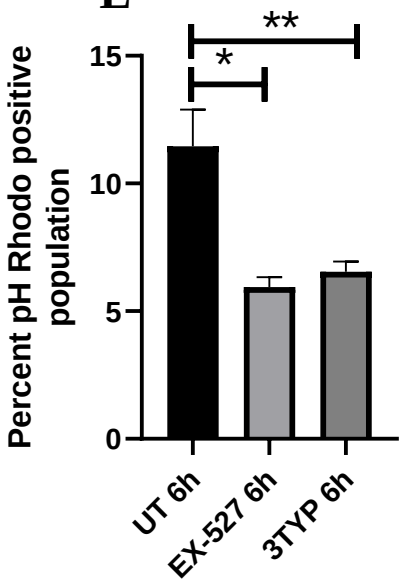
Percent pH Rhodo positive population
15
10
5
0
*
**
UT 6h
EX-527 6h
3TYP 6h

F

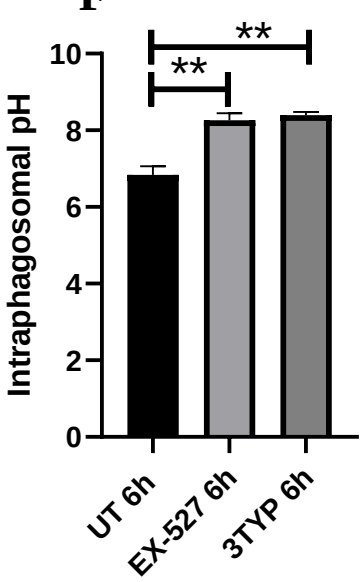
Intraphagosomal pH
10
8
6
4
2
0
**
**
UT 6h
EX-527 6h
3TYP 6h

Fig. S4- SIRT1 and SIRT3 knockdown or inhibition leads to loss of acidification of SCV

A-C- Flow cytometric analysis of SCV pH of infected RAW264.7 macrophages under knockdown condition of SIRT1 or SIRT3 at 6h post-infection. Data is representative of N=2,n=3. Unpaired two-tailed Student's t-test was performed to obtain the p-values. ***** $p < 0.001$, ** $p<0.01$, * $p<0.05$**

D-F- Flow cytometric analysis of SCV pH of infected RAW264.7 macrophages under inhibitor treatment of SIRT1 or SIRT3 at 6h post-infection. Data is representative of N=2,n=3. Unpaired two-tailed Student's t-test was performed to obtain the p-values. ***** $p < 0.001$, ** $p<0.01$, * $p<0.05$**

SUPPLEMENTARY FIG. S5

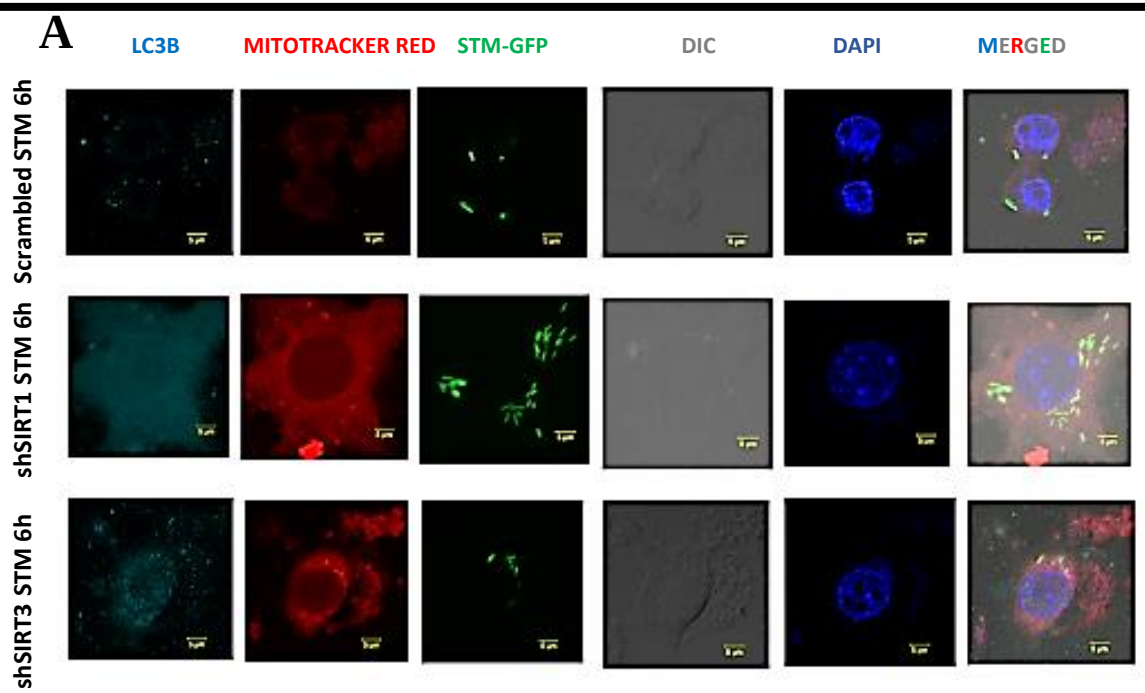

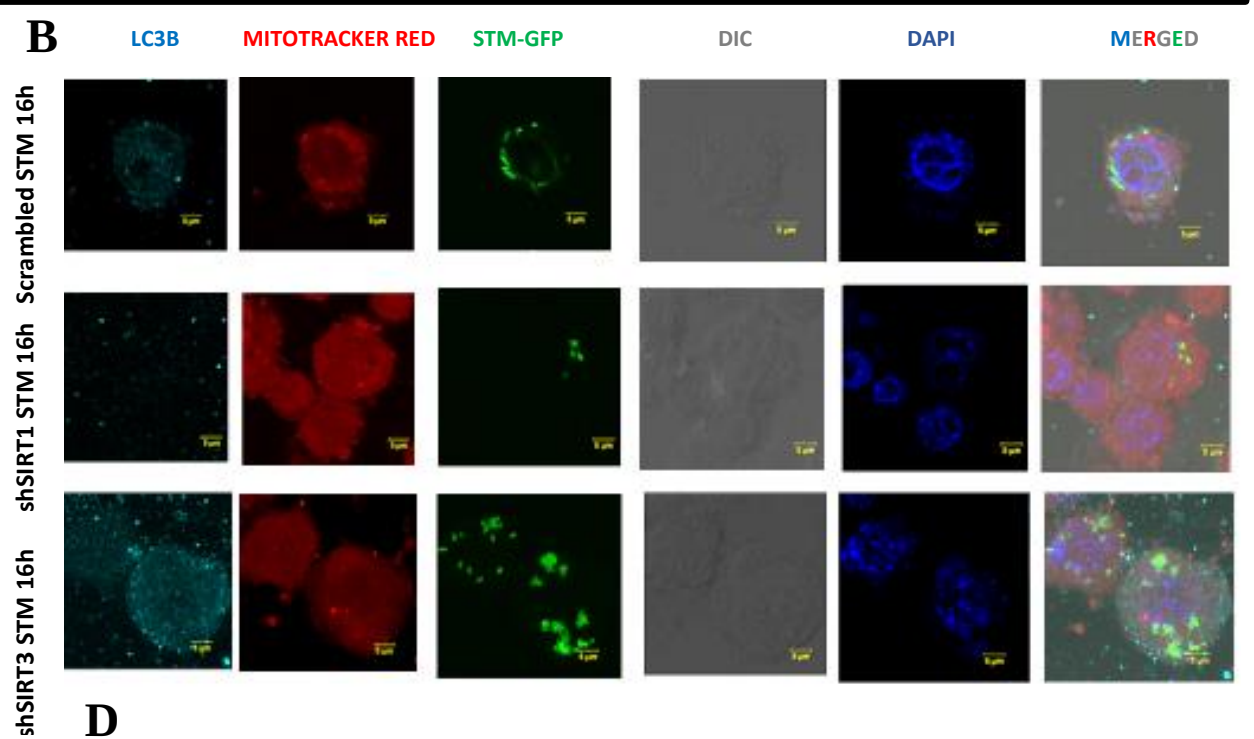

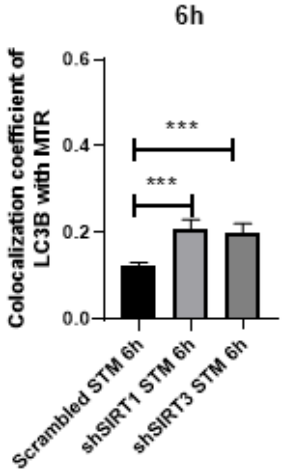

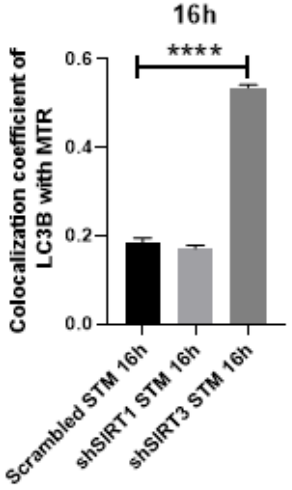

Fig. S5- SIRT1 or SIRT3 knockdown triggers mitophagy in the *S.* Typhimurium-infected macrophages

A-B-Representative confocal images of SIRT1 or SIRT3 knockdown RAW264.7 macrophages exhibiting colocalization of LC3B with mitotracker Red to detect mitophagy upon *S.* Typhimurium infection at 6hr (A) and 16hr (B) post-infection. Data is representative of N=2, n=80 (microscopic field).

C-D-Quantitative representation of the colocalization co-efficient of LC3B with that of mitotracker Red as shown in the confocal images (A-B). Unpaired two-tailed Student's t test was performed to obtain the p values. ***** p < 0.001, ** p<0.01, * p<0.05**

SUPPLEMENTARY FIG. S6

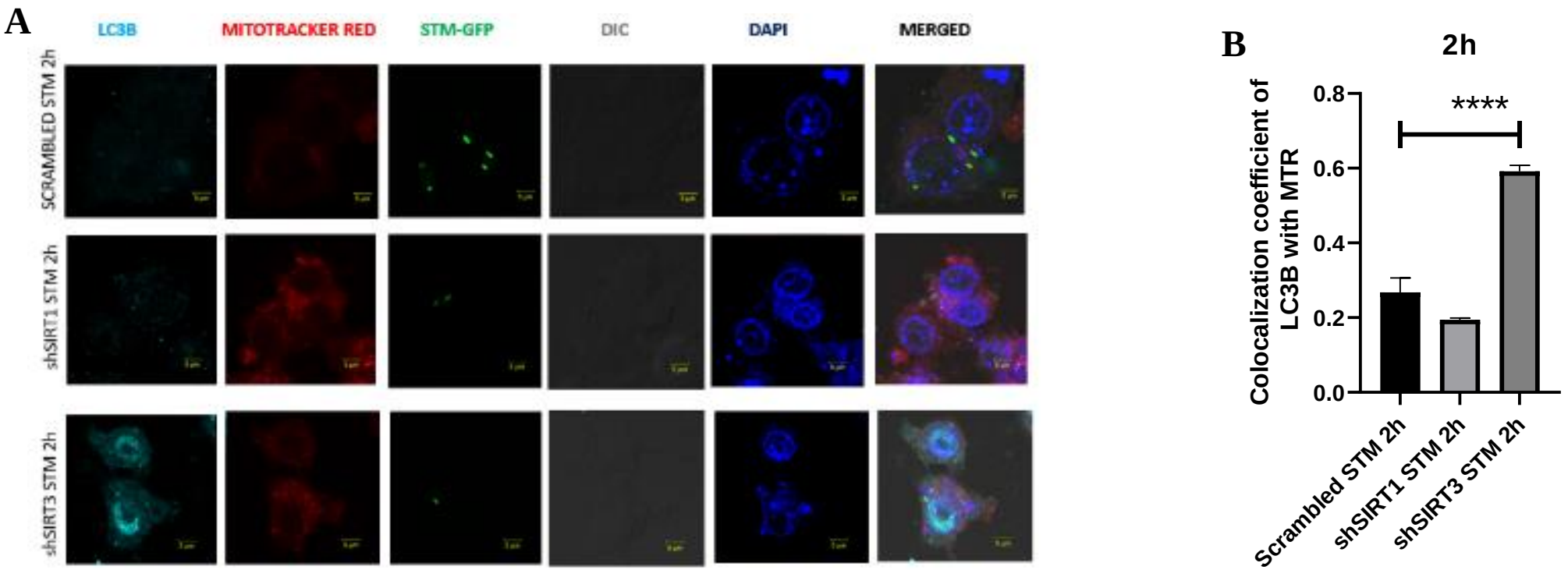

Fig. S6- SIRT3 knockdown triggers mitophagy in the *S.* Typhimurium-RAW264.7 infected macrophages at early time points of 2hr post-infection

A-Representative confocal images of SIRT1 or SIRT3 knockdown RAW264.7 macrophages exhibiting colocalization of LC3B with mitotracker Red to detect mitophagy upon *S.* Typhimurium infection at 2hr post-infection. Data is representative of N=2, n=80 (microscopic field).

B-Quantitative representation of the colocalization co-efficient of LC3B with that of mitotracker Red as shown in the confocal images A. Unpaired two-tailed Student's t test was performed to obtain the p values. ***** p < 0.001, ** p<0.01, * p<0.05**

SUPPLEMENTARY FIG. S7

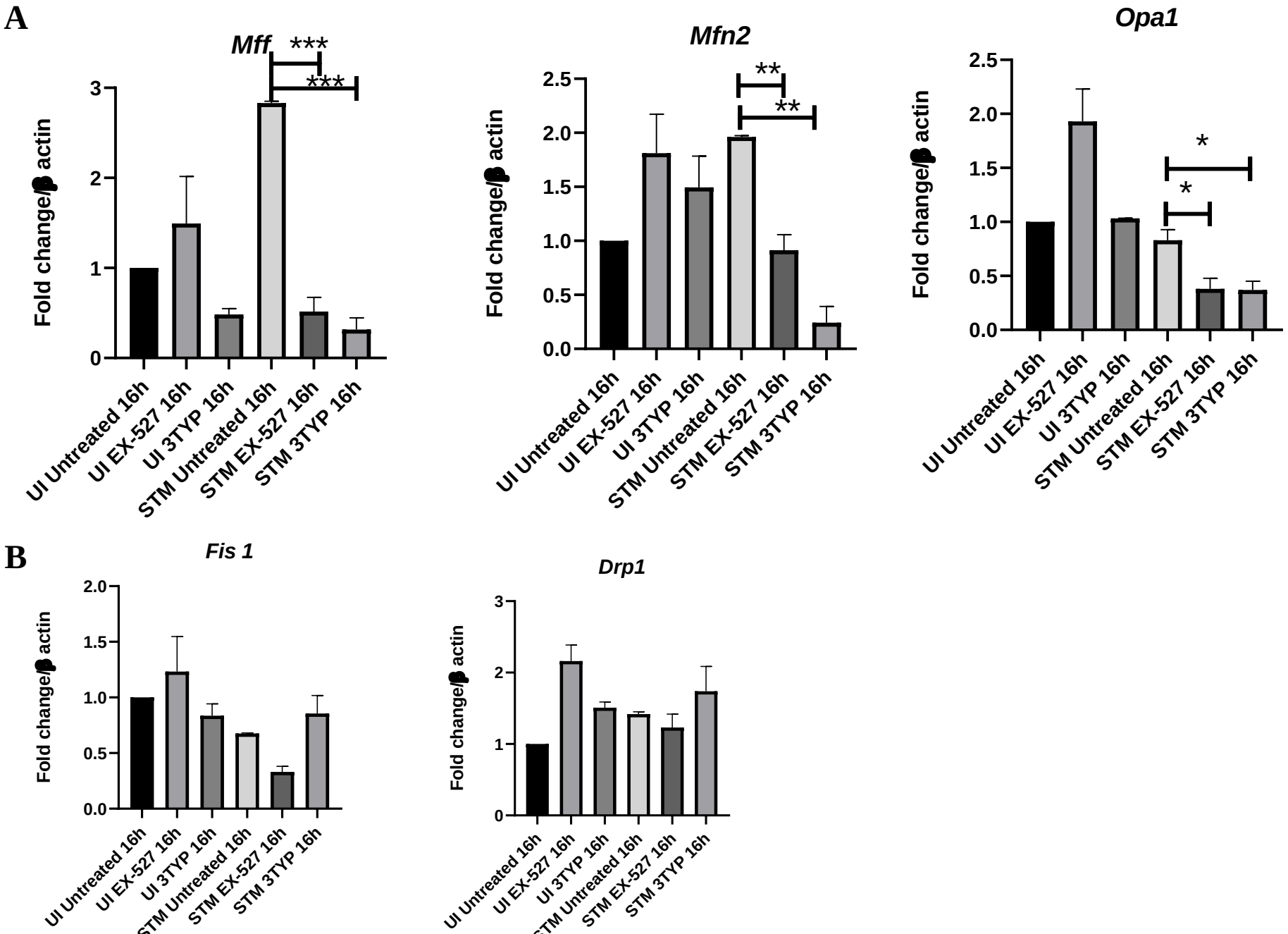

Fig. S7- SIRT1 and SIRT3 inhibition causes alteration in mitochondrial fusion-fission dynamics in STM-infected peritoneal macrophages

A-qRT-PCR mediated expression analysis of mitochondrial fusion genes in *S.* Typhimurium infected peritoneal macrophages at 16hr post infection under inhibitor treatment of SIRT1 or SIRT3 at a concentration of 1µM. Data is representative of N=3,n=2. Unpaired two-tailed Student's t test was performed to obtain the p values. ***** p < 0.001, ** p<0.01, * p<0.05**

B-qRT-PCR mediated expression analysis of mitochondrial fission genes in *S.* Typhimurium infected peritoneal macrophages at 16hr post infection under inhibitor treatment of SIRT1 or SIRT3 at a concentration of 1µM. Data is representative of N=3,n=2. Unpaired two-tailed Student's t test was performed to obtain the p values. ***** p < 0.001, ** p<0.01, * p<0.05**

SYNOPSIS

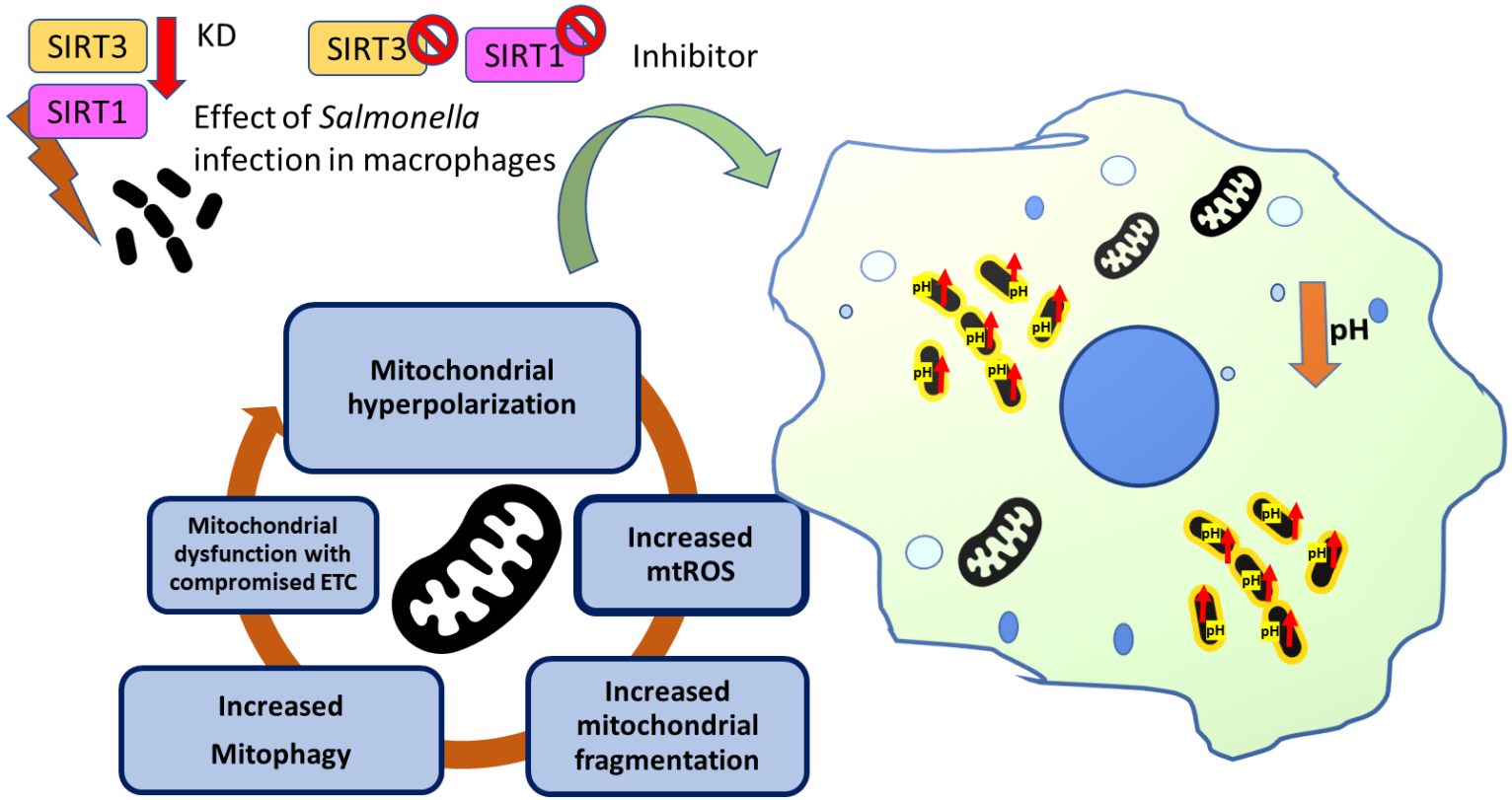

- The loss of SIRT1 and SIRT3 function, achieved through shRNA-mediated knockdown or inhibitor treatment, leads to increased mitochondrial dysfunction in *Salmonella*-infected macrophages. This dysfunction manifests as alterations in mitochondrial bioenergetics and an upsurge in mitochondrial superoxide generation.
- The presence of dysfunctional mitochondria triggers mitophagy and affects the balance of mitochondrial fusion-fission dynamics in the infected macrophages.
- The perturbation in mitochondrial bioenergetics contributes to an acidification of the cytosolic pH in infected macrophages, which, in turn, skews the intravacuolar pH and the pH within the intracellular *Salmonella*. This altered pH environment ultimately results in decreased expression of the *Salmonella* Pathogenicity Island-2 (SPI-2) effector genes.